5-1-2015

Mechanisms of Enhanced Pulmonary Vasoconstriction and Calcium Sensitization Following Chronic Hypoxia

Charles Elbert Norton III

Charles Elbert Norton III

Candidate

Cell Biology and Physiology

Department

This thesis is approved, and it is acceptable in quality and form for publication:

Approved by the Thesis Committee:

Thomas Resta, Chairperson

Nikki Jernigan

William Shuttleworth

Benjimen Walker

MECHANISMS OF ENHANCED PULMONARY VASOCONSTRICTION AND CALCIUM SENSITIZATION FOLLOWING CHRONIC HYPOXIA

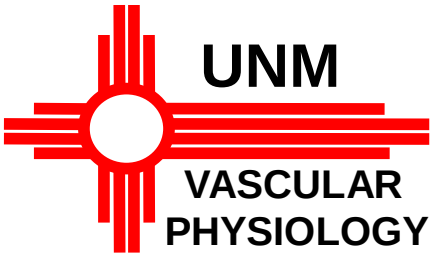

by

CHARLES ELBERT NORTON III

B.S. BIOLOGY, B.A. CHEMISTRY UNIVERSITY OF NEW MEXICO, 2010

DISSERTATION

Submitted in Partial Fulfillment of the
Requirements for the Degree of

Doctor of Philosophy
Biomedical Sciences

The University of New Mexico
Albuquerque, New Mexico

May 2015

ACKNOWLEDGEMENTS

I thank my mentor and advisor, Dr. Tom Resta, for his support and guidance for the past eight years. I would additionally like to thank my committee members Dr. Ben Walker, Dr. Nikki Jernigan, and Dr. Bill Shuttleworth. Their input and support throughout my graduate career has been vital to my success as a scientist and the completion of my dissertation. I also wish to thank the Vascular Physiology Group, members past and present, for their input at lab meetings, journal clubs, and around the laboratory. I feel privileged to have been able to receive my training in such a collaborative intellectual environment. I wish to specifically highlight the contributions of Joshua Sheak for his assistance with the matrix metalloproteinase western blot experiments in these studies.

I also want to thank my parents for their support and for promoting the value of a graduate degree. Finally I would like to express my gratitude to the friends who supported me seasons 1-8.

MECHANISMS OF ENHANCED PULMONARY VASOCONSTRICTION AND CALCIUM SENSITIZATION FOLLOWING CHRONIC HYPOXIA

by

CHARLES ELBERT NORTON III

B.S. BIOLOGY, B.A. CHEMISTRY, UNIVERSITY OF NEW MEXICO, 2010

ABSTRACT

CH results in pressure dependent basal tone and enhanced depolarization- and endothelin-1 (ET-1)-induced vasoconstriction in the pulmonary circulation through Rho kinase (ROK)-dependent Ca^{2+} sensitization, responses that may contribute to the development of pulmonary hypertension (PH) in this setting. The free radical superoxide (O_2^-) has been implicated in these responses. Because NADPH oxidases (NOX) play a role in the development of PH, we hypothesized that membrane depolarization, increases in

intraluminal pressure, and ET-1 signaling lead to pulmonary vascular smooth muscle (VSM) myofilament Ca^{2+} sensitization and augmented vasoconstrictor reactivity following CH through NOX-derived O_2^- production. As epidermal growth factor receptor (EGFR) and Src kinases can mediate NOX activation, we further hypothesized that Src-induced EGFR activation mediates this response.

Vasoconstrictor responses to ET-1 and KCl were greater in Ca^{2+} permeabilized, endothelium-disrupted, pressurized, pulmonary arteries from CH (4 wk at 0.5 atm) rats compared to controls, and this effect of CH was abolished by NOX inhibition. NOX inhibition additionally prevented KCl-dependent O_2^- production in CH arteries. Furthermore, inhibition of EGFR and Src kinases also prevented augmented ET-1- and KCl-induced vasoconstriction and the development of basal tone. Rats treated chronically with an EGFR inhibitor (gefitinib) displayed reduced right ventricular pressure and diminished arterial remodeling associated with CH-dependent PH. We additionally determined that vascular smooth muscle membrane depolarization contributes to basal tone but not vasoconstriction to ET-1 in CH arteries by clamping membrane potential with valinomycin. Our studies support a novel role for a Src kinase/EGFR/NOX 2 signaling axis in the enhanced pulmonary vascular smooth muscle VSM Ca^{2+} sensitization, vasoconstriction and PH following CH.

TABLE OF CONTENTS

LIST OF FIGURES

Chapter 1 – Introduction

PULMONARY HYPERTENSION

Hypoxemia, a reduction in arterial oxygen levels, can be caused by diminished inspired O_2 or by impaired gas transport within the lung. Chronic hypoxia (CH; Appendix A: Abbreviations and Acronyms, page 148) results from prolonged exposure to high altitude or as a consequence of conditions that impede oxygenation of the blood resulting from chronic obstructive pulmonary diseases (COPD) which has recently risen to the third leading cause of death in the United States (92) and can result in right heart failure and death. CH causes pulmonary hypertension (PH), defined clinically as pulmonary arterial pressure exceeding 25 mmHg at rest (269). Thus, understanding the mechanisms of CH-induced PH is important for the treatment of the disease.

Mechanisms of Chronic Hypoxia-Induced Pulmonary Hypertension

Normally, the pulmonary circulation is a low pressure, low resistance network of blood vessels. However, under pathological conditions such as CH or COPD, there are structural and functional changes within the pulmonary vasculature including vasoconstriction (discussed in next section), vascular remodeling, and polycythemia (Fig. 1). These changes lead to increases in pulmonary vascular resistance in accordance with Poiseuille's law:

$$\text{Resistance} = 8\eta L / \pi r^4$$

where, η is viscosity, L is length, and r is vessel radius. While this equation relates to resistances in straight, rigid tubes containing a Newtownian fluid, it

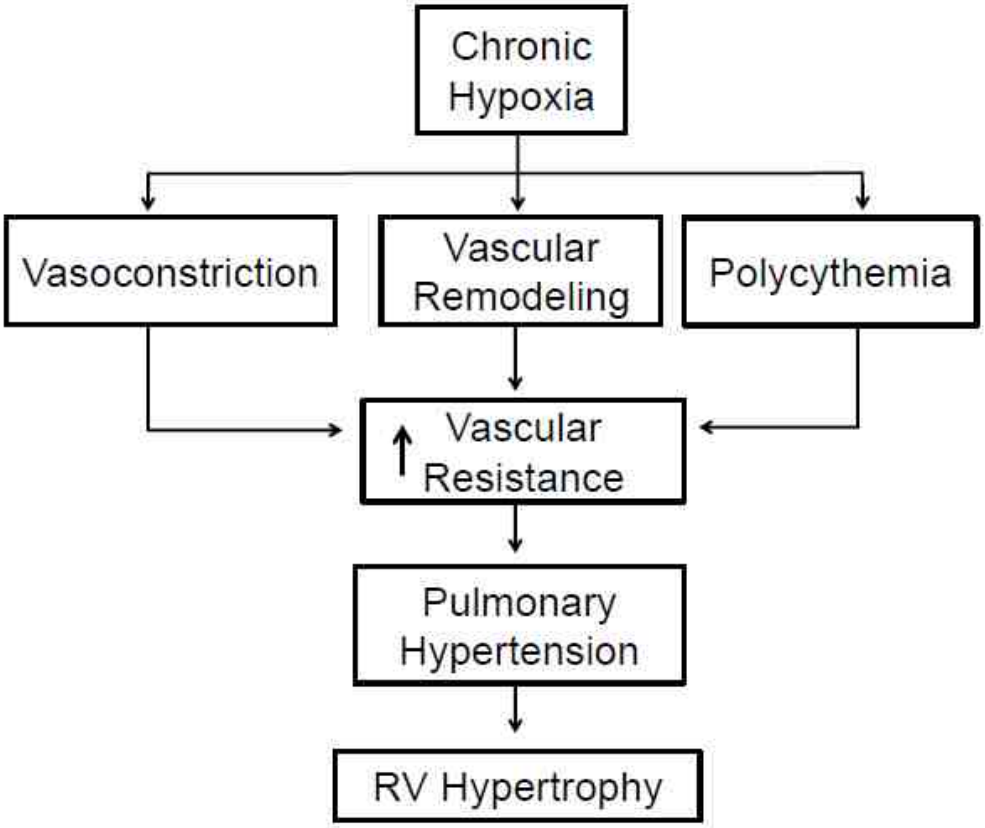

Figure 1: Schematic illustrating contributing factors to chronic hypoxia (CH)-induced pulmonary hypertension. CH causes vasoconstriction, vascular remodeling, and polycythemia. These result in elevated vascular resistance, the development of pulmonary hypertension, and right ventricular (RV) hypertrophy.

serves as an approximation for the hemodynamic components that determine resistance to flow within the pulmonary vasculature.

Polycythemia, an increase in the percent volume of circulating red bloods cells, results in an increase in blood viscosity, and therefore according to Poiseuille's law would lead to an increase in pulmonary vascular resistance. Hypoxia activates hypoxia inducible factor (HIF)-1α which induces the erythropoiesis that drives the polycythemic response (85; 102).

Erythropoiesis normally occurs at a low basal rate to replace old red blood cells and can be stimulated when blood loss results in a decrease in the number of red blood cells and resultant tissue hypoxia. Erythropoietin, the glycoprotein hormone mediator of this response, is synthesized in the kidney and acts on erythropoietin receptors on erythroid progenitor cells in the bone marrow to induce erythropoiesis (54). Other factors that contribute to this response include testosterone, somatotropin, and insulin-like growth factor 1, although erythropoietin is necessary for the response (102). This response functions to maintain red blood cell mass constant day to day and to hasten red blood cell recovery after hemorrhage.

In response to hypoxia, the transcription factors HIF-1 and HIF-2 result in an increase in erythropoietin production by fibroblasts in the renal cortex of the kidney (245; 291). The C-terminus of the HIF-α subunits contains O_2-dependent degradation domains that are prolylhydroxylated in the presence of O_2 (28; 99; 100; 308), which leads to ubiquitination and proteasomal degradation (95; 209).

Therefore, under hypoxic conditionsHIF-1α and HIF-2α levels increase, facilitating cooperation with the constitutively present HIF-β subunits and the transcriptional coactivators p300 and cAMP response element-binding protein (29). These complexes will then bind to the DNA and result in enhanced transcription of erythropoietin. Hypoxia also decreases GATA-2-dependent inhibition of erythropoietin synthesis (279). Combined, these actions result in polycythemia which facilitates greater oxygen carrying capacity in the blood which serves a beneficial role during hypoxemia. However, polycythemia also increases blood viscosity and could contribute to elevated pulmonary vascular resistance during prolonged hypoxia or chronic lung disease.

It has long been understood that structural changes occur within the pulmonary circulation in response to hypoxia. Studies in CH animals demonstrated that remodeling of small pulmonary arteries begins within 2 days of hypoxia exposure (163). This response involves proliferation and hypertrophy of the smooth muscle and an increase in the muscularization of previously non-muscularized vessels. Numerous signaling molecules contribute to the vascular remodeling response including endothelin-1 (ET-1) (4; 49), serotonin (5-HT) (63), and thromboxanes (123). ET-1, produced by the endothelium, stimulates both ET_A and ET_B receptors on pulmonary artery vascular smooth muscle cells, promoting cell proliferation (43), which contributes to the proliferative response following hypoxia as ET-1 levels are increased during CH. 5-HT production is also increased by hypoxia (61) which leads to mitogenesis of smooth muscle and fibroblasts (299). It is likely that increases in intracellular Ca^{2+} associated with

these stimuli plays a key role in the remodeling as increased vascular smooth muscle (VSM) $[Ca^{2+}]_i$ has been linked to remodeling in both human patients suffering idiopathic PH (73; 309) and animal models of PH (268).

Remodeling also occurs within the adventitial and intimal layer of the vessel (260). Increased fibroblast and myofibroblast numbers in the vessel wall substantially contribute to thickening of the vessel wall (230; 249). Endothelial proliferation and intimal thickening occur in some forms of PH and may contribute to morphological changes as well (164). Additionally, the recruitment of immune cells such as macrophages, monocytes, mast cells, dendritic cells, and T-cells (cytotoxic and T-helper) has been demonstrated in vessels from lungs with idiopathic PH (238), while decreases in natural killer cells have been observed (197). Furthermore, these cell types contribute to pulmonary vascular remodeling in monocrotaline-treated rats (197), and likely contribute to the inflammatory response associated with PH. These immune cells have been observed both in the adventitial and intimal layers of the vessel (9; 203; 204; 238; 256; 280). However, the mechanisms by which immune cells contribute to PH remain to be fully elucidated.

CHRONIC HYPOXIA AND VASOCONSTRICTION

Changes in vessel diameter that occur with vasoconstriction can additionally be integral in determining pulmonary vascular resistance (Fig. 1). There are several factors that contribute to elevated vasoconstriction in the pulmonary circulation including hypoxic pulmonary vasoconstriction, enhanced

agonist-induced vasoconstriction, and the development of basal arterial tone (Fig. 2).

The contractile state of VSM is regulated by the level of phosphorylation of the myosin light chain. The myosin regulatory light chain is phosphorylated by myosin light chain kinase (MLCK) which facilitates actin myosin interaction and shortening of the contractile apparatus (272). MLCK is activated by calmodulin. Calmodulin signaling is set in motion when four Ca^{2+} ions are bound to it, making phosphorylation of the myosin light chain dependent upon changes in VSM $[Ca^{2+}]_i$.

Ca^{2+}-Dependent Vasoconstriction

Pulmonary VSM cells contain L-type voltage gated Ca^{2+} channels (VGCC) that couple membrane depolarization to Ca^{2+} entry. Given that VSM cells (VSMC) from CH animals are more depolarized than those of control animals (179), it is likely L-type VGCCs contribute to the elevations in basal Ca^{2+} in the setting of PH, as rats treated chronically verapamil, an L-type VGCC blocker, developed reduced hypoxic PH (257). Consistent with this finding are reports that basal Ca^{2+} is elevated in the setting of PH (76; 310).

The sarcoplasmic reticulum acts as a Ca^{2+} sink within the cytoplasm. The sarcoplasmic endoplasmic reticulum Ca^{2+} ATPase (SERCA) uptakes Ca^{2+} from the cytoplasm. Store operated Ca^{2+} entry (SOCE) occurs following depletion

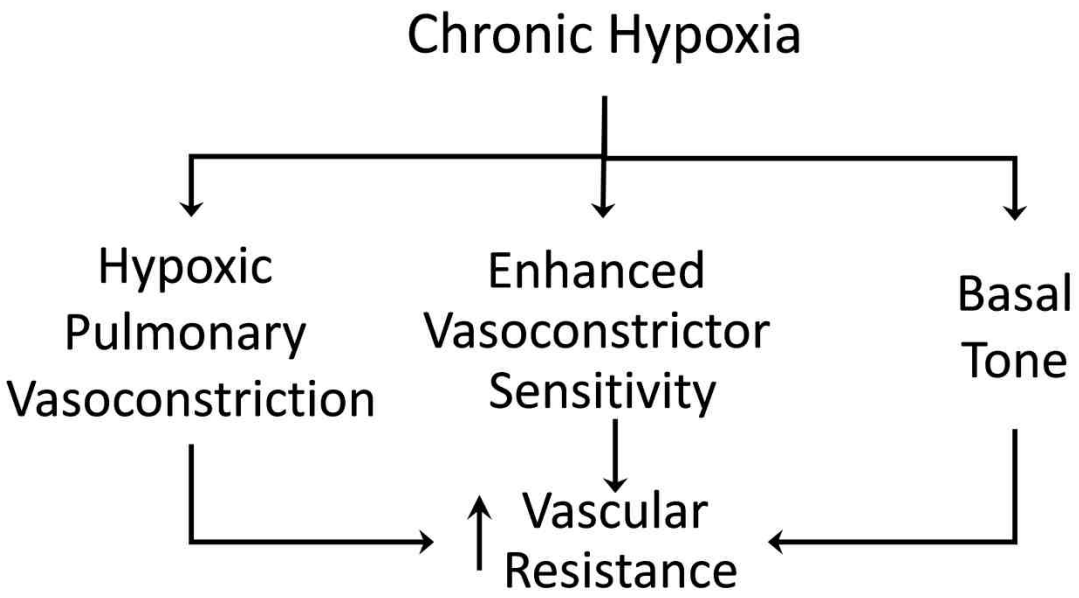

Figure 2. Schematic illistrating mechanisms of vasoconstriction following CH.

of the sarcoplasmic reticulum stores leading to further increases in cytosolic Ca^{2+} (110; 200). Stromal interaction molecule (STIM1) appears to be the Ca^{2+} sensor within the sarcoplasmic reticulum that couples store depletion to Ca^{2+}entry (53; 144). While the cellular players mediating this response are still being identified, roles for canonical transient receptor potential (TRPC) channels, Orai1, and acid sensing ion channels (ASIC) have been identified (104; 149; 268). SOCE contributes to enhanced vasoconstriction in CH rats with recognized functions for STIM1 (144) and ASIC (105; 183; 206) in this response.

Receptor-operated Ca^{2+} entry (ROCE) contributes to agonist-induced increases in $[Ca^{2+}]_i$. Diacylglycerol (DAG), produced by phospholipase C following G_q-coupled receptor stimulation, activates receptor-operated non-selective cation channels to mediate Ca^{2+} influx. While previous reports from our laboratory in Sprague Dawley rats demonstrate decreased SOCE and ROCE following CH (103), SOCE and ROCE are elevated in pulmonary hypertensive Wistar rats, mice and humans (76; 251; 285; 310).

Ca^{2+} Sensitization

In addition to increasing VSM $[Ca^{2+}]_i$, many stimuli can also increase the sensitivity of the contractile apparatus to Ca^{2+}. This is achieved by inhibition of myosin light chain phosphatase (MLCP). Active MLCP dephosphorylates the myosin light chain resulting in decreased myosin actin interaction. Agonists that are coupled to G_q receptors can lead to Ca^{2+} sensitization through PKC signaling

via increases in VSM $[Ca^{2+}]_i$ and DAG. PKC is a serine/threonine kinase that regulates both VSM proliferation and contractility (10; 19). PKC elicits Ca^{2+} sensitization through phosphorylation of CPI-17 (Thr 38) which subsequently inhibits the catalytic subunit of MLCP, PP1 (115; 118).

Rho kinase (ROK), another serine/threonine kinase, serves as an additional mechanism by which Ca^{2+} sensitization occurs. Binding of the small GTPase RhoA to the Rho binding domain of ROK causes a conformational change and activation of the kinase(255). ROK phosphorylates MLCP at two sites (Thr 696 and Thr 853) (114). Phosphorylation at Thr 697 inhibits MLCP activity, while phosphorylation at Thr 853 interferes with binding of myosin by the MYPT1 subunit (65).

CH increases both RhoA activity and ROK expression in pulmonary arteries (96; 108). This corroborates findings that chronic ROK inhibition prevents CH-induced PH (96). Studies by Nagaoka and colleagues showed that ROK is a significant contributor to enhanced pulmonary vascular resistance following CH (177). These studies demonstrated that acute administration of the ROK inhibitor drastically decreased pulmonary vascular resistance in CH rats and nearly normalized pressure to the level of the normotensive control animals (177). This group also demonstrated that acute inhalation of a ROK inhibitor decreases pulmonary arterial pressures in fawn-hooded rats which spontaneously develop PH and in rats with monocrotaline-induced PH (176). These studies, among others (96; 160), suggest that ROK contributes to the development of PH via enhanced vasoconstriction.

Hypoxic Pulmonary Vasoconstriction

Under normal physiological conditions hypoxic pulmonary vasoconstriction (HPV) occurs in response to alveolar hypoxia to direct blood flow away from poorly ventilated (as a result of airway constriction or obstruction) regions of the lungs. The vasoconstriction then diverts blood to the better ventilated areas of the lung matching perfusion to the level of alveolar ventilation. In the situation of chronic hypoxia or COPD, however, where all or most of the lung is hypoxic, this will lead to elevated pulmonary vascular resistance.

The HPV response has been divided into two phases, phase I and II. Phase I HPV appears to be intrinsic to the VSM as the response persists following endothelial disruption (130), and that isolated pulmonary arterial smooth muscle cells (PASMC) contract in response to acute exposure to hypoxia (152). Phase I HPV requires Ca^{2+}, and is comparatively short in duration.

There is currently some controversy as to how hypoxia is sensed. Both theories suggest that mitochondrial reactive oxygen species (ROS) are involved; however, while one theory suggests there is an increase in ROS, the other suggests that they are decreased. Archer and colleagues have proposed that pulmonary arteries have a tonic level of ROS production that is inhibited by decreased O_2 tension (165). This decrease in ROS is proposed to reduce the cytosol, inhibit K^+ channels, depolarize the VSM cell, activate L-type Ca^{2+} channels, ultimately resulting in contraction (296). Alternatively, an increase in PASMC mitochondrial ROS in response to hypoxia (215) is proposed to cause

Ca^{2+} release from the sarcoplasmic reticulum that activates store operated Ca^{2+} entry channels (228; 293) to mediate vasoconstriction. The second phase of HPV requires the endothelium and is mediated through Ca^{2+}sensitization (130; 227). Several laboratories have identified a role for endothelin-1 (ET-1) derived from the endothelium in this response (140; 235). Alternatively, a role for gap junctions has been proposed in phase II of HPV (119), supporting a role for coupling of the smooth muscle and endothelium. Additional findings support a role for conducted depolarization in the endothelium to elicit epoxyeicosatrienoic acid (EET) release and subsequent vasoconstriction to hypoxia (286).

Interestingly, prolonged exposure to hypoxia blunts the HPV response (159; 216). This attenuated response appears to be mediated by decreased K^+ channel expression and activity (216). While there is still some residual constriction to acute hypoxia following CH, these findings suggest that other mechanisms play a larger role in the elevated arterial tone observed following CH.

Enhanced Vasoconstrictor Sensitivity

The contractile state of the VSM can be influenced by hormones, neurotransmitters, and other paracrine agents. Many of these factors such as ET-1, uridine trisphosphate (UTP), and serotonin (5-HT) bind to G_q-coupled receptors. G_q-coupled signaling results in activation of phospholipase C (PLC) which cleaves phophatidylinositol 4,5-bisphosphate (PIP_2) into inositol trisphosphate (IP_3) and DAG. IP_3 binds to and activates IP_3 receptors on the

sarcoplasmic reticulum, resulting in increases in intracellular $[Ca^{2+}]_i$. The associated decrease in sarcoplasmic Ca^{2+} is further capable of mediating SOCE. DAG is capable of both activation of receptor-operated channels and increasing PKC activity both of which further lead to vasoconstriction. A role for ROK-induced Ca^{2+} sensitization has also been identified in pulmonary vasoconstriction to ET-1 (109).

Active vasoconstriction contributes to PH in humans (151; 170) and rats (192), as revealed by findings in both species that pulmonary arterial pressure decreases in response to acute vasodilator inhalation. It has been known for some time that agonist-induced pulmonary vasoconstriction is augmented in rodent models of PH, as it was demonstrated that isolated lungs from CH rats were hyper-responsive to agonists such as angiotensin and prostaglandin $F_{2\alpha}$ ($PGF_{2\alpha}$) (159). Later studies have demonstrated enhanced reactivity to U-46619, ET-1, 5-HT, and norepinepherine in pulmonary hypertensive animals (109; 207; 212; 290). ET_A and ET_B receptor expression is increased by hypoxia (132). CH also increases prepro ET-1 mRNA, as well as circulating levels of ET-1 (49), likely through regulation by HIF-1 (93). In addition to vasoconstriction, ET-1 signaling has also been shown to stimulate the growth of VSM cells (244; 303). Furthermore, ET-1 receptor inhibition has been shown to prevent hypoxic PH (196) and reverse established PH (49), suggesting that ET-1-induced vasoconstriction and vascular remodeling may contribute to CH-induced PH.

Membrane depolarization serves as a vasoconstrictor stimulus in arteries, including those in the pulmonary circulation. KCl-dependent pulmonary

vasoconstriction is augmented in isolated lungs from CH rats (26; 184). Interestingly, studies in isolated arteries suggest that this mechanism is dependent on Ca^{2+} sensitization as pulmonary arteries from CH rats demonstrate increased vasoconstriction to KCl despite a blunted Ca^{2+} response compared to arteries from control animals (26).

Development of Basal Tone

Pressure-dependent VSM tone was first characterized in the systemic circulation (14). The maintained arterial constriction in response to distending force exerted by increased intraluminal pressure serves as an autoregulatory mechanism allowing blood flow to remain relatively constant within small arteries across various intraluminal pressures (44). Within the pulmonary circulation, little evidence exists for pressure-dependent tone in the healthy normoxic circulation (262). However, following CH, pulmonary arteries develop basal tone (27; 177; 304). Our laboratory has found that ROK mediates pressure dependent tone in arteries from rats with CH-induced pulmonary hypertension (27).

REACTIVE OXYGENSPECIES

Endogenous reactive oxygen species (ROS) are important physiological second messenger molecules that regulate VSM phenotype (17; 261) and contractility (17) in the normal pulmonary circulation. ROS are produced in the endothelial, VSM, and adventitial cells of the blood vessel. Virtually all cell types within the vasculature are capable of producing both superoxide (O_2^-) and hydrogen peroxide (H_2O_2) (50; 155; 267). O_2^- is produced when an electron is

donated to molecular oxygen (O_2). Dismutation of O_2^- by superoxide dismutase (SOD) produces H_2O_2, a more stable ROS. While there is basal O_2^- production, constitutive activity of SOD keeps these levels low in the normotensive pulmonary circulation (302). The resultant H_2O_2 is eliminated by catalase, glutathione peroxidase, and peroxiredoxins, which convert H_2O_2 into H_2O and other metabolites (224).

ROS contribute to the development of PH (46; 60). Excessive ROS production has been implicated in both the vascular remodeling (98; 138) and vasoconstrictor responses (69; 109; 138) associated with CH-induced PH. ROS cause endothelial dysfunction (70; 313). One well known effect of O_2^- on vascular contractility arises from its affinity for nitric oxide (NO), which it rapidly scavenges to form the reactive nitrogen species peroxynitrite ($ONOO^-$) (233). Oxidative stress within the endothelium is also capable of oxidation of BH4, an essential cofactor for endothelial nitric oxide synthase (eNOS), leading to eNOS uncoupling that diminishes NO production and increases O_2^- production (133). This diminished NO bioavailability impairs endothelium-dependent dilation that can be restored by treatment with antioxidants (55; 289). The free radical O_2^- hasalsobeen linked to Ca^{2+} sensitization and vasoconstriction in VSM of pulmonary arteries (122). H_2O_2, conversely, has been shown to have both vasodilator and vasoconstrictor properties in the pulmonary circulation (30; 136).

Alterations in superoxide dismutase (SOD) levels may also contribute to the elevated ROS observed following CH. SOD is an enzyme that catalyzes the conversion of O_2^- to H_2O_2. There are three isoforms of SOD, with SOD1 located

in the cytoplasm, SOD2 in the mitochondria, and SOD3 in the extracellular space.SOD1 and 3 utilize copper and zinc as cofactors, whereas SOD2, the mitochondrial enzyme, has manganese in its reactive center. Many forms of pulmonary hypertension are associated with dysfunction of SOD (6; 48; 68; 112; 188; 206; 214). Indeed levels of SOD1 and SOD3 are reduced in both rodent and piglet models of pulmonary hypertension (48; 68; 206), while reduced SOD2 expression has been observed in fawn hooded rats and humans with idiopathic pulmonary hypertension (Group I) (6; 237). Reductions in SOD activity exacerbate increases in ROS production from enzymatic sources and may facilitate basal tone and enhanced vasoconstriction following CH. Changes in the regulation of H_2O_2 degradation in animal models of PH also has the potential to regulate pulmonary arterial ROS levels (206).

Hypoxia has been demonstrated to increase pulmonary arterial ROS levels (116; 287). An increase in vasoconstrictor reactivity is associated with this increase in ROS in pulmonary hypertensive piglets, and the source of ROS in this setting appears to be NADPH oxidase (NOX) (69). O_2^--dependent RhoA activation also contributes to enhanced pulmonary vasoconstrictor reactivity following CH though Ca^{2+} sensitization mechanisms (26; 109). While the ROS species contributing to this response appears to be O_2^-, the vascular source of this factor has not yet been identified (Fig. 3). However, experiments demonstrating increased vasoreactivity to KCl and ET-1 in endothelium-disrupted pulmonary arteries suggest that endothelial sources of ROS, such as uncoupled eNOS, do not directly contribute to this response (26; 109; 184).

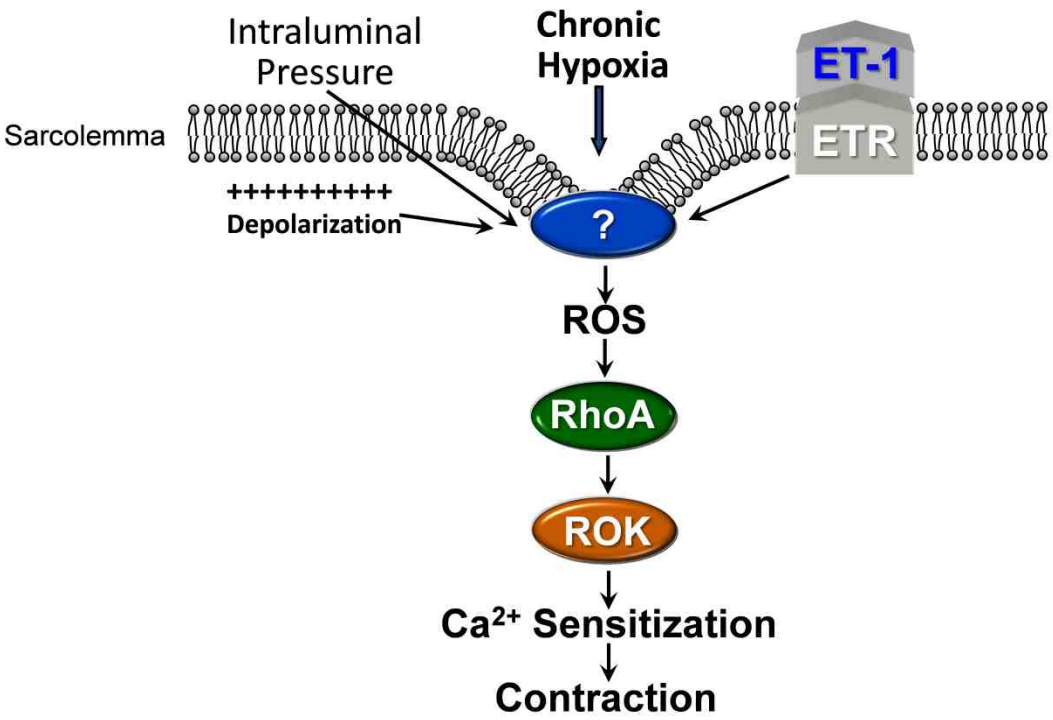

Figure 3. Increases in intraluminal pressure, membrane depolarization, and ETR signaling lead to ROK-dependent Ca^{2+} sensitization in pulmonary VSM.

Enzymatic Sources of ROS

One source of ROS within the vasculature is NOX. NOX isoforms are the only enzymes whose primary function is the production of ROS. NOX subtypes 1, 2, and 4 are the most abundant forms in VSM (153), and they are a major source of O_2^- in the smooth muscle and endothelium (169). The catalytic subunits of NOX 1 and 2 are activated by phosphorylation of the cytosolic subunits NOXO1 and NOXA1 in the case of NOX 1, and $p47^{phox}$ and $p67^{phox}$ in the case of NOX 2 (Fig. 4) (21; 38; 153). A small GTP-binding protein, Rac1, is also a critical signaling mediator of both NOX 1 and 2 signaling (21; 38). NOX 4 does not contain the cytosolic regulatory subunits of NOX 1 and 2 (21; 38).

Alterations in NOX expression and function have been identified in multiple forms of PH. CH increases expression of NOX 4 in pulmonary arteries (168), whereas NOX 2 has been shown to contribute to the development of CH-induced PH in mice (138). Furthermore, Rac1 and $p47^{phox}$ expression are elevated in lungs from pulmonary hypertensive lambs (81).

Another source of vascular ROS is the mitochondria. Under normal physiological conditions, the mitochondria convert up to 5% of molecular oxygen to O_2^- (199). Generally mitochondrial ROS are buffered by antioxidants such as SOD2 (64). However, pulmonary hypertensive chickens have increased ROS production mediated by dysfunction of mitochondrial complexes I and III (97). Preliminary findings from our laboratory support a role for mitochondrial ROS in the development of intermittent hypoxia-induced PH (253).

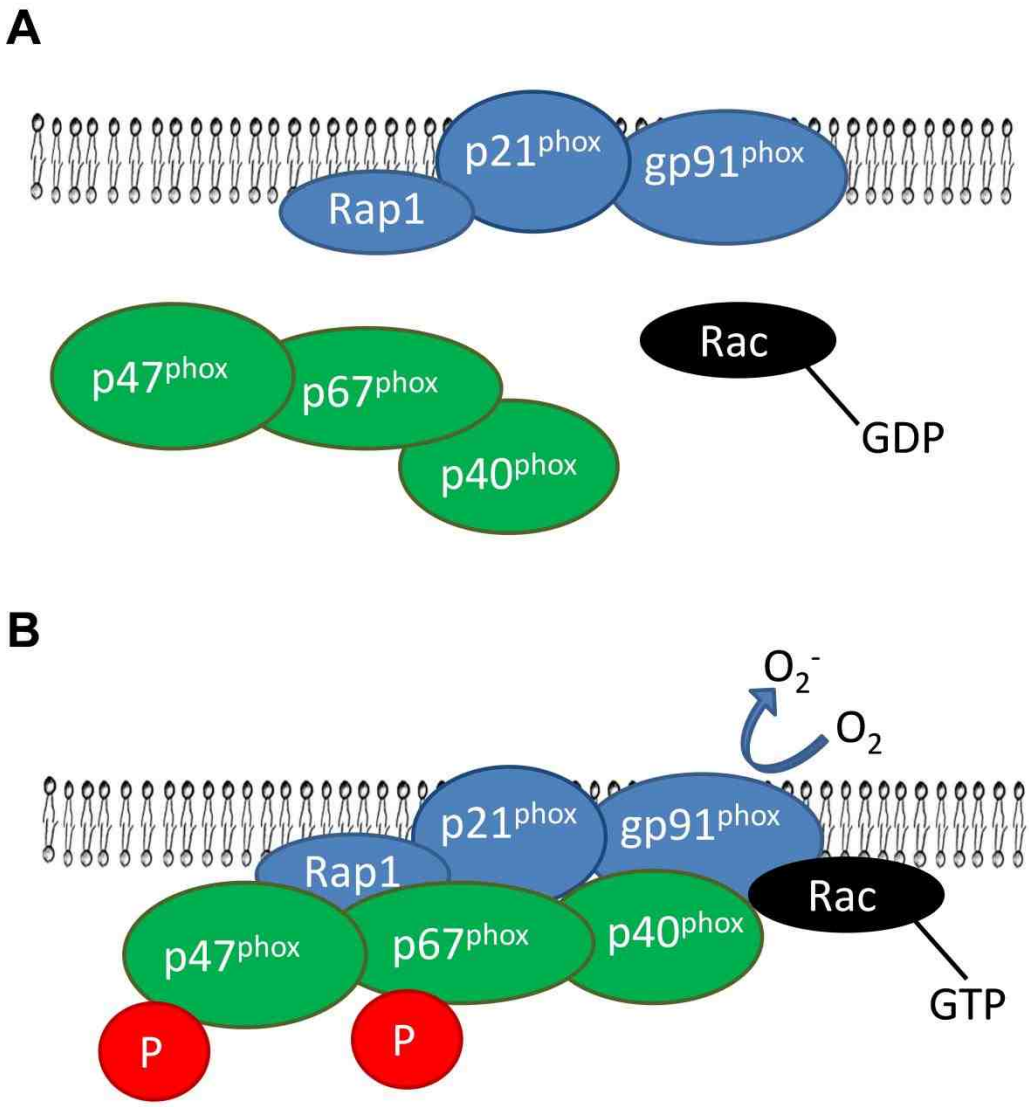

Figure 4. Schematic of NADPH oxidase 2 components including membrane components Rap1, $p21^{phox}$, and $gp91^{phox}$, cytosolic subunits $p47^{phox}$, $p67^{phox}$, and $p40^{phox}$, and Rac1 in inactive (A) and active (B) states.

Xanthine oxidase (XO) is an additional source of ROS within the vasculature. It is an enzyme that catalyzes oxidative hydroxylation of purine substrates and generates O_2^-. XO can be activated by hypoxia in cultured PASMCs (88). Additional studies found that hypoxia increases lung XO activity and that treatment of rats with allopurinol, a XO inhibitor, blunts CH-induced PH and associated pulmonary vascular remodeling (91).

Interestingly, membrane depolarization and membrane stretch may activate NOX in macula densa (142) and endothelial cells (32; 158; 254), whereas G-protein-coupled receptor (GPCR) stimulation in the systemic circulation can result in vasoconstriction via NOX (180). Therefore, NOX enzymes serve as likely candidates for ROS production following depolarization, membrane stretch, and ET-1 receptor (ETR) signaling in the hypertensive pulmonary circulation.

EPIDERMAL GROWTH FACTOR RECEPTOR

The epidermal growth factor receptor (EGFR) plays a role in the development of monocrotaline-induced PH in rats (42; 162) and mediates PH in mice that overexpress transforming growth factor (TGF)-α (129). EGFR is a 1186-amino acid growth factor receptor that is primarily stimulated by the ligands EGF and TGF-α and is involved in growth and proliferation (297; 319). It is well established that upon ligand binding to EGFR there is an increase in receptor dimerization and autophosphorylation of the tyrosine 845 residues followed by enzyme activation (306; 307). This is associated with migration of EGFR from lipid domains in the plasma membrane to the general membrane component

(166). EGFR activation is also characterized by phosphorylation on the tyrosine1068 residue (13; 74).

EGFR is an upstream activator of NOX and Rac 1 in glomerular mesangial cells (314) and of RhoA in renal tubule epithelial cells (111). Interestingly, depolarization can activate EGFR in both PC12 cell and cardiomyocytes (56; 270; 318). EGFR also contributes to the development of myogenic tone in the systemic circulation (5), suggesting that it could play a role in the mediation of pressure-dependent basal tone following CH. Additionally, EGFR signaling has been implicated in systemic vasoconstriction to agonists such as angiotensin II (15), phenylepherine (87; 281), and enhanced pulmonary vasoconstriction to KCl (184).

SRC FAMILY KINASES

Src family kinases are potential candidates for mediating EGFR activation following CH. They are a group of 9 kinases characterized by its prototypical member c-Src. As intracellular proteins with no known ability to detect changes in the extracellular milieu, activation of Src family kinases is regulated by other cell surface receptors (23; 35; 148; 205; 223; 250). Many cellular processes are regulated by Src family kinases, including focal adhesion formation, migration, cell cycle progression, apoptosis, differentiation, and gene transcription (3; 25; 275). Growth factor receptors are key initiators of Src kinase signaling (23; 25). Additionally, focal adhesion kinases can interact with Src family kinases where they play an essential role in events resulting from activation of integrins (205; 223). Activation of Src kinases is achieved through protein-protein interactions

involving the phosphotyrosine binding Src homology domain 2 (SH2) and SH3 regions (20; 39; 175). Phosphorylation of the tyrosine 416 residue also contributes to kinase activation (232).

Src family kinases can be activated by an array of GPCRs (35; 125; 148; 250). Some data point to a direct interaction between Src and Gα subunits (150). Many GPCRs contain SH3 binding motifs (137), and other data indicate a role for GPCR phosphorylation in this response (62). Src family kinases couple membrane stretch to Rac1 and NOX signaling through EGFR-dependent mechanisms in mesangial cells (314). Additionally, NOX1 is involved in angiotensin II-mediated hypertension in the systemic circulation (157). These findings make Src kinases a prime candidate for coupling depolarization, membrane stretch, and ETR receptor stimulation to EGFR-dependent NOX activation and ROS production following CH (184).

Src kinases can activate EGFR either directly (18; 236; 263) or through matrix metalloproteinases (87; 146; 190; 234). Src can directly phosphorylate EGFR on two residues, Tyr-1101 and Tyr-845 (18). However, Src dependent ligand cleaving can also result in EGFR activation. The best characterized mechanism of EGFR activation in through a process known as ectodomain shedding (208). The principle ligands of EGFR are synthesized as precursor molecules that can be proteolyzed to produce soluble ligands. The primary classes of molecules implicated in this response are matrix metalloproteinases and ADAMs (a disintegrin and a metalloproteinase) (7; 82; 208).

MATRIX METALLOPROTEINASES

Matrix metalloproteinases (MMPs) are a class of zinc-dependent enzymes (193). They are involved in the degradation of numerous extracellular proteins, but can additionally produce bioactive ligands (229; 259). MMPs can be regulated by tissue inhibitors of metalloproteinases (TIMPs). TIMPs 1-4 have been identified mammals (22). TIMPs are capable of inhibiting all MMPs except for MMP14 (300).

Alterations in MMP expression have been detected in numerous forms of PH (72; 89; 156; 241; 242), although the general trend is for increased expression. Findings by Lepetitet. al. show increased MMP2 activity and decreased MMP3 expression in arteries from patients with idiopathic PH (131). Consistent with this result, increased MMP2 and 9 expression and activity were observed in rats with monocrotaline- and hypoxia-induced PH (72; 124; 240; 284). Endothelial (240), VSM (213; 226), and adventitial fibroblast (167) cells are all capable of MMP production in a variety of vascular beds. Interestingly, MMP2 production in pulmonary arterial fibroblasts can be increased by hypoxia (167), and maternal hypoxia increases MMP2 and MMP9 activity in neonatal rat brains (276). Additional MMPs may be secreted by immune cells within the vasculature (294).

Some of the best characterized roles for MMPs in the pulmonary vasculature are growth and angiogenesis (283). Members of the gelatinase family (due to their ability to degrade gelatin), particularly MMPs 2 and 9, are critical for sprouting angiogenesis (283). MMPs are capable of regulation of

proliferation, migration, and apoptosis of endothelial cells and VSMCs (211; 283; 311).

While little is known about the role of MMPs in pulmonary vasoconstriction, several isoforms have been implicated in systemic vasoconstriction. Agonist-induced activation of MMP-7 contributes to EGFR-dependent vasoconstriction in the mesenteric circulation of Sprague-Dawley rats (87). MMPs 2 and 9 have been shown to be involved in EGFR transactivation and myogenic tone in the murine circulation (146), while MMP 2 has been implicated in the development of angiotensin II-induced hypertension (189). Interestingly, Src kinases can activate both of these MMPs in T cells (243).

ADAMs area family of metalloproteases that are closely related to MMPs. EGF cleaved by ADAM-17 contributes to cell proliferation of cancer cells and angiogenesis (195). Intriguingly, ADAM-17 has also been shown to be critical mediator of angiotensin II-induced EGFR activation in aortic VSM and hepatic stem cells (190; 191), and has additionally been linked to ET-1 receptor signaling (234). Additionally, while regulation of ADAM-17 expression can be regulated by HIF in synovial cells (31), very little is known about the role of these proteins in PH.

RATIONALE AND SPECIFIC AIMS

Pulmonary vascular dysfunction resulting from CH leads to increased pulmonary vascular resistance and PH in patients with COPD and in residents at high altitude. It is widely considered that pulmonary arterial constriction is central

to this disease process. Vasoconstrictor responses to CH are multifaceted, including acute hypoxic pulmonary vasoconstriction, elevated basal tone, and enhanced vasoconstrictor reactivity to both membrane depolarizing stimuli and many receptor-mediated agonists. Studies from our laboratory have revealed a prominent role for RhoA-mediated myofilament Ca^{2+} sensitization in each of these vasoconstrictor components (26; 27; 109). However, the mechanisms that link vascular smooth muscle (VSM) stretch, vasoconstrictor receptors, and membrane depolarization to RhoA-dependent vasoconstriction in the hypertensive pulmonary circulation are largely unknown. Our lack of knowledge regarding mechanisms by which CH mediates pulmonary VSM contraction is an important problem, because without it, we are unlikely to understand the significance of the relevant signaling pathways to the etiology of PH or to develop effective treatments and preventative measures for this condition. Therefore, the overall objective of this study was to determine mechanisms by which CH imparts pulmonary basal tone and augmented receptor-mediated vasoconstriction. We have previously reported that enhanced agonist- and depolarization-induced VSM Ca^{2+} sensitization following CH is mediated by ROS (26; 109). Furthermore, CH leads to greater pressure-dependent depolarization and vasoconstriction compared to small pulmonary arteries from control rats (26; 184). However, whether membrane depolarization-induced ROS generation contributes to elevated basal tone and vasoconstriction in hypertensive pulmonary arteries had not been previously established. Experiments showing that NOX 2 knockout mice do not develop PH (138) suggest that NOX 2 could be

the source or ROS mediating the studied responses. Furthermore, EGFR and Src kinases have been implicated in stretch-dependent NOX activation in mesangial cells (179; 314) providing the rationale for the investigation of these two proteins in the studied responses. Therefore, our studies investigated the **central hypothesis that chronic hypoxia confers basal pulmonary arterial tone and augmented depolarization-induced and receptor-dependent vasoconstriction through Src/EGFR/NOX 2 signaling and myofilament Ca^{2+} sensitization.** We tested this hypothesis by addressing the following specific aims:

Specific Aim 1.

Establish the contribution of NOX 2 signaling to enhanced pulmonary arterial vasoconstrictor reactivity following CH.

Hypothesis and Approach.

We hypothesized that CH imparts basal tone and enhances depolarization-induced and ET-1-dependent vasoconstriction in small pulmonary arteries through NOX 2-mediated myofilament Ca^{2+} sensitization. Protocols for this study employed isolated, pressurized small pulmonary arteries (100-200 μm ID) from control and CH rats using a preparation that allows simultaneous measurement of ID and vessel wall $[Ca^{2+}]_i$ or ROS production at physiological intraluminal pressures. To minimize complicating influences of the endothelium, all experiments were conducted in vessels disrupted of endothelium. These experiments were performed in the presence and absence of NOX 2 and Rac1

inhibition. NOX 2 expression and Rac1 activity were also measured in pulmonary arteries.

Specific Aim 2.

Identify the role of EGFR and Src kinase signaling in augmented pulmonary vasoconstrictor reactivity following CH

Hypothesis and Approach.

We hypothesized that CH-dependent basal tone and enhanced depolarization-induced and ET-1-mediated vasoconstriction require Src/EGFR signaling. Experiments in this aim were designed to address the contribution of EGFR and Src to enhanced vasoconstrictor reactivity and ROS production in isolated small pulmonary arteries following CH and determine the effects of Src and EGFR inhibition on Rac1 activation. We further tested a role for MMPs in enhanced vasoconstriction to ET-1. Additional experiments examined the contribution of EGFR to the development of PH by measuring right ventricular pressure, right ventricular hypertrophy, and vascular remodeling in animals treated chronically with an EGFR inhibitor or its vehicle.

Specific Aim 3.

Assess the contribution of pressure-dependent and ET-1-induced membrane depolarization to augmented pulmonary vasoconstrictor reactivity following CH.

Hypothesis and Approach.

Pulmonary VSM is depolarized in arteries from CH rats compared to controls. As previously stated, while membrane depolarization can activate L-

type Ca^{2+} channels and lead to constriction, we have observed a direct effect of membrane depolarization to lead to Ca^{2+} sensitization, independent from L-type channel activation that occurs in arteries from CH rats (27). Increases in intraluminal pressure (likely through stretch-activated cation channels in pulmonary VSM) and ET-1 receptor stimulation can result in pulmonary VSM membrane depolarization (179; 248). We hypothesized that CH increases vasoconstrictor responsiveness by coupling stretch and ET-1-mediated VSM membrane depolarization to myofilament Ca^{2+} sensitization. Protocols for this aim assessed arterial diameter, vessel wall $[Ca^{2+}]_i$, and membrane potential in the presence and absence of the potassium ionophore valinomycin to clamp membrane potential in order to determine the contribution of depolarization to enhanced vasoconstrictor reactivity in arteries from CH rats. The ability of membrane depolarization to mediate vasoconstriction to ET-1 was tested in a similar manner.

Chapter 2 – Methods

GENERAL METHODS

Experimental Groups and Chronic Hypoxic Exposure Protocol

Male Sprague Dawley rats (Harlan Industries, ~300-380g) were used for all studies. CH rats were housed in hypobaric chambers maintained at a pressure of ~380 mmHg for four weeks (27; 109; 179; 220). Age matched control rats were housed in an adjacent room at ambient pressure (~630 mmHg in Albuquerque, NM). All animals were maintained on a 12:12-h light-dark cycle. All protocols employed in this study were reviewed and approved by the Institutional Animal Care and Use Committee of the University of New Mexico School of Medicine (Albuquerque, NM).

Indices of Pulmonary Hypertension

Right Ventricular Hypertrophy and Polycythemia

Right ventricular hypertrophy was assessed as an index of PH as described previously (217; 220). After isolation of the heart, the atria and major vessels were removed from the ventricles. The right ventricle (RV) was then separated from the left ventricle and septum (LV + S). The sections of the heart were then weighed and Fulton's index (RV/LV+S) was used to assess the degree of right ventricular hypertrophy. Polycythemia was assessed by measuring hematocrit (%) from blood collected in microcapillary tubes following direct cardiac puncture.

Right Ventricular Pressure

Right ventricular systolic pressure (RVSP) was measured as an index of pulmonary arterial pressure in anesthetized rats (2% isoflurane and 98% O_2 gas mixture). An upper transverse laparotomy was performed to expose the diaphragm. A 25-gauge needle, connected to a pressure transducer (model P23 XL, Spectramed), was inserted into the RV via a closed-chest transdiaphragmatic approach, and the transducer output amplified by a Harvard Instruments amplifier. All data were recorded, and heart rate was calculated with a computer-based data-acquisition system (AT-CODAS, DATAQ Instruments).

Arterial Wall Thickness

Following assessment of right ventricular pressures, lungs were fixed similar to experiments our laboratory has performed previously (217; 218). After a median sternotomy, heparin (100 U in 0.1 ml) was injected directly into the right ventricle. The pulmonary artery was then cannulated with a 13-gauge needle stub, and the trachea was cannulated with a 17 gauge needle stub. The preparation was immediately perfused at 0.8 ml/min by a Masterflex microprocessor pump drive (model 7524-10) with physiological saline solution (PSS) containing (in mM) 129.8 NaCl, 5.4 KCl, 0.5 NaH_2PO_4, 0.83 $MgSO_4$, 19 $NaHCO_3$, 1.8 $CaCl_2$, and 5.5 glucose with 4% bovine serum albumin (wt/vol) added as a colloid. Papaverine (10^{-4} M) was also included in the PSS to maintain the vasculature in a dilated state during subsequent fixation. The left ventricle was cannulated with a plastic tube (4 mm outer diameter). The perfusion rate was gradually increased to 60 $ml \cdot min^{-1} \cdot kg$ body wt^{-1}. Perfusate was pumped

through a water-jacketed bubble trap maintained at 38°C before entering the pulmonary circulation. Experiments were performed with lungs in zone three conditions, achieved by elevating the perfusate reservoir until venous pressure (Pv) was ~12 mmHg. Previous work from our laboratory suggests that maximal recruitment and thus maximal vascular surface area is achieved at this flow and Pv(57). The vasculature was initially washed with 250 ml of PSS, followed by 250 ml of fixative (0.1 M phosphate-buffered saline with 4% paraformaldehyde, 0.1% gluteraldehyde, and 10^{-4} M papaverine). Lungs were additionally inflated with fixative via the trachea to a pressure of 25 cm H_2O during perfusion. The trachea was ligated with 2-0 silk, the arterial and venous lines simultaneously clamped, and the lungs immersed in fixative. A transverse section (2–3 mm thick) of tissue from the left lobe was removed and rinsed in phosphate-buffered saline. Sections were dehydrated in increasing concentrations of ethanol, cleared in xylene, and mounted in paraffin.

Transverse sections of the left lung were cut (4 μm thick) and mounted onto Superfrost Plus slides (Fisher Scientific). Sections were stained for elastin (Sigma Accustain Elastic Stain kit), and arteries were identified by the presence of an internal elastic lamina(217; 219). Vessels were examined with a ×40 objective on a Nikon Optiphot microscope, and images were generated with a digital charge-coupled device camera (Photometrics CoolSNAP) and processed with MetaMorph software (Universal Imaging). Measurements were performed on 16-51 arteries (<50 μm inner diameter) and 4–25 arteries (50–100 μm diameter) per rat from 5 rats/group. These measurements assessed from the outer margin

of the external elastic lamina, and luminal (80) diameter and were made using a blinded analysis. External and internal arterial diameters were calculated from the medial the medial and luminal circumferences, respectively. Arterial wall thickness was assessed by subtracting luminal radius from external radius and expressed as a percentage of external diameter according to the following formula:

[(2X wall thickness)/external diameter] X 100

Additional lung sections were prepared to examine changes in the number of fully and partially muscularized arteries (183). Sections were incubated with rabbit anti-smooth muscle α-actin (1:200, Abcam) overnight at 4°C. Smooth muscle α-actin was detected by incubating the slides with DyLight 549-donkey anti-rabbit (1:400, 3.5 h, Jackson ImmunoResearch). Twenty images from the right and left lobes were randomly collected per animal using a ×20 objective on a confocal microscope (TCS SP5, Leica). Numbers of fully and partially muscularized arteries were counted per animal.

Isolation of Small Pulmonary Arteries

Rats were anesthetized with pentobarbital sodium (200 mg/kg ip), and the heart and lungs were exposed by midline thoracotomy. The heart and left lung were removed and immediately placed in cold PSS. A 4th or 5th order intrapulmonary artery [~150 μm inner diameter (ID)] without side branches, approximately ~1mm in length, was dissected free from the lung parenchyma and transferred to a Living Systems vessel chamber. The proximal end of the

artery was cannulated with a tapered glass pipette and held in place by a single strand of silk ligature. The artery was then gently flushed with PSS to remove blood from the lumen and a strand of moose mane was inserted into the distal end of the artery to disrupt the endothelium. Endothelial disruption allows for the focus on VSM function independent of endothelial influences. The distal end of the artery was then cannulated and pressurized to 12 mmHg with a servo-controlled peristaltic pump (Living Systems). The absence of vessel leakage was confirmed by turning off the servo-control function and ensuring the vessel maintained pressure. All vessels with apparent leaks were discarded (26; 27; 109).

Measurement of Vessel Diameter

Isolated, cannulated pressurized vessels were transferred to the stage of a Nikon Eclipse TS100 microscope for measurement of changes in vessel diameter (Fig. 5). This setup allows for assessment of VSM function independent of circulating factors, innervation, or shear stress. The preparation was superfused with PSS equilibrated with a 10% O_2, 6%, CO_2, and balance N_2 gas mixture and maintained at 37 °C. A vessel chamber cover was position to allow this same gas mixture to flow over the top of the vessel chamber bath. An Imaging Source camera was used to obtain bright-field images of the vessels and dimensional analysis was performed by IonOptix software to measure ID by edge detection. A viability check was performed to by constriction to 5 µM UTP as previously reported (27; 109). Endothelial disruption was confirmed by lack of a vasodilatory response to 1 µM acetylcholine (ACh).

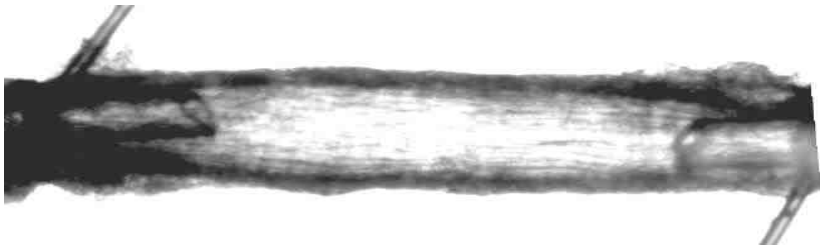

Figure 5: Representative image of isolated pulmonary artery from a CH rat.

To directly assess mechanisms of myofilament Ca^{2+} sensitization independent of changes in vessel wall $[Ca^{2+}]_i$, we clamped $[Ca^{2+}]_i$ in some arteries by permeabilizing with the Ca^{2+} ionophore, ionomycin (3 μM, Sigma), as previously described(109). All Ca^{2+} permeabilized vessels were equilibrated with PSS containing a calculated free Ca^{2+} concentration of 300 nM. This concentration of Ca^{2+} was chosen to provide optimal vasoreactivity to KCl while having minimal effects on resting tone based on preliminary studies.

Measurement of Vessel Wall $[Ca^{2+}]_i$

Pressurized arteries (Fig. 5) were loaded abluminally with the ratiometric, Ca^{2+} sensitive, fluorescent indicator fura-2 AM (Molecular Probes) as previously described (27; 103; 107; 108; 184; 185; 251). Prior to loading, fura-2 AM (1mM in anhydrous DMSO) was mixed 2:1 with a 20% solution of pluronic acid (Invitrogen). This mixture was diluted in PSS, resulting in a final concentrationof2 μM fura-2 AM and 0.05% pluronic acid. Arteries were incubated in this solution for 45 minutes at room temperature while being equilibrated with a 10% O_2 gas mixture. Subsequently, vessels were rinsed for 20 minutes with aerated PSS (37 °C) to wash out excess dye and facilitate hydrolysis of AM groups by intracellular esterases. Fura-2-loaded vessels excited alternatively at 340 and 380 nm with an IonOptix Hyperswitch dual excitation light source, and the respective 510 nm emissions we collected by a photomultiplier tube. Background-subtracted 340/380 emission ratios were calculated with IonOptix Ion Wizard Software and recorded simultaneously with ID measurements (described above) throughout the experiment.

Measurement of DHE Fluorescence in Pulmonary Arteries

Fluorescence detection of dihydroethidium (DHE; Molecular Probes) oxidation was used as a measure of O_2^-levels in pressurized, endothelium-disrupted, Ca^{2+}-permeabilized arteries from control and CH rats, as reported previously (26; 109; 184; 185). Cells are permeable to DHE, which is converted to the fluorescent products ethidium and 2-hydroxyethidium in an O_2^--dependent manner (315). Arteries were prepared for experimentation as described above and transferred to the stage of a Nikon Diaphot microscope. After 30 min of equilibration, arteries were loaded with DHE (10 μM DHE and 0.05% pluronic acid). Vessels were incubated in this solution for 30 min at room temperature in the dark and then rinsed for 5 min with PSS (37°C) to wash out excess dye. Fluorescent images were obtained using a standard tetramethyl-rhodamineisothiocyanate (TRITC, excitation ~550 nm and emission ~600 nm) filter before (for background subtraction) and after loading the vessel with DHE. Images (1 per minute) were generated with a charge-coupled device camera (PhotometricsSenSys 1400) and processed with MetaFluorsoftware (Molecular Devices). Normalized fluorescence intensity is defined as average gray-scale values for all pixels in the field above background.

Membrane Potential Measurement

Small pulmonary arteries prepared as described above were used to measure VSM membrane potential. Arteries were maintained at 12 mmHg unless otherwise stated. VSM cells were impaled with microelectrodes (50- to 100-MΩ tip resistance) containing 3 M KCl from the adventitial surface.

Membrane potential was recorded with a Neuroprobe amplifier (model 1600, A-M Systems). Analog output from the amplifier was low-pass filtered at 1 kHz and sent to a Tektronix RM502A oscilloscope and Dataq data acquisition system. Membrane potential recordings used for analysis contained 1) a sharp negative deflection in potential and the microelectrode was advanced into the cell, 2) a stable E_m for at least 30 seconds, and 3) an abrupt return to ~0 mV following retraction of the electrode from the cell. Movement of vessels in response to changes in pressure and KCl or ET-1 stimulation prevented the acquisition of continuous recordings from the same cell. Therefore membrane potential was recorded in several (4-6) cells under both baseline conditions and in response to stimulation. The mean membrane potential of all VSM cells recorded from a single artery under each set of conditions were averaged into a single n for statistical purposes (179; 184).

Measurement of DHE Fluorescence in Isolated PASMCs

Pulmonary arterial smooth muscle cells (PASMC) were isolated from arteries from CH and control rats treated with papain (9.5 U/mL, Sigma), collagenase (1750 U/mL, Sigma), and dithiothreitol (1 mM, Sigma) in reduced Ca^{2+} HBSS at 37 °C for 30 min. The cell suspension was placed on glass cover slips and cultured for 3-4 days in Ham's F-12 media with 5% fetal bovine serum and 1% penicillin streptomycin in a humidified incubator in an atmosphere of 5% CO_2-95% air at 37 °C. PASMC were treated with HEPES PSS containing ET-1 (10^{-8} M), ET-1+AG1478 (EGFR inhibitor), or vehicle conditions to determine the role of EGFR in ET-1-stimulated O_2^- production. Cells were then treated with the

fluorescent O_2^- indicator DHE (5 μM in 0.05% pluronic acid, Molecular Probes) and the nuclear stain TO-PRO®-3 (1:2,000, Molecular Probes) for 15 minutes at 37 °C and subsequently fixed in 2% paraformaldehyde (206). Fluorescent images were acquired with a 63X objective on a Leica confocal microscope. Mean fluorescence intensity was averaged from 5 images/animal. Each image was thresholded using ImageJ (NIH) to select for positively stained areas above background (cells not treated with DHE).

Western Blotting

Pulmonary arteries collected from the entire pulmonary arterial tree were dissected in ice-cold HEPES-PSS and snap frozen in liquid N_2. Samples were homogenized in 10 mM Tris-HCl containing 255 mM sucrose, 2 mM EDTA, 12 μM leupeptin, 4 μM pepstatin A, 1 μM aprotinin (Sigma) and centrifuged at 10,000 *g* at 4°C to remove insoluble debris, following which the supernatant was collected. Pulmonary artery lysates were separated by SDS-PAGE (Tris·HCl gels, Bio-Rad) and transferred to polyvinylidenedifluoride membranes. Blots were blocked for 1 hr at RT with 5% milk and 0.05% Tween 20 (Bio-Rad) in Tris-buffered saline (TBS) containing 10 mM Tris-HCl and 50 mM NaCl (pH 7.5). Primary antibodies were incubated overnight. Some blots were labeled by chemiluminescence (ECL, Pierce Thermo Scientific) and bands were detected by exposing the blots to chemiluminescence-sensitive film (KODAK). These blots were normalized to total protein as assessed by Coomassie staining. Other blots were incubated with a fluorescent secondary antibody and then imaged on an

Odyssey fluorescent imaging system (LI-COR). Total protein expression was normalized to the level of β-actin. Bands were quantified using ImageJ.

Calculations and Statistics

All data are expressed as means ± SE. Values of *n* refer to number of animals in each group. A *t*-test, one-way ANOVA, two-way ANOVA, or repeated measures ANOVA was used to make comparisons when appropriate. If differences were detected by ANOVA, individual groups were compared with the Student-Newman-Keuls or Bonferroni test. A probability of $P < 0.05$ was considered significant for all comparisons.

PROTOCOLS FOR SPECIFICAIM 1

Establish the contribution of NOX 2 signaling to enhanced pulmonary arterial vasoconstrictor reactivity following CH.

<u>Protocol Series 1.1:</u> Role of NOX 2 in depolarization-induced vasoconstriction following CH.

Vessel ID and vessel wall $[Ca^{2+}]_i$ were measured in response to increasing depolarizing concentrations of KCl (30-120 mM KCl) in small, endothelium disrupted, pulmonary arteries from CH and control rats as described above (26; 184). Some vessels were permeabilized to Ca^{2+} in order to focus on the Ca^{2+} sensitization component of the vasoconstriction response. We confirmed that arteries were Ca^{2+} permeabilized by loading arteries with fura-2AM and measuring vessel wall $[Ca^{2+}]_i$. Experiments were performed in the presence of the NOX inhibitors apocynin (30 μM, Sigma) (261) and DPI (10 μM, Sigma) (301) in addition to the specific NOX2 inhibitor gp91ds-tat or its scrambled control

peptide (50 μM, Tufts) (221; 222) (Fig. 6). We confirmed that gp91ds-tat did not alter membrane potential with sharp electrode measurements. These experiments were repeated in arteries pretreated with the Rac1 inhibitor NSC23766 (50 μM, Cayman) (143) or vehicle to identify the contribution of the NOX2 accessory protein, Rac1, to depolarization-dependent vasoconstriction and ROS production following CH. NSC23766 was chosen for its selectivity for Rac1 over other members of the Ras family, particularly RhoA. To further characterize the ROS species mediating this response, vasoconstrictor responses to KCl were assessed in arteries from CH and control rats in the presence of polyethylene glycol (PEG)-SOD (120 U / mL, Sigma) (70), PEG-catalase (250 U / mL, Sigma) (48), or vehicle.

In parallel protocols, we determined effects of NOX inhibition on depolarization-induced O_2^- generation in isolated arteries from CH and control rats using the fluorescent indicator dihydroethidium (DHE) (17). We conducted these experiments in the presence of apocynin, gp91ds-tat, NSC23766 or their respective vehicles to determine the contribution of NOX 2 and Rac1 in mediating increased depolarization-induced ROS production in pulmonary arteries from CH rats. To determine the effect of depolarization on Rac1 activity and expression, western blots were performed on homogenatesofCa^{2+} permeabilized intrapulmonary arteries from CH and control rats stimulated with 60 mM KCl or vehicle. Using a GTP-pulldown assay (Cytoskeleton) (314), GTP bound Rac1 (indicative of activation) was normalized to total Rac1.

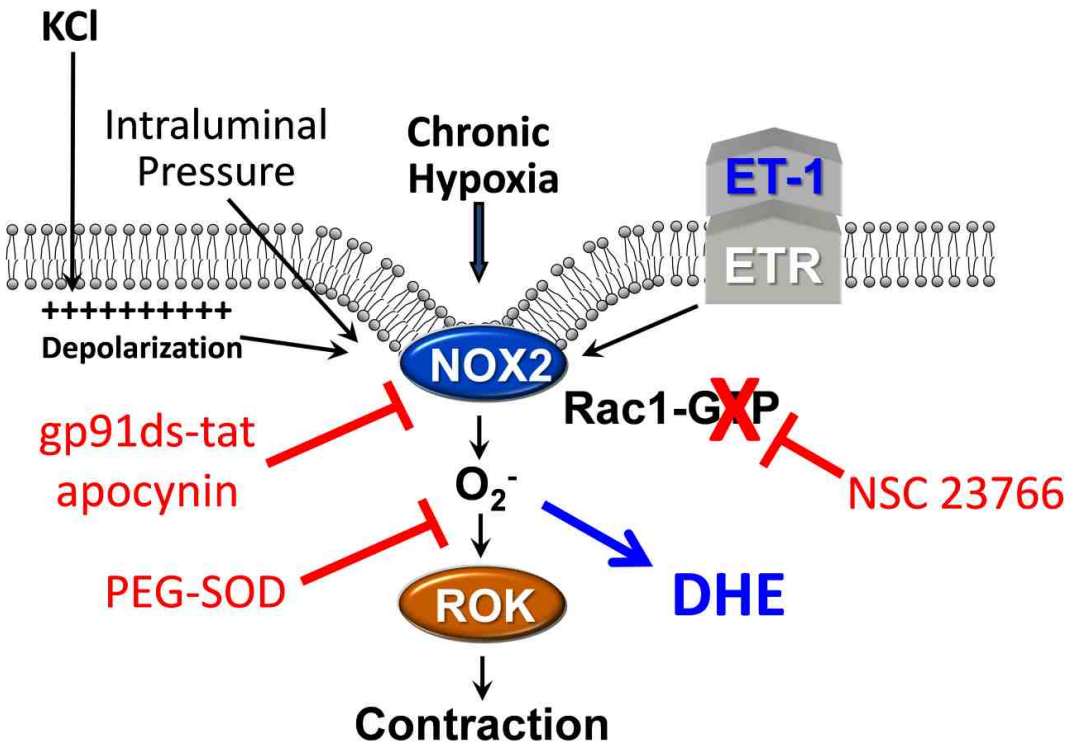

Figure 6: Diagram of experimental protocols for Specific Aim 1.

Protocol Series 1.2: Contribution of NOX 2 to CH-induced basal tone.

Vessel diameter and vessel wall $[Ca^{2+}]_i$ were measured in small pulmonary arteries in response to increasing intraluminal pressure steps (5-45 mmHg). In contrast to Protocol series 1.1, arteries used for basal tone measurements were not Ca^{2+} permeabilized as the development of basal tone is not associated with a significant change in Ca^{2+} (27). We performed pressure steps under both Ca^{2+}-containing and Ca^{2+}-free conditions. Basal tone was calculated as the percent difference in ID between Ca^{2+} containing and Ca^{2+} free conditions at each pressure step (Fig. 7) (27). To evaluate the contribution of NOX 2 to this response, vasoconstrictor and Ca^{2+} responses to increasing intraluminal pressure were measured in arteries from CH and control rats in the presence of apocynin, gp91ds-tat, or their respective vehicles. These experiments were repeated in arteries pretreated with the Rac1 inhibitor, NSC23766, the ROS scavengers PEG-SOD and PEG-catalase, or vehicle.

Protocol Series 1.3: Role of NOX 2 in augmented ET-1-mediated vasoconstriction following CH.

Similar to Protocol Series 1.1, vessel ID and vessel wall $[Ca^{2+}]_i$ were measured in response to increasing concentrations of ET-1 (10^{-10}-10^{-7} M, Sigma) in Ca^{2+} permeabilized pulmonary arteries from CH and control rats in the presence of gp91ds-tat, or its scrambled control peptide to determine the contribution of NOX to enhanced ET-1 constriction following CH.

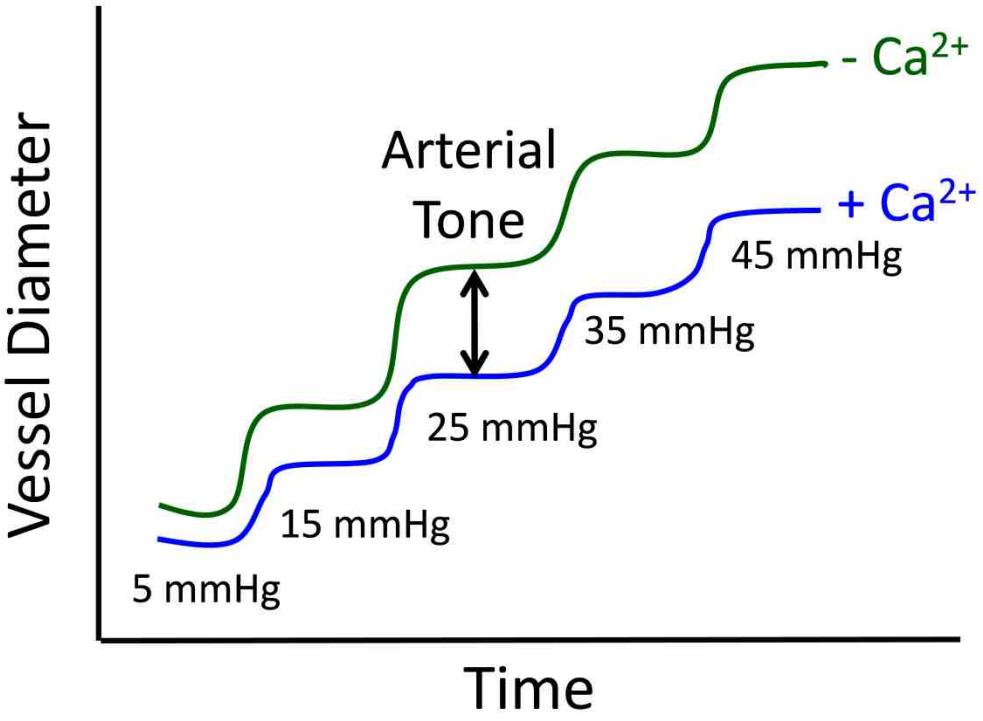

Figure 7: Pressure-dependent arterial tone was assessed by increasing intraluminal pressure in 10 mmHg steps under Ca^{2+}-replete and Ca^{2+}-free conditions. Arterial tone was calculated as the % difference in vessel ID between Ca^{2+}-replete and Ca^{2+}-free conditions.

Protocol Series 1.4: Effects of CH on pulmonary arterial NOX expression.

NOX 2 expression was compared between intrapulmonary arteries from CH and control rats by western blotting (as described in the general protocol section). Pulmonary arterial NOX 2 catalytic subunit expression was measured using a mouse monoclonal NOX 2 ($gp91^{phox}$) antibody (1:2,000, BD Biosciences) (59). Expression was normalized to β-actin to account for any variance in protein loading.

PROTOCOLS FOR SPECIFIC AIM 2

Identify the role of EGFR and Src kinase signaling in augmented pulmonary vasoconstrictor reactivity following CH.

Protocol Series 2.1: Role of EGFR and Src in enhanced depolarization-induced vasoconstriction following CH.

Depolarization-induced vasoconstriction and ROS production were assessed in the presence and absence of the EGFR inhibitor AG 1478 (1 μM, Cayman) in Ca^{2+} permeabilized pulmonary arteries from CH and control rats similar to Protocol Series 1.1 (Fig. 8). This concentration of AG1478 prevents stretch induced EGFR activation in mesangial cells (314). We additionally examined the role of Src in mediating enhanced depolarization-induced vasoconstriction using the Src inhibitors SU6656 (10 μM, Cayman) and PP2 (10 μM, Cayman). These Src inhibitors at the stated concentrations have been shown to prevent Src activation in mesangial cells in work that was corroborated by siRNA (314).

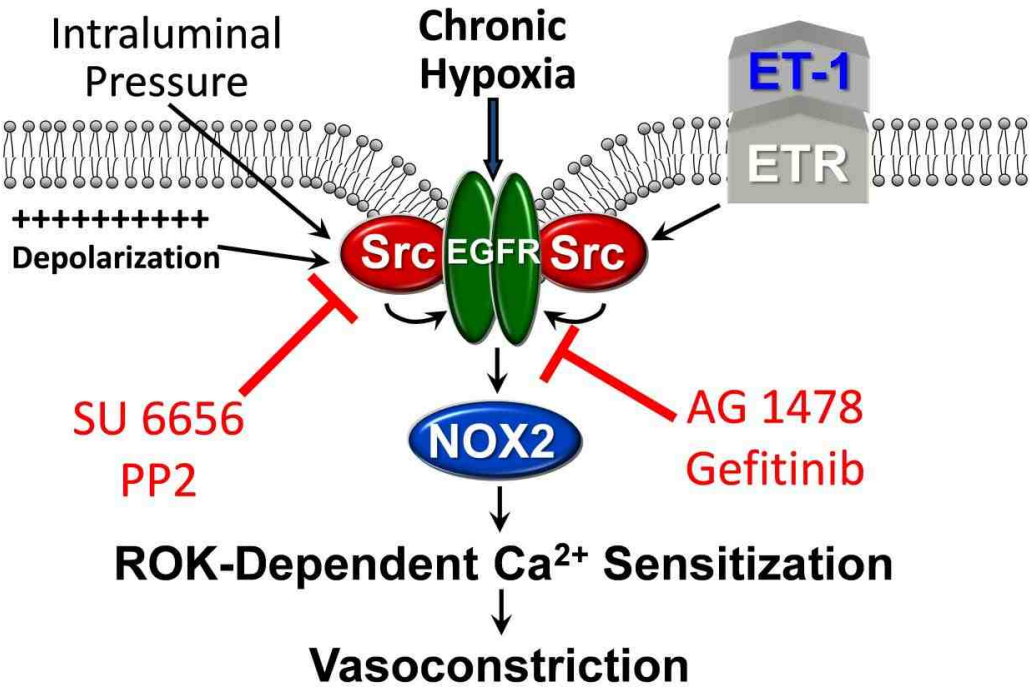

Figure 8: Diagram of Specific Aim 2 assessing the role of Src kinases and EGFR in enhanced vasoconstrictor reactivity following CH.

Similar to protocols measuring Rac1 activity (Aim 1), we measured EGFR activation (indicated by phosphorylation of the tyrosine residue 1068 (13; 74) by western blot with antibodies for both phospho-EGFR (1:500, Cell Signaling) in pulmonary arteries from CH and control rats (314). These experiments compared pulmonary arterial homogenates stimulated with 60 mM KCl or vehicle. Phospho-EGFR was normalized to total EGFR expression (1:500, Cell Signaling) (314). We assessed the role of EGFR in mediating depolarization-induced Rac1 activation following CH by measuring Rac1 activity in the same manner as Protocol Series 1.1, but in the presence and absence of the EGFR inhibitor AG 1478.

Protocol Series 2.2: Role of EGFR and Src in basal tone following CH.

Pulmonary arterial ID and vessel wall $[Ca^{2+}]_i$ were measured in response to increasing pressure steps as described in Protocol Series 1.2 in the presence or absence of the EGFR inhibitors AG 1478 and gefitinib (1 μM, Cayman). These protocols were repeated in the presence of the Src kinase inhibitor SU6656.

Protocol Series 2.3: Contribution of EGFR and Src to enhanced ET-1-mediated vasoconstriction following CH.

We measured vasoconstrictor responses to ET-1 in Ca^{2+} permeabilized arteries from control ad CH rats as described in Protocol Series 1.3 in the presence or absence of AG 1478 and SU6656. Src kinase phosphorylation (1:1,000, Cell Signaling) (273) on tyrosine 416 (indicative of activation) was measured by western blot in pulmonary arterial homogenates from CH and

control rats and normalized to total Src kinase expression (1:1,000, Cell Signaling) (273). To assess the role of EGFR in ET-1 induced ROS production, we measured DHE fluorescence in isolated PASMCs from CH and control rats treated with vehicle, ET-1, or ET-1 and AG-1478.

Protocol Series 2.4: Mechanisms of EGF-induced vasoconstriction.

To determine whether CH induces this pathway at the point of EGFR or downstream, ID and vessel wall $[Ca^{2+}]_i$ were measured in non-Ca^{2+} permeabilized arteries from CH and control rats in response to increasing concentrations of EGF (Sigma). Experiments were performed in the presence of HA1077 (10 μM, Sigma), gp91ds-tat, AG 1478, and SU 6656 to determine the roles of ROK, NOX, EGFR, and Src kinases respectively.

Protocol Series 2.5: Role of matrix metalloproteinases in enhanced pulmonary vasoconstriction following CH.

To determine if EGFR is being activated by Src kinases though MMP dependent (18; 236; 263) or MMP independent mechanisms (87; 146; 190; 234), the broad spectrum MMP inhibitor GM6001 (15 μM, Millipore) (37) was used to examine the role of metalloproteinases in augmented vasoconstriction to ET-1 following CH similar to protocols 1.3 and 2.3 (Fig. 9). Subsequent experiments examined effects of inhibitors of ADAM 17 (TAPI-1, 10 μM, Santa Cruz) (174), MMP 2 [MMP 2 inhibitor 3 (also known as ARP 100), 100 nM, Millipore] (189), and MMP9 (MMP 9 inhibitor 2, 10 μM, Millipore) (52) on this response. MMP 2 inhibitor 3 has a relatively high selectivity at this dose for MMP 2 (IC_{50} values:

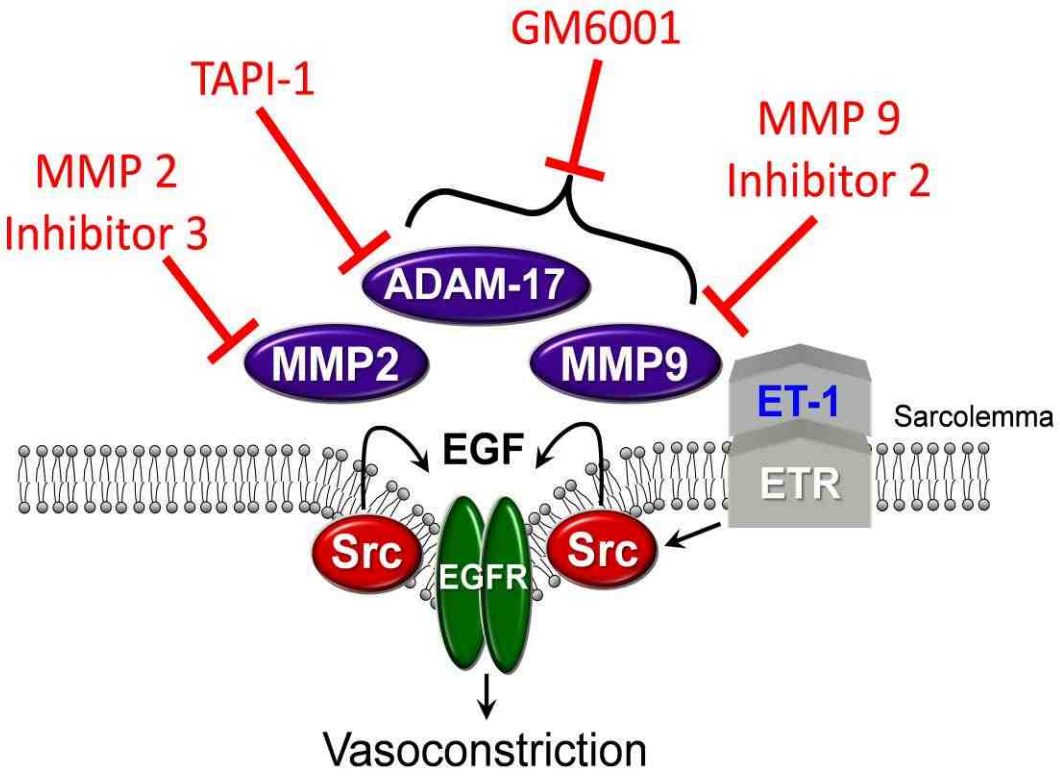

Figure 9: Diagram of Specific Aim 2.5 examining the role of MMPs in enhanced vasoconstriction to ET-1 following CH.

MMP 2, 12 nM; MMP 9, 200 nM; MMP 1, 50µM; MMP 3, 3 µM; MMP 7, 50 µM) (178; 231), while MMP 9 inhibitor 2 is targeted to the hemopexin domain that exists on MMP 9, but not other MMPs (52).

Western blots were performed to determine potential changes in MMP expression following CH. Primary antibodies to ADAM 17 (1:1,000, Abcam) (24), MMP2 (1:500, Abcam) (240) and MMP 9 (1:2,500, Abcam) (240) were used to determine if CH alters expression of these proteins.

Protocol Series 2.6: Role of ETR in metabotropic transduction of membrane depolarization and increased intraluminal pressure to enhanced vasoreactivity following CH.

As some GPCRs have been implicated in transducing both mechanical(113; 161) and depolarizing stimuli (141; 154) to VSM contraction, we hypothesized that ETR function as a proximal signaling mediator coupling membrane depolarization and vessel wall stretch to myofilament Ca^{2+} sensitization and vasoconstriction following CH. To test this hypothesis, we assessed pressure-dependent basal tone and vasoconstrictor responses to KCl in pulmonary arteries similar to previous protocols. Experiments were performed in the presence of both the selective ET_A receptor agonist BQ-123 (10 µM, Sigma) and the ET_B antagonist BQ-788 (10 µM, Sigma) (109) to determine if membrane depolarization or membrane stretch transduce their signal through ETRs. These ETR antagonists, at the used concentrations, have been shown to nearly abolish ET-1 mediated vasoconstriction in pulmonary arteries (109).

Protocol Series 2.7: Contribution of EGFR to CH-induced PH.

To determine if EGFR is critical in the development of CH-induced PH, we treated CH and control animals daily with pills containing the EGFR inhibitor gefitinib (30 mg/kg/day, Cayman), or vehicle pills (Bioserv dough with 10% peanut butter). This concentration of drug administered orally for 14 days was able to attenuate monocrotaline-induced PH in Sprague-Dawley rats (42). We then measured right ventricular pressure (RVP), right ventricular hypertrophy, vascular remodeling, and hematocrit in these animals as we have done previously in our laboratory (general methods) (217; 219).

PROTOCOLS FOR SPECIFIC AIM 3

Assess the contribution of pressure-dependent and ET-1-induced membrane depolarization to augmented pulmonary vasoconstrictor reactivity following CH.

Protocol Series 3.1: Contribution of membrane depolarization in CH-dependent basal tone.

Pressure-response curves were conducted in the presence of the K^+ ionophore valinomycin (5 μM, Sigma) (288) and 16 mM KCl to normalize VSM membrane potential in CH arteries to that of control arteries and to prevent stretch-induced depolarization (Fig. 10). Using the Nernst equation to predict membrane potential, and assuming K^+ is the only membrane permeant ion, 16 mM extracellular K^+ in combination with valinomycin should set membrane potential to ~-60 mV (membrane potential of a control artery under

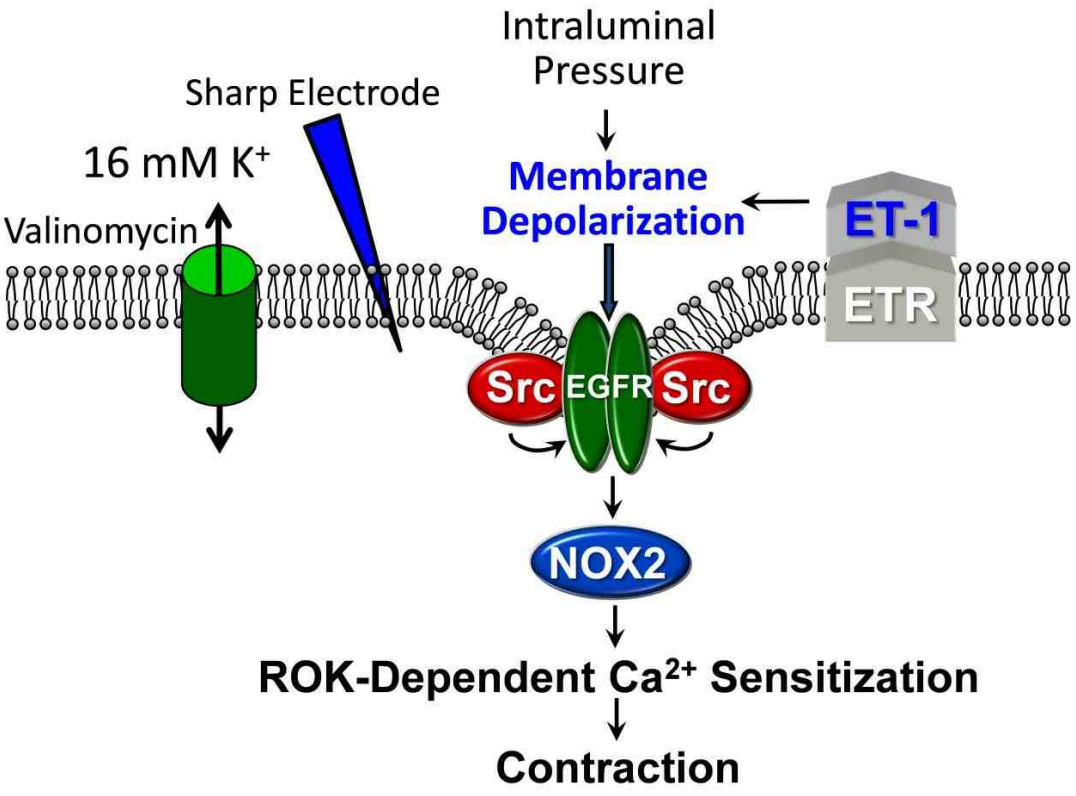

Figure 10: Diagram of experimental protocols for Specific Aim 3.

baseline conditions). The ability of valinomycin to prevent depolarization was validated using sharp electrode measurement of membrane potential. Assessment of pressure-dependent basal tone was further evaluated in separate sets of arteries from each group treated with pinacidil (100 μM, Sigma) (106; 128), an ATP-sensitive potassium channel (K_{ATP}) agonist, to hyperpolarize VSM membrane potential. This concentration of pinacidil is able to nearly maximally dilate the pulmonary circulation in isolated saline perfused lungs (106). These experiments with pinacidil were performed in the presence of the L-type Ca^{2+} inhibitor diltiazem (50 μM, Sigma) (26) to prevent changes in VSM $[Ca^{2+}]_i$ resulting from alterations in membrane potential.

<u>Protocol Series 3.2:</u> Role of membrane depolarization in receptor-mediated vasoconstriction following CH.

Vasoconstrictor responses to ET-1 were measured in Ca^{2+} permeabilized arteries treated with valinomycin and 16 mM KCl as in Protocol Series 3.1 in order to examine the potential contribution of membrane depolarization to enhanced vasoconstriction to ET-1 in CH arteries. The ability of valinomycin to prevent depolarization to ET-1 was validated using sharp electrode measurement of membrane potential.

Chapter 3 – Results

General

CH resulted in polycythemia (hematocrit of62.0 ± 3.4% in CH rats and 46.7 ± 2.7% in controls, n=89-92/group) and right ventricular hypertrophy (RV/LV+S of 0.55 ± 0.01 in CH rats and 0.28 ± 0.01 in controls, n=28/group) indicative of the development of PH consistent with previous observations in our laboratory (16; 217; 219; 252). CH also elevated RVSP (Fig. 11A) and resulted in increased arterial wall thickness in small pulmonary arteries (<50 μm diameter, Fig. 11B).

SPECIFIC AIM 1

Establish the contribution of NOX 2 signaling to enhanced pulmonary arterial vasoconstrictor reactivity following CH.

Hypothesis:

We hypothesize that CH imparts basal tone and enhances depolarization-induced and ET-1-dependent vasoconstriction in small pulmonary arteries through NOX 2-mediated myofilament Ca^{2+} sensitization.

Role of NOX 2 in depolarization-induced vasoconstriction following CH

The role of NOX, as a source of O_2^-, in mediating enhanced membrane depolarization-dependent vasoconstriction following CH was initially tested in nonpermeabilized pulmonary arteries using the general NOX inhibitor apocynin. Apocynin decreased reactivity to KCl in CH arteries, while having no effect in control arteries (Fig. 12 A) supporting a role for NOX in this response.

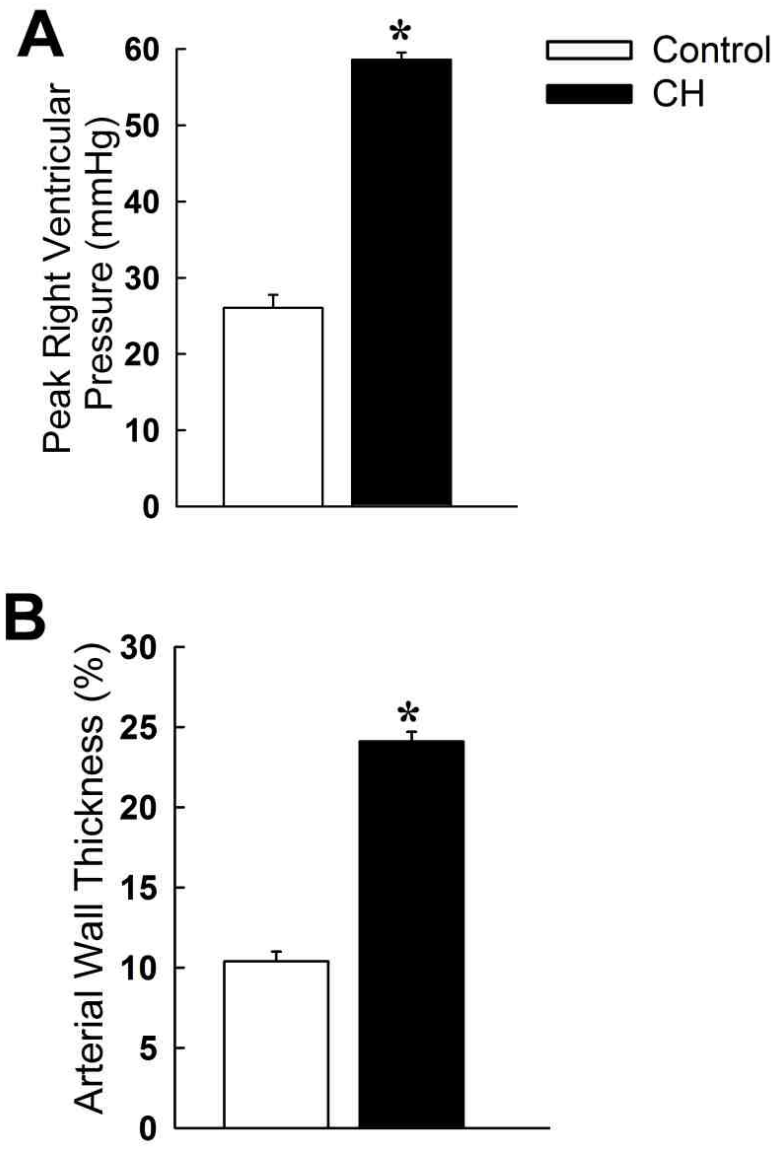

Figure 11. **CH leads to increased RVSP and arterial remodeling**. Peak right ventricular pressures (A) and arterial wall thickness (B) following CH or control exposure. Values are means ± SE n=5/group; *p<0.05 vs. control.

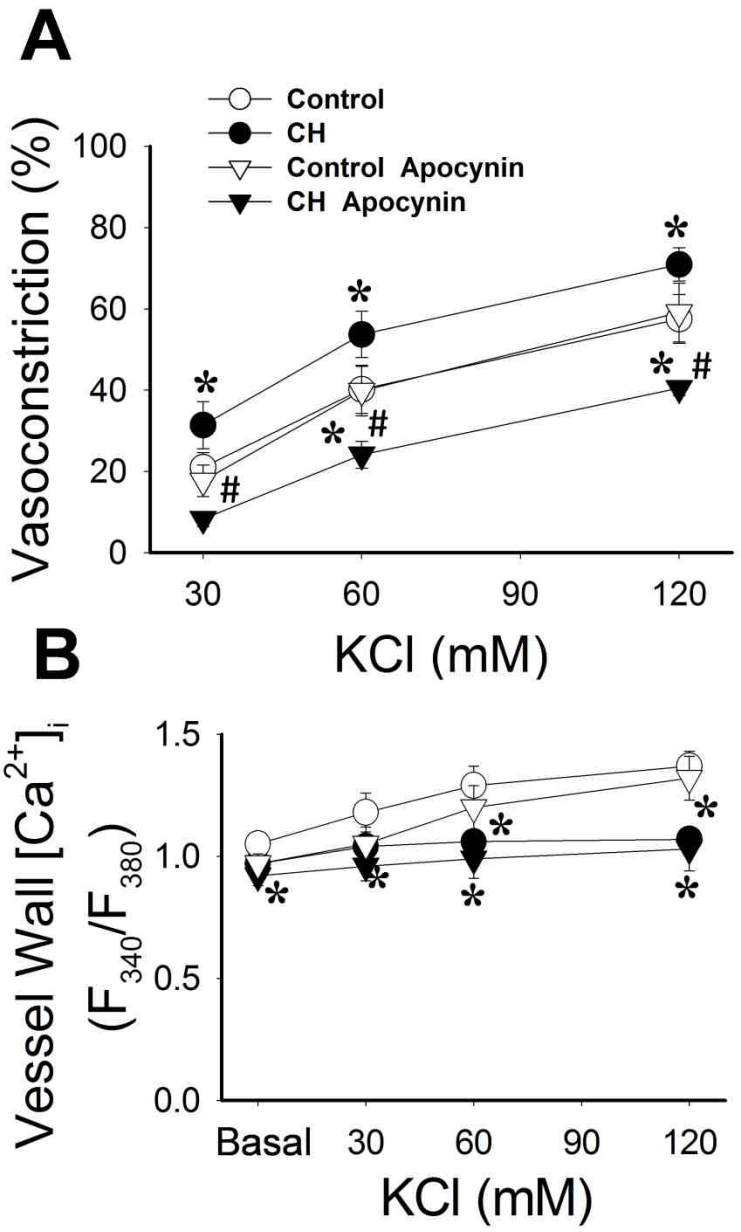

Figure 12. **Augmented KCl-induced vasoconstriction following CH is NOX-dependent in nonpermeabilized pulmonary arteries**. Vasoconstrictor responses (A) and vessel wall Ca^{2+} (B) to KCl in pressurized, endothelium-disrupted pulmonary arteries from CH and control rats in the presence of the NOX inhibitor apocynin (30 μM) or vehicle. Values are means ± SE n=5-7/group; *p<0.05 vs. respective control. #p<0.05 CH apocynin vs. CH vehicle.

Interestingly, KCl caused an increase in vessel wall Ca^{2+} in control arteries, but not CH arteries (Fig. 12B).

To more directly address the role of NOX in enhanced depolarization-dependent VSM Ca^{2+} sensitization following CH, we further examined effects of NOX inhibitors on KCl-dependent vasoconstriction in Ca^{2+}-permeabilized arteries. The nonselective NOX inhibitors apocynin (Fig. 13A) and DPI (Fig. 13B) attenuated KCl-dependent vasoconstriction in arteries from CH, but not control rats, and normalized responses between groups. Similar inhibitory effects were observed using the specificNOX2 inhibitory peptide, gp91ds-tat (also known as Nox2ds-tat) (41), compared to the scrambled peptide (Fig. 14A). We detected no differences in basal Ca^{2+} and observed no Ca^{2+} responses to KCl in arteries treated with apocynin, DPI, or gp91ds-tat (Fig. 14B).

O_2^- production was measured by fluorescence detection of dihydroethidium (DHE) oxidation in endothelium-disrupted, Ca^{2+}-permeabilized arteries from control and CH rats pressurized to 12 mmHg. CH exposure resulted in elevated basal and KCl-induced O_2^-levels in pressurized pulmonary arteries (Fig.15). In contrast, KCl did not alter O_2^- production in control arteries. In arteries from CH animals, apocynin lowered basal DHE fluorescence to the level of controls, while both apocynin and DPI prevented KCl-dependent increases in O_2^- production (Fig. 15A and 15B, respectively). gp91ds-tat also decreased basal DHE fluorescence compared to the scrambled peptide in arteries from CH rats, and prevented the effect of KCl to elevate DHE fluorescence in these

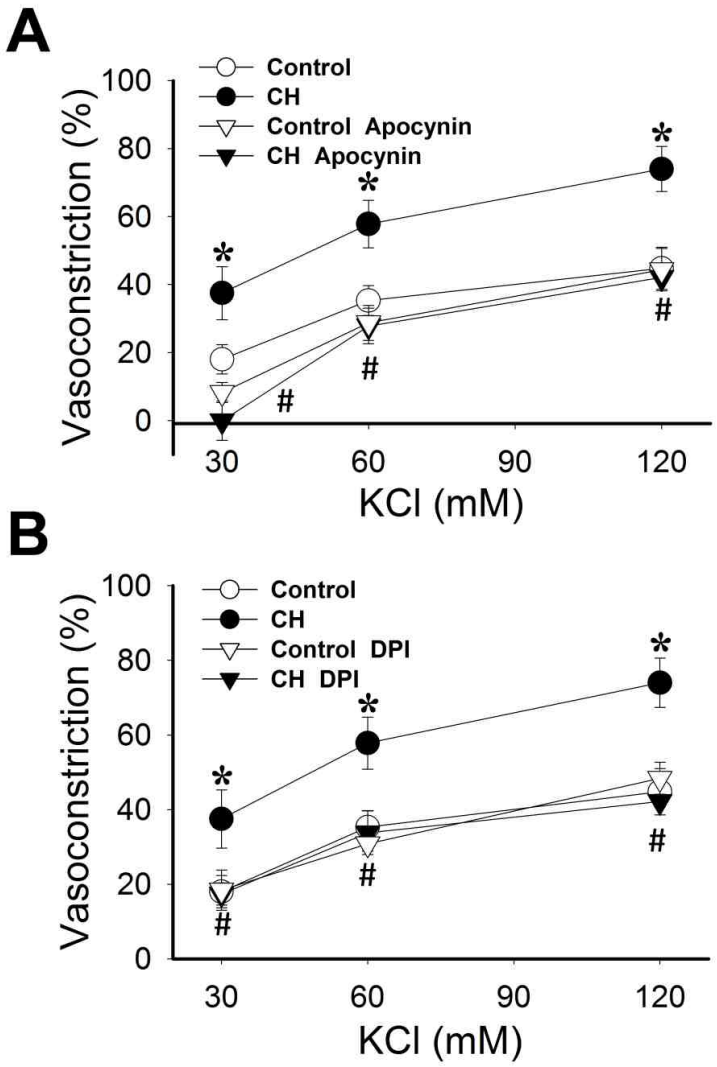

Figure 13. **NOX is required for greater KCl-mediated Ca^{2+} sensitization and constriction in Ca^{2+} permeabilized arteries from CH rats**. Vasoconstrictor responses to KCl in pressurized, Ca^{2+} permeabilized, endothelial disrupted pulmonary arteries from CH and control rats in the presence of the NOX inhibitors (A) apocynin (30 µM), DPI (50 µM), or vehicle. Values are means ± SE n=4-5/group; *p<0.05 vs. control. #p<0.05 vs. CH vehicle.

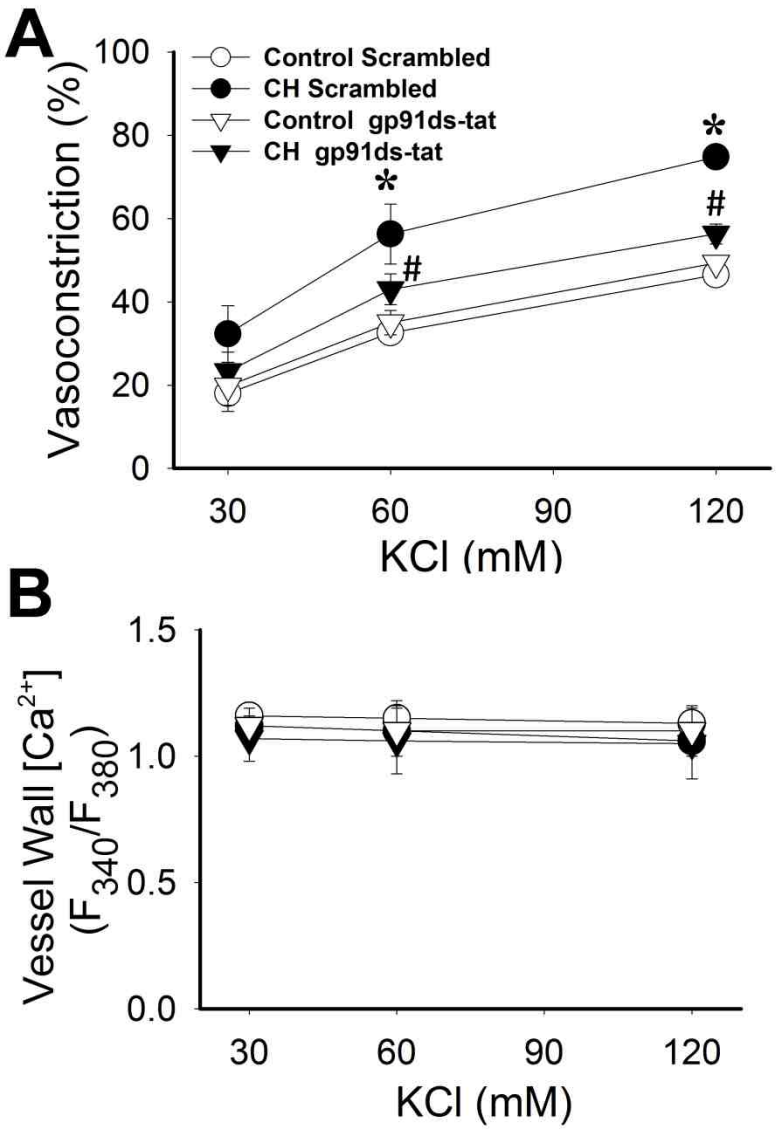

Figure 14 **Enhanced KCl-mediated vasoconstriction and Ca^{2+} sensitization in arteries from CH rats requires NOX 2**. Vasoconstrictor (A) and Ca^{2+} (B) responses to KCl in pressurized, Ca^{2+} permeabilized, endothelium disrupted pulmonary arteries from CH and control rats in the presence of the specific NOX 2 inhibitor, gp91ds-tat (50 μM), or its scrambled control peptide. Values are means ± SE n=4-5/group; *p<0.05 vs. control. #p<0.05 vs. CH vehicle.

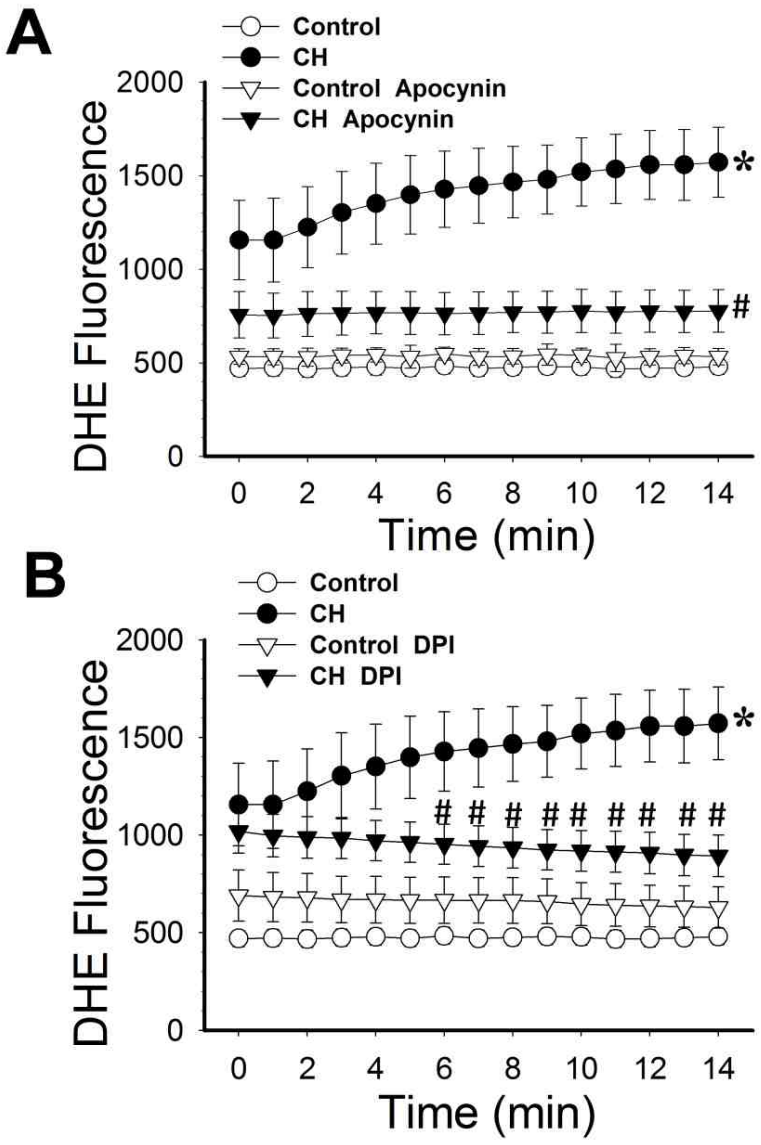

Figure 15. **CH-induced increases in basal and depolarization-stimulated O_2^- levels in pressurized arteries are NOX-dependent**. DHE fluorescence under basal conditions and following administration of KCl (60 mM) in pressurized, endothelium-disrupted, Ca^{2+} permeabilized pulmonary arteries from CH and control rats in the presence of (A) apocynin, (B) DPI, or their respective vehicles. KCl was administered 1 min into recording. Values are means ± SE n=4-5/group; *p<0.05 vs. control at each time point. #p<0.05 vs. CH vehicle. τp<0.05 vs. CH vehicle.

vessels (Fig. 16), suggesting that NOX 2 plays a primary role in depolarization induced O_2^- generation and pulmonary vasoconstriction.

To confirm that inhibitory influences of gp91ds-tat on KCl-induced vasoconstriction and production in CH arteries were not due to the peptide causing VSM membrane hyperpolarization, we measured membrane potential with sharp electrodes in pressurized arteries from each group. In accordance with previous findings (26), VSM membrane potential was depolarized in arteries from CH rats under both basal and KCl-stimulated conditions (Fig. 17). Inhibition of NOX 2 was without effect on membrane potential in arteries from either group.

Previous work from our laboratory has demonstrated that the O_2^- spin trap agent, tiron, prevents enhanced vasoconstriction to KCl following CH exposure (26). To further characterize the ROS involved in this response, we assessed the relative contributions O_2^- and H_2O_2 to enhanced KCl-induced vasoconstriction following CH. Experiments were conducted in the presence of the O_2^- scavenger, PEG-SOD, or the H_2O_2 scavenger, PEG catalase. Similar to tiron (26), PEG-SOD attenuated reactivity to KCl in pulmonary arteries from rats exposed to CH, while having no effect in control vessels (Fig. 18A). In contrast, PEG-catalase did not alter vasoconstriction to KCl in either group (Fig. 18B).

We next wanted to determine if the NOX component Rac1 plays an important role to mediate this response. To test this possibility, we measured depolarization-induced vasoconstriction and DHE fluorescence in the presence

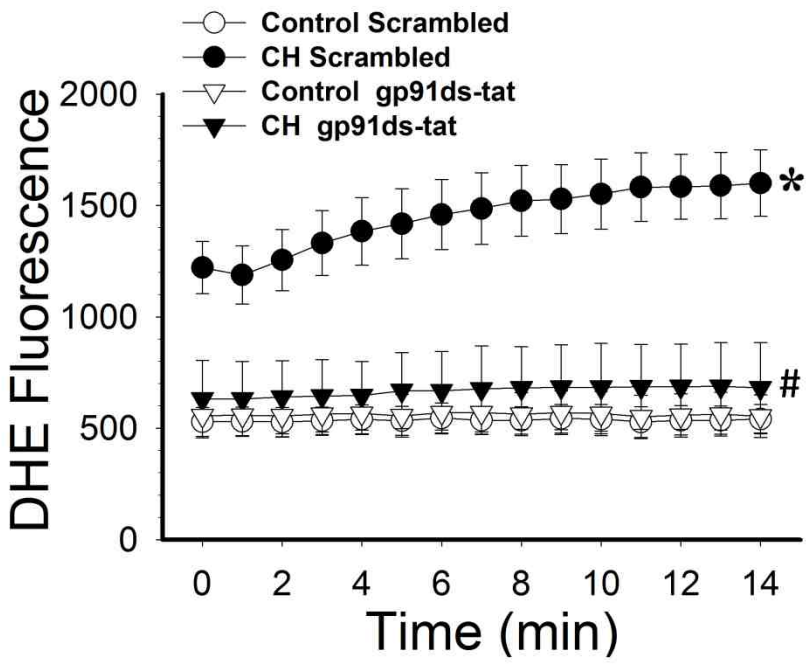

Figure 16. **NOX 2 is necessary for CH-induced increases in basal and depolarization-stimulated O_2^- levels in pressurized arteries**. DHE fluorescence under basal conditions and following administration of KCl (60 mM) in pressurized, endothelium-disrupted, Ca^{2+} permeabilized pulmonary arteries from CH and control rats in the presence of the specific NOX 2 inhibitor, gp91ds-tat (50 μM), or its scrambled control peptide. KCl was administered 1 min into recording. Values are means ± SE n=4-5/group; *p<0.05 vs. control at each time point. #p<0.05 vs. CH vehicle. τp<0.05 vs. CH vehicle.

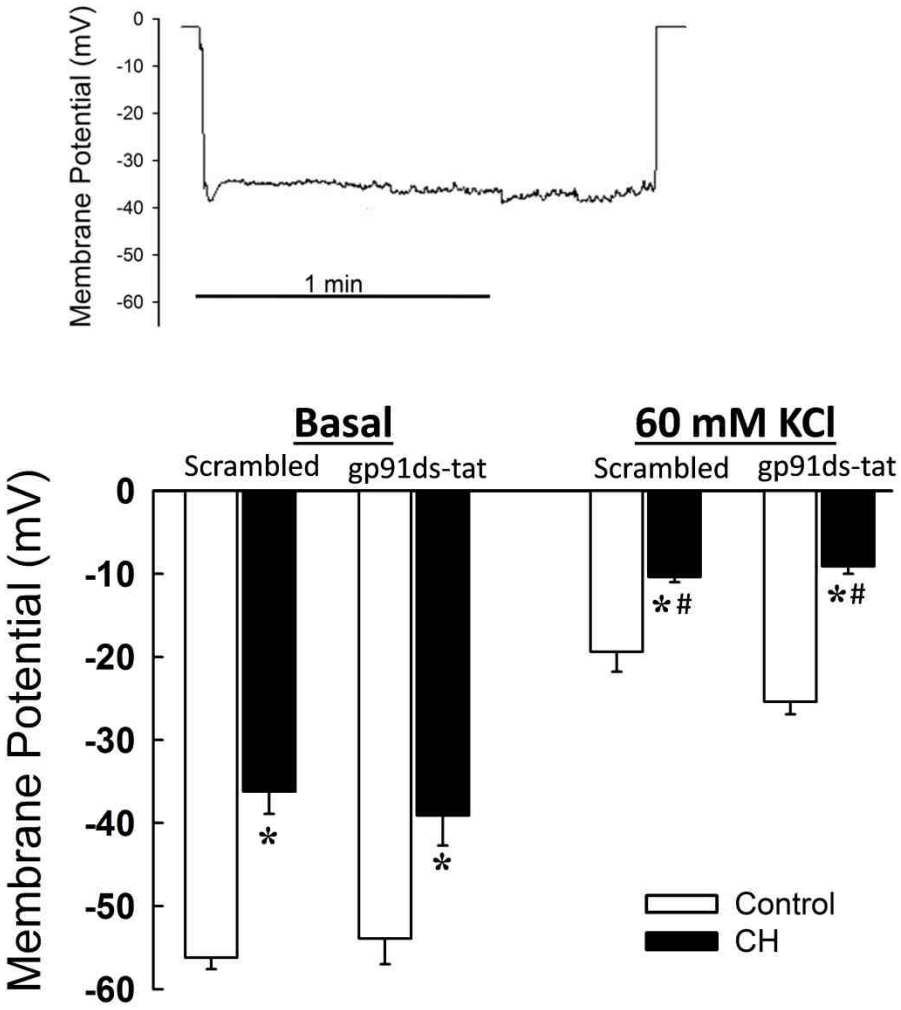

Figure 17. **NOX 2 inhibition does not alter pulmonary VSM membrane potential**. Sharp electrode measurements (raw trace and mean data) of membrane potential in response to KCl in pressurized, Ca^{2+} permeabilized, endothelial disrupted pulmonary arteries from CH and control rats in the presence of the specific NOX 2 inhibitor, gp91ds-tat (50 μM), or its scrambled control peptide. Values are means ± SE n=4-5/group; *p<0.05 vs. control. #p<0.05 vs. CH vehicle.

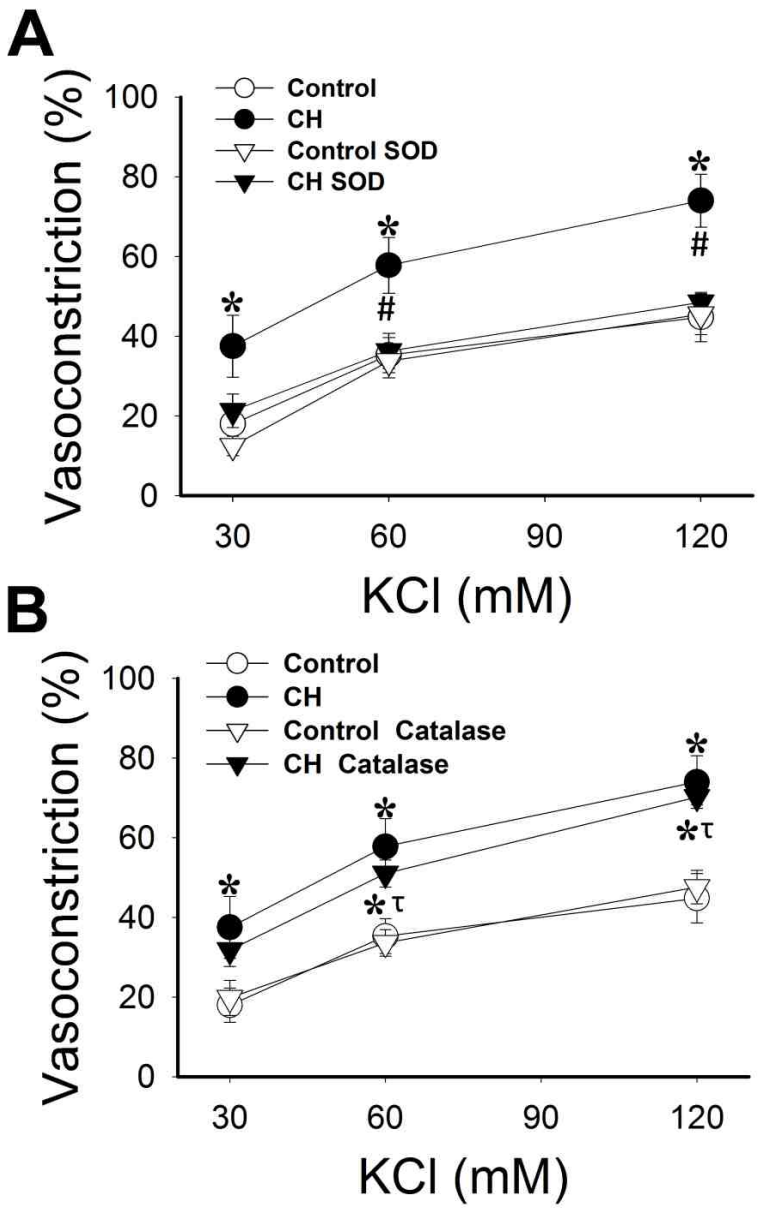

Figure 18. **O_2^-, but not H_2O_2, mediates depolarization-induced myofilament Ca^{2+} sensitization and constriction in Ca^{2+} permeabilized arteries from CH rats.** Vasoconstrictor responses to KCl in pressurized, endothelium-disrupted, Ca^{2+} permeabilized pulmonary arteries from CH and control rats in the presence of (A) PEG-SOD (120 U/mL) or (B) PEG-catalase (250 U/mL). Values are means ± SE n=4-5/group; *p<0.05 vs. control. #p<0.05 vs. CH vehicle. τp<0.05 vs. CH catalase vs. CH SOD.

or absence of the Rac1 inhibitor NSC 23766. Similar to our findings with NOX inhibition, Rac1 inhibition prevented KCl-mediated increases in vasoreactivity (Fig. 19) and DHE fluorescence (Fig. 20) in CH arteries, while having no effect in control arteries. Similar to effects of O_2^- scavenging (109; 184) or NOX inhibition (Figs. 15 and 16), Rac1 inhibition prevented elevated basal O_2^- levels in arteries from CH rats.

KCl-dependent Rac1 activation was assessed by performing a Rac1-GTP pulldown assay in ionomycin-treated (300nM Ca^{2+}) pulmonary arteries from control and CH rats. While not significant, Rac1-GTP tended to be increased in arteries from CH rats under basal conditions (Fig. 21). KCl stimulation caused a robust increase in Rac1 activation in arteries from rats exposed to CH, while having no significant effect in control arteries. No differences were detected in total Rac1 expression (normalized to β actin, Fig. 22).

Contribution of NOX 2 to CH-induced basal tone

The role of NOX as a source of O_2^- mediating basal arterial tone development following CH was tested in nonpermeabilized pulmonary arteries using the NOX inhibitors apocynin and gp91ds-tat. Both general NOX (Fig. 23) and specific NOX 2 (Fig. 24A) inhibition attenuated the development of pressure-dependent basal tone in CH arteries while having no effect in control arteries. Vessel wall Ca^{2+} was not different between CH and control arteries at any pressure step (Fig. 24B).

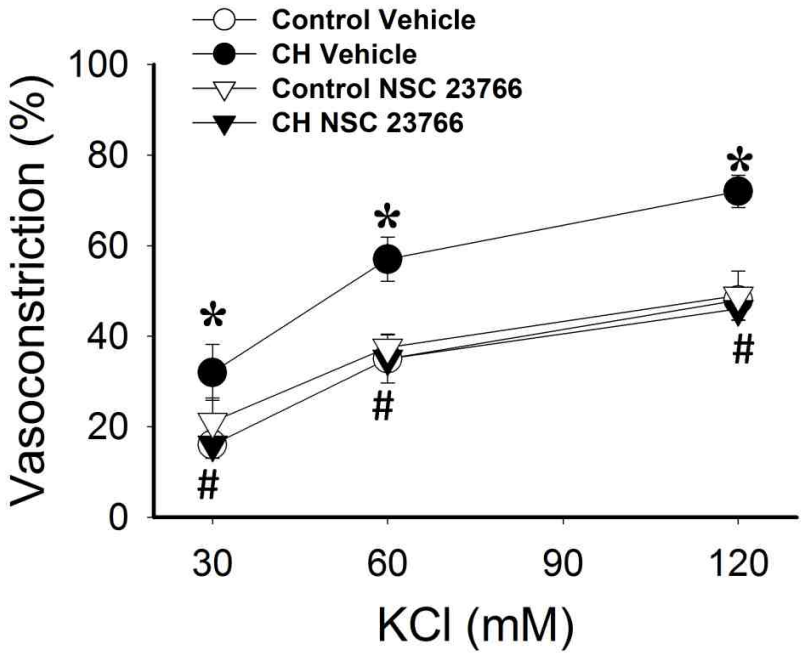

Figure 19. **Enhanced depolarization-dependent vasoconstriction following CH requires Rac1**. Vasoconstrictor responses to KCl in pressurized, Ca^{2+} permeabilized, endothelial disrupted pulmonary arteries from CH and control rats in the presence of the Rac1 inhibitor, NSC 23766 (50 µM), or its vehicle. Values are means ± SE n=4/group; *p<0.05 vs. control. #p<0.05 vs. CH vehicle.

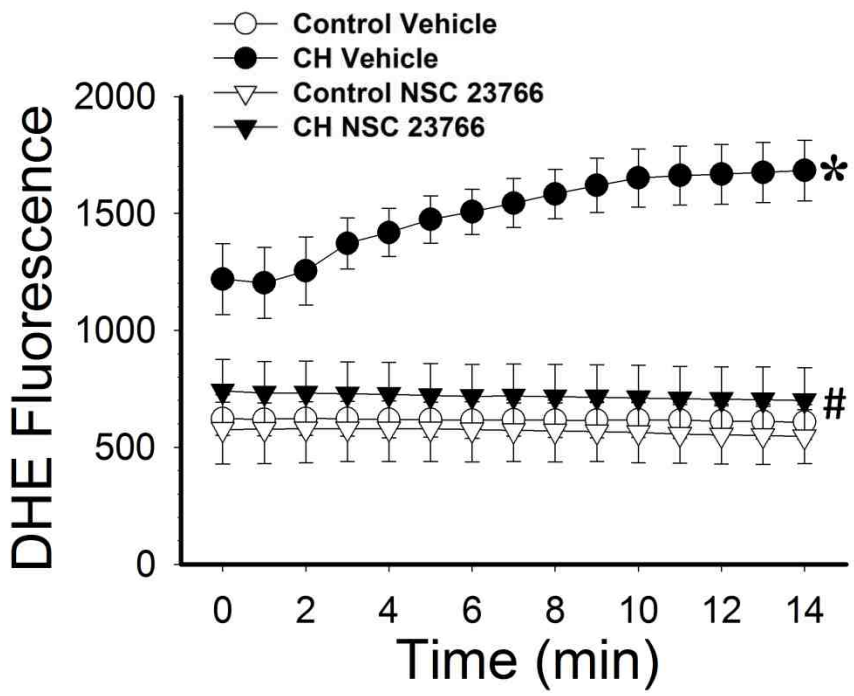

Figure 20. **Rac1 is necessary for CH-induced increases in basal and depolarization-stimulated O_2^- levels in pressurized arteries**. DHE fluorescence under basal conditions and following administration of KCl (60 mM) in pressurized, endothelium-disrupted, Ca^{2+} permeabilized pulmonary arteries from CH and control rats in the presence and absence of the NSC 23766 (50 µM). KCl was administered 1 min into recording. Values are means ± SE n=4/group; *p<0.05 vs. control at each time point. #p<0.05 vs. CH vehicle.

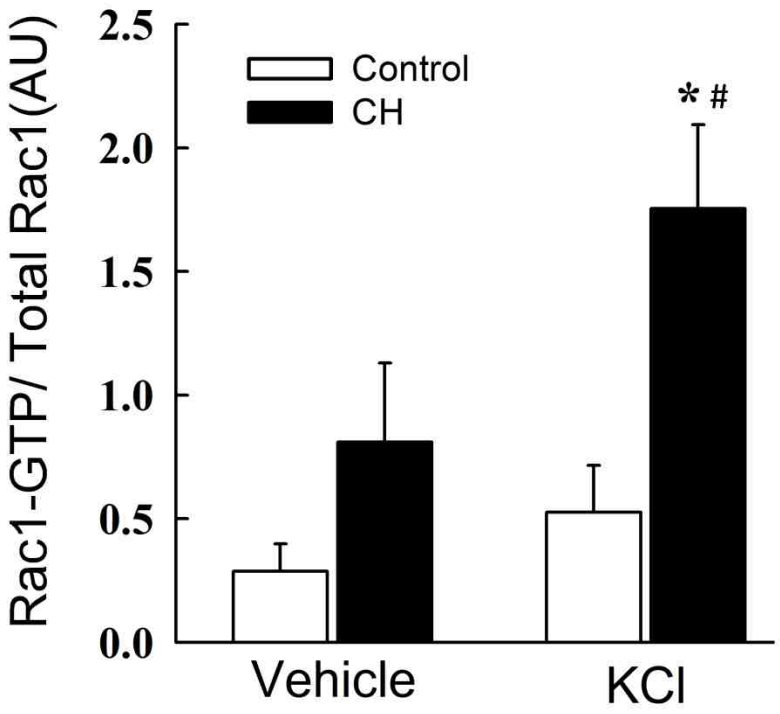

Figure 21. **Depolarization mediates Rac1 activation in arteries from CH rats.** Mean densitometric data for GTP bound (active) Rac1 normalized to total Rac1 in homogenates from control and CH intrapulmonary arteries. Active Rac1 was measured under baseline conditions, and following 10 min stimulation with KCl (60 mM). Values are means ± SE n=4/group; *p<0.05 vs. control KCl. #p<0.05 vs. CH vehicle.

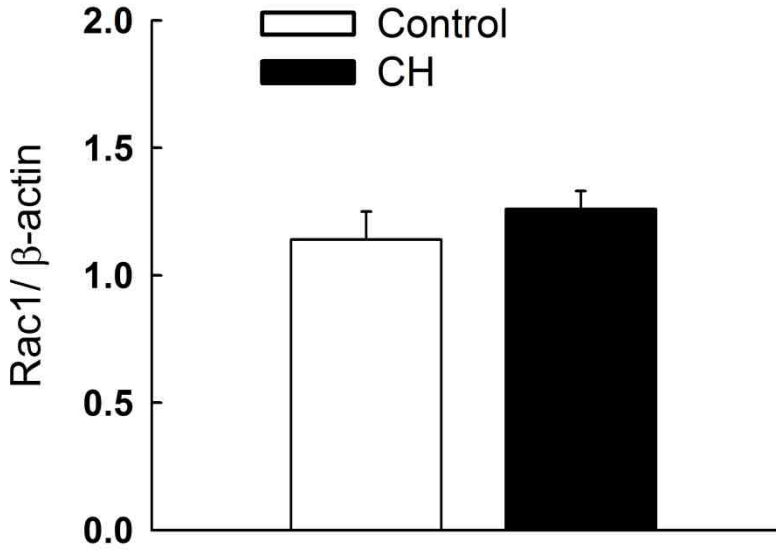

Figure 22. **Rac 1 expression is not altered by CH**. Mean densitometric data for total Rac1 normalized to β-actin in arterial homogenates from control and CH intrapulmonary arteries. Values are means ± SE n=8/group; no significant differences were detected.

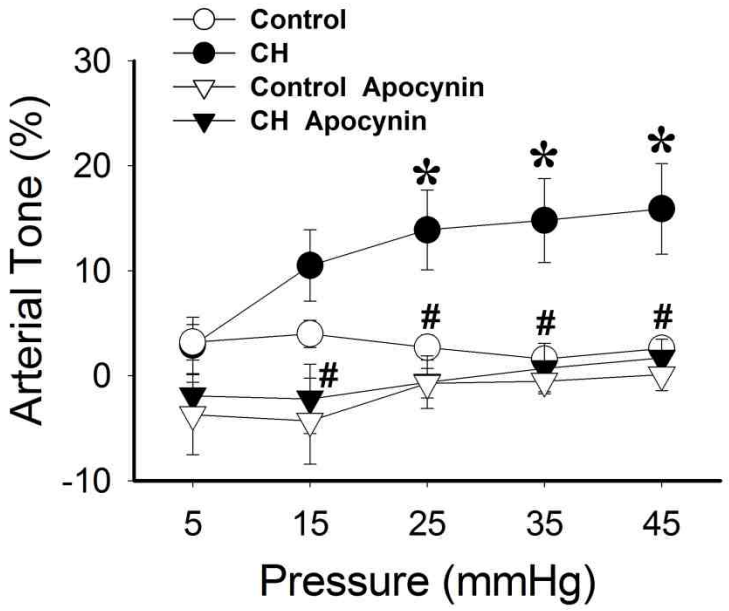

Figure 23. **Pressure-dependent basal tone in arteries from CH rats requires NOX**. Basal arterial tone (% of passive ID) as a function of increasing intraluminal pressure in arteries from CH and control rats in the presence of the NOX inhibitor apocynin (30 μM) or its vehicle. All arteries were endothelium-disrupted. Values are means ± SE n=4-5/group; *p<0.05 vs. control. #p<0.05 vs. CH vehicle.

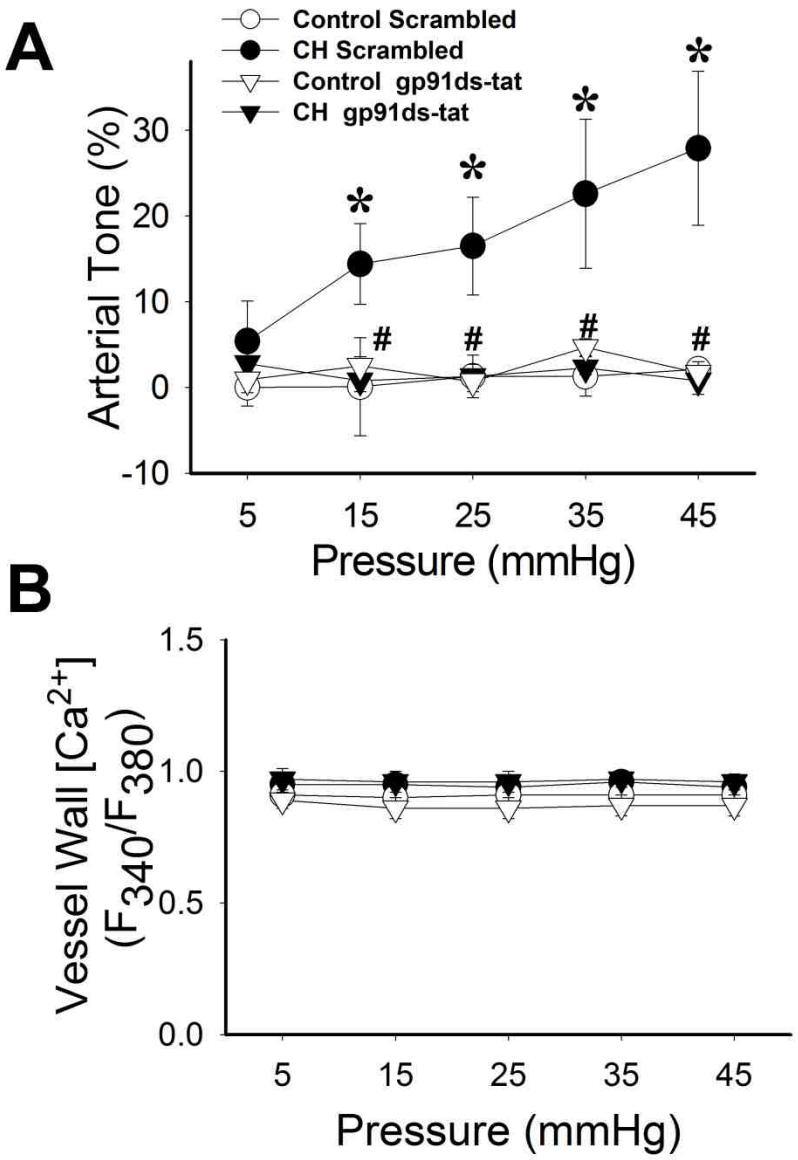

Figure 24. **Pressure-dependent basal tone in arteries from CH rats requires NOX 2**. Basal arterial tone (% of passive ID, A) and vessel wall Ca^{2+} (B) as a function of increasing intraluminal pressure in arteries from CH and control rats in the presence of the NOX 2 inhibitor gp91ds-tat (50 μM), or its scrambled control peptide. All arteries were endothelium-disrupted. Values are means ± SE n=4-5/group; *p<0.05 vs. control. #p<0.05 vs. CH vehicle.

To address the role of Rac1 in this response, experiments were repeated in the presence of the Rac1 inhibitor NSC 23766. Similar to NOX inhibition, blocking Rac1 activation prevented the development of basal arterial tone (Fig. 25).

Previous reports suggest that O_2^- is the ROS responsible for basal tone development following CH (27). To further characterize the ROS species involved in this response, pressure step protocols were conducted in the presence of the O_2^- scavenger, PEG-SOD, or the H_2O_2 scavenger, PEG catalase. PEG-SOD attenuated pressure-dependent basal tone in pulmonary arteries from rats exposed to CH, while having no effect in control vessels (Fig. 26A). In contrast, PEG-catalase did not alter responses in either group (Fig. 26B).

Role of NOX 2 in augmented ET-1-mediated vasoconstriction following CH

We examined the effect of gp91ds-tat on ET-1-dependent vasoconstriction in Ca^{2+} permeabilized arteries to determine if NOX 2 is important in mediating agonist-induced Ca^{2+} sensitization. Similar to KCl-induced vasoconstriction (Fig. 12), NOX 2 inhibition attenuated vasoconstriction to ET-1 in arteries from CH, but not control rats (sample trace Fig. 27, mean data Fig. 28). Responses between CH and control groups treated with the NOX 2 inhibitor were not different from each other. Inhibition of the NOX component, Rac1, additionally prevented enhanced vasoconstrictor sensitivity to ET-1 in arteries from CH rats (Fig. 29).

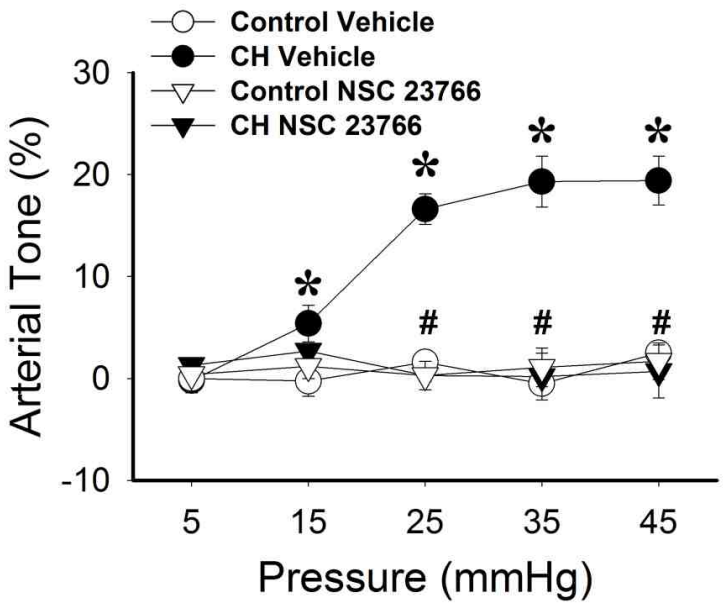

Figure 25. **Pulmonary basal tone requires Rac1**. Basal arterial tone in the presence or absence of the Rac1 inhibitor NSC 23766 (50 μM). All arteries were endothelium-disrupted. Values are means ± SE n=4-5/group; *p<0.05 vs. control. #p<0.05 vs. CH vehicle.

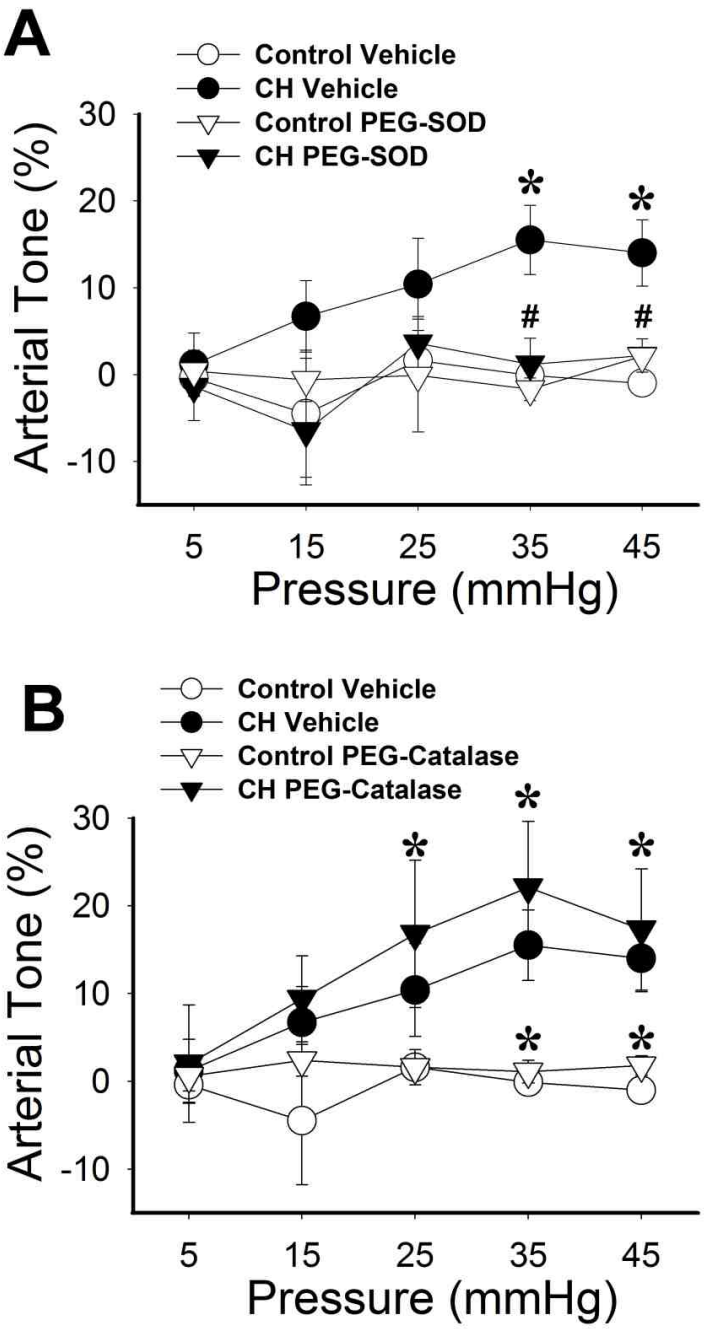

Figure 26. **O_2^- mediates pressure-dependent pulmonary basal tone following CH.** Basal arterial tone in pressurized, endothelium-disrupted, pulmonary arteries from CH and control rats in the presence of (A) PEG-SOD or (B) PEG-catalase. Values are means ± SE n=4-5/group; *p<0.05 vs. control. #p<0.05 vs. CH vehicle.

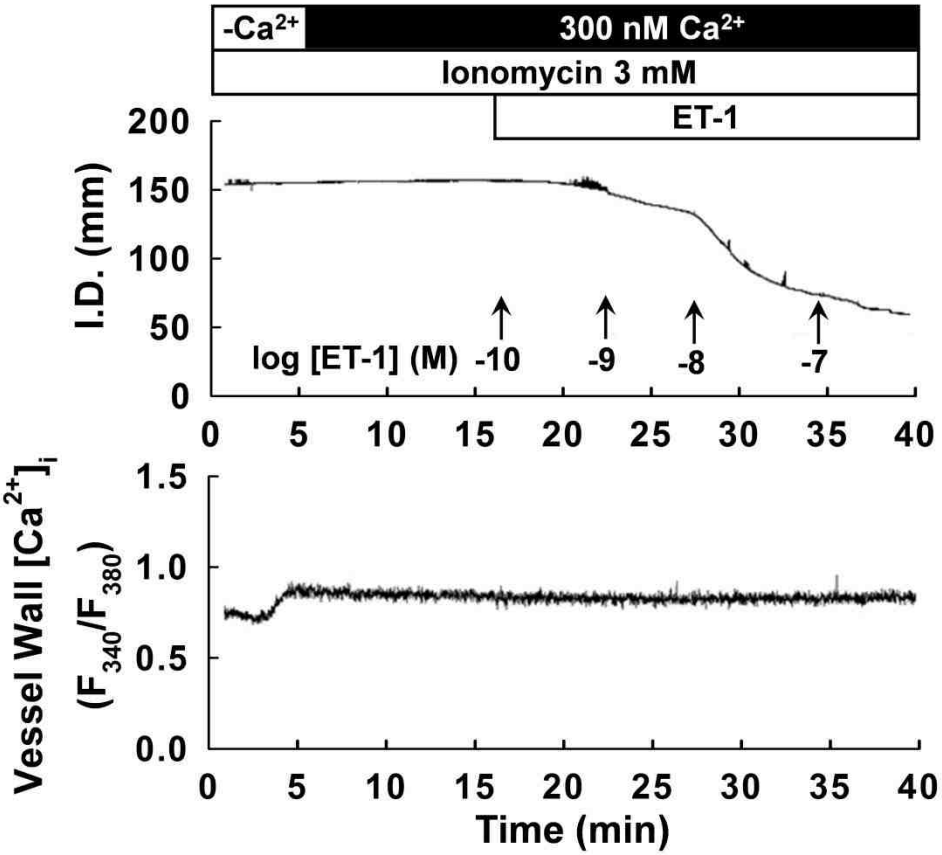

Figure 27. **Sample trace of ET-1 constriction in a Ca^{2+} permeabilized artery**. Raw traces of vasoconstrictor responses to ET-1 and vessel wall Ca^{2+} in a pressurized, endothelium-disrupted Ca^{2+} permeabilized pulmonary artery from a CH rat.

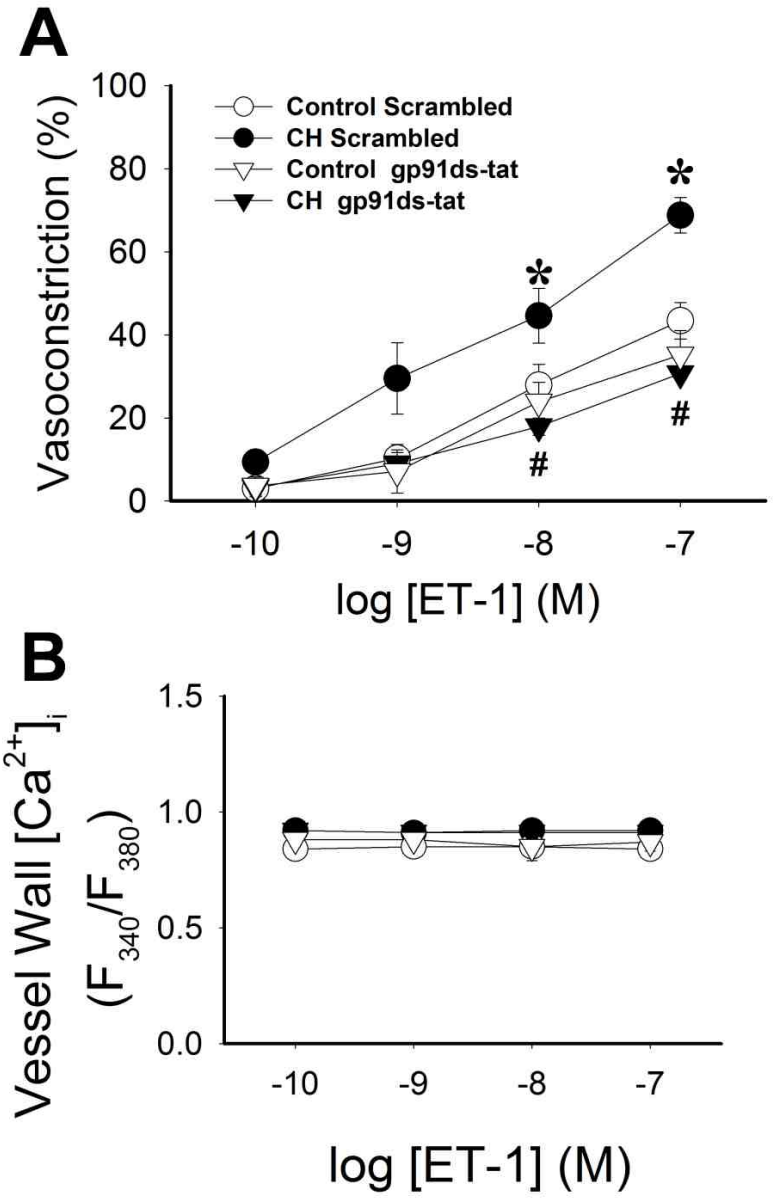

Figure 28. **Augmented ET-1-induced vasoconstriction following CH is NOX 2-dependent**. Vasoconstrictor (A) and vessel wall Ca^{2+} (B) responses to ET-1 in pressurized, endothelium-disrupted Ca^{2+} permeabilized pulmonary arteries from CH and control rats in the presence of the NOX 2 inhibitory peptide gp91ds-tat (50 μM) or its scrambled control peptide. Values are means ± SE n=5-7/group; *p<0.05 vs. respective control. #p<0.05 CH gp91ds-tat vs. CH scrambled.

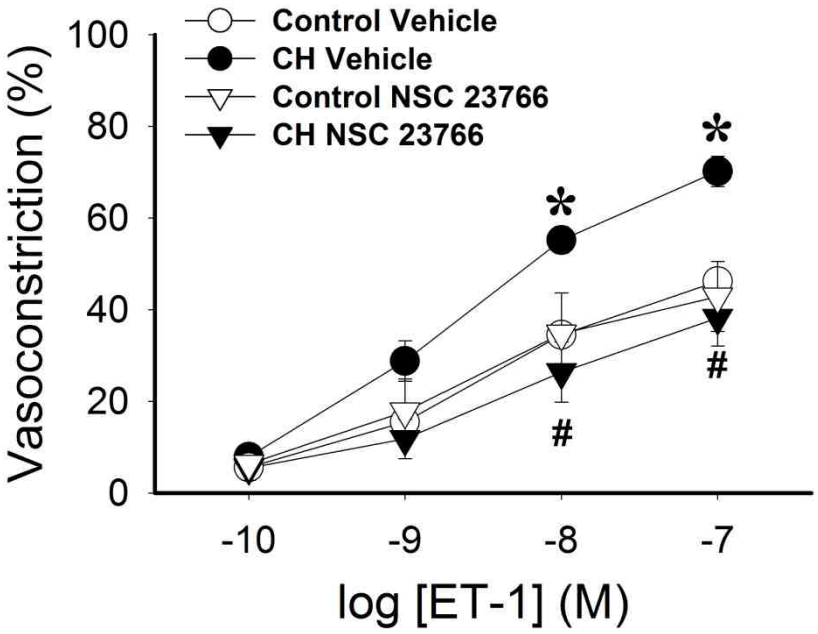

Figure 29. **Augmented ET-1-induced vasoconstriction following CH is Rac1-dependent**. Vasoconstrictor responses to ET-1 in pressurized, endothelium-disrupted pulmonary arteries from CH and control rats in the presence of the Rac1 inhibitor NSC23776 (50 µM) or vehicle. Values are means ± SE n=4-5/group; *p<0.05 vs. respective control. #p<0.05 CH NSC23776 vs. CH vehicle.

Effects of CH on pulmonary arterial NOX expression

To address whether enhanced pulmonary vasoreactivity and O_2^- production following CH are associated with an increase in NOX 2 expression, we measured levels of the catalytic subunit of NOX 2 ($gp91^{phox}$) in intrapulmonary arteries from CH and control rats. However, we observed no difference in NOX 2 levels between control and CH arterial homogenates when normalized to β actin expression (Fig. 30).

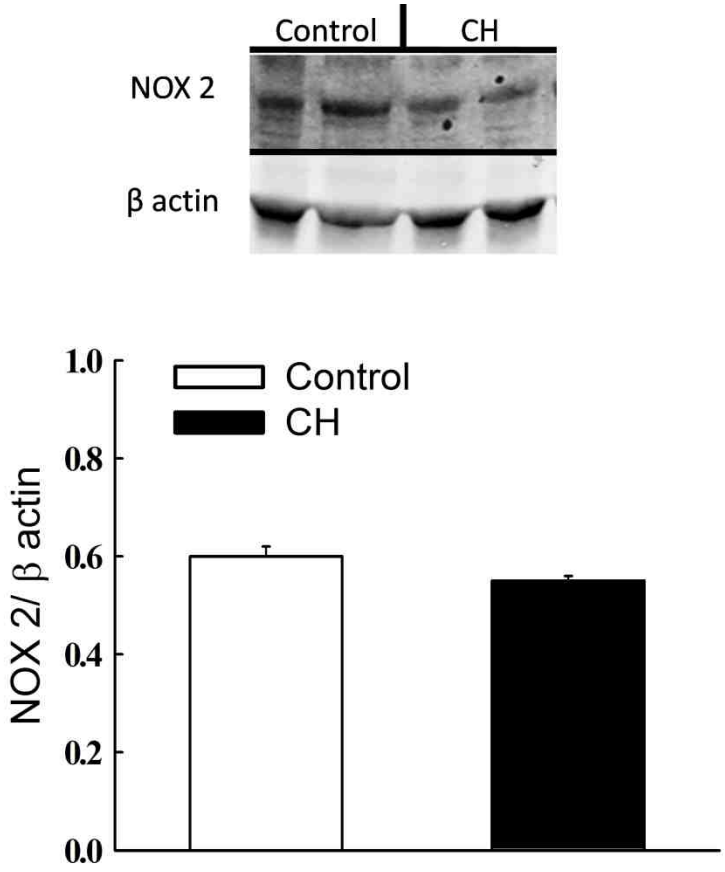

Figure 30. **Pulmonary arterial NOX 2 expression is not altered by CH exposure**. Representative Western blots and mean densitometric data for NOX 2 and β actin in intrapulmonary arteries from CH and control rats. Values are means ± SE n=4/group. There were no significant differences.

Aim 1 Major Findings

- NOX 2 mediates augmented KCl-dependent pulmonary arterial vasoconstriction, Ca^{2+} sensitization, and O_2^- production following CH (Figs. 14 and 16).

- Basal tone in arteries from pulmonary hypertensive animals requires NOX 2 (Fig. 24).

- The enhanced pulmonary arterial constriction to ET-1 following CH requires NOX 2 (Fig. 28).

- Rac1 is required for both basal tone and enhanced vasoconstrictor sensitivity to KCl and ET-1 in pulmonary arteries from animals exposed to CH (Figs. 19, 25, and 29).

- Pulmonary arterial NOX 2 catalytic subunit expression (gp91phox) is unaltered by CH exposure (Fig. 30).

SPECIFIC AIM 2

Identify the role of EGFR and Src kinase signaling in augmented pulmonary vasoconstrictor reactivity following CH.

Hypothesis:

We hypothesize that CH-dependent basal tone and enhanced depolarization-induced andET-1-mediated vasoconstriction require Src/EGFR signaling.

Role of EGFR and Src in enhanced depolarization-induced vasoconstriction following CH

To address the contribution of EGFR to enhanced depolarization-dependent VSM Ca^{2+} sensitization following CH, we further examined effects of the EGFR inhibitor AG 1478 on KCl-dependent vasoconstriction in Ca^{2+}-permeabilized arteries. AG 1478 attenuated KCl-dependent vasoconstriction in arteries from CH rats, while having no effect on arteries from control animals (Fig. 31). Inhibition of EGFR also normalized responses between groups. Additionally, to determine the effects of EGFR inhibition on ROS production, we measured DHE fluorescence over time following administration of KCl in pulmonary arteries in the presence and absence of the EGFR inhibitor. In contrast to NOX or Rac1 inhibition (Figs. 15,16, and 20), inhibition of EGFR did not prevent the effect of CH to increase basal O_2^- generation (Fig. 32). However, AG 1478 prevented KCl-dependent increases in DHE fluorescence in the arteries from rats exposed to CH.

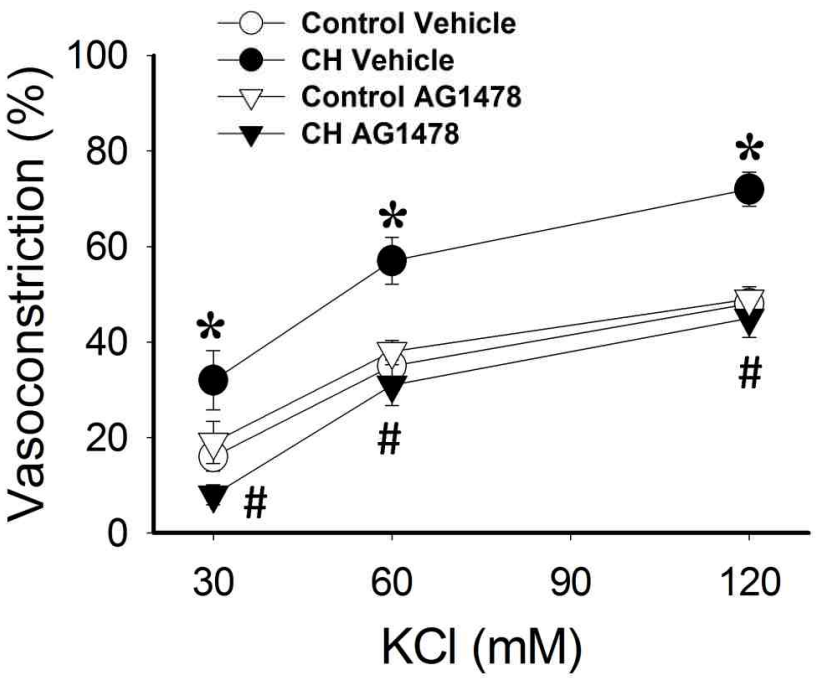

Figure 31. **EGFR is necessary for enhanced KCl-mediated vasoconstriction and Ca^{2+} sensitization in arteries from CH rats**. Vasoconstrictor responses to KCl in pressurized, Ca^{2+} permeabilized, endothelial disrupted pulmonary arteries from CH and control rats in the presence of the EGFR inhibitor, AG 1478 (1 μM), or its scrambled control peptide. Values are means ± SE n=4-5/group; *p<0.05 vs. control. #p<0.05 vs. CH vehicle.

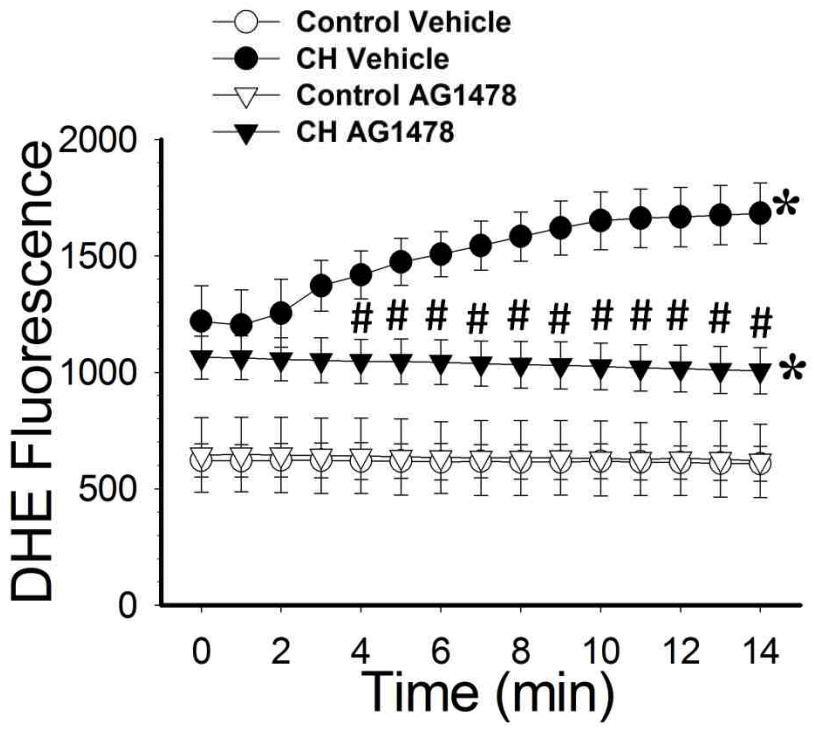

Figure 32. **EGFR contributes to CH-dependent increases in depolarization-stimulated O_2^- levels in pulmonary arteries**. DHE fluorescence under basal conditions and following administration of KCl (60 mM) in pressurized, endothelium-disrupted, Ca^{2+} permeabilized pulmonary arteries from CH and control rats in the presence or absence of AG 1478 (1 µM). KCl was administered 1 min into recording. Values are means ± SE n=4-5/group; *p<0.05 vs. control at each time point. #p<0.05 vs. CH vehicle. τp<0.05 vs. CH vehicle.

Next, we sought to define the signaling relationship between EGFR and KCl-dependent Rac1 activation in Ca^{2+}-permeabilized pulmonary arteries from control and CH rats with a Rac1-GTP pull-down assay. EGFR inhibition abolished KCl-induced increases in Rac1 activity observed in CH arteries (Fig. 33).

EGFR activity was assessed as the ratio of phosphorylated (Tyr 1068) to total EGFR levels. Basal levels of phosphorylated EGFR were not different between control and CH arteries (Fig. 34). KCl led to an increase in active (phosphorylated) EGFR in CH arteries while having no effect in control arteries. No differences were detected in total EGFR expression (normalized to β actin, Fig. 35).

We next tested the role of Src kinases in this response with the inhibitors PP2 and SU6656. Similar to EGFR and NOX inhibition, blockade of Src kinases attenuated KCl-induced vasoconstriction in pulmonary arteries from CH rats (Fig. 36). Interestingly, at the highest concentration of KCl (120 mM) Src kinase inhibition did not fully normalize reactivity to the level of controls.

Contribution of EGFR and Src to basal tone following CH

We hypothesized that similar to depolarization-dependent vasoconstriction, EGFR and Src kinases are important mediators of pressure-dependent basal arterial tone in arteries from pulmonary hypertensive rats. Consistent with this hypothesis, we observed that the EGFR inhibitors AG 1478 and gefitinib prevented pressure-dependent tone in pulmonary arteries from CH rats (Fig. 37 A and B). We additionally sought to examine the role of Src kinase

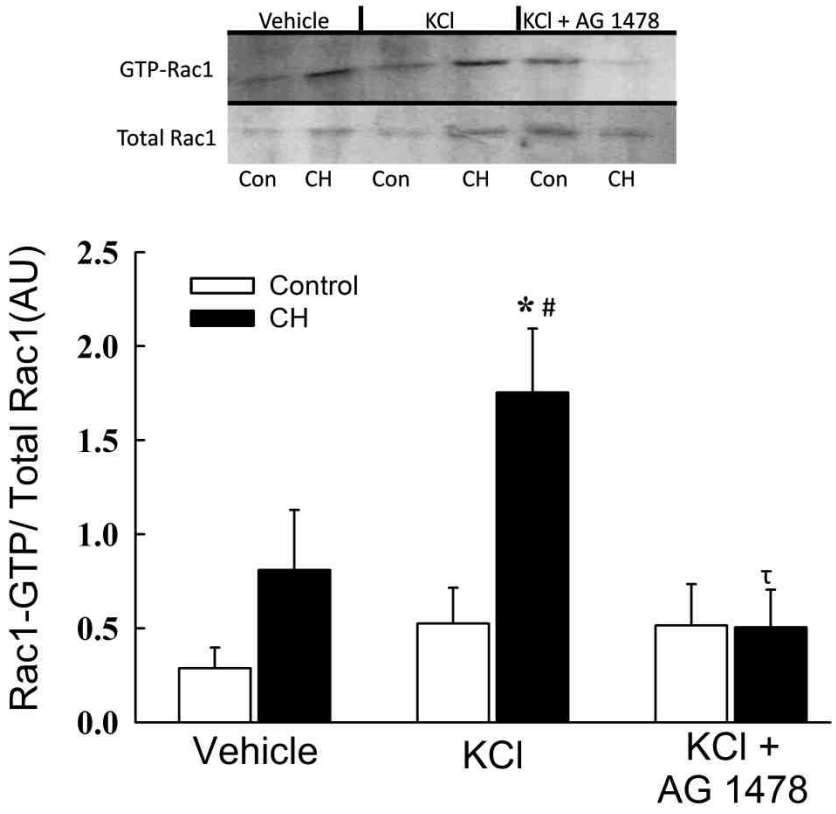

Figure 33. **Depolarization mediates EGFR-dependent Rac1 activation in arteries from CH but not control rats.** Representative Western blots and mean densitometric data for GTP bound (active) Rac1 normalized to total Rac1 in homogenates from control and CH intrapulmonary arteries. Active Rac1 was measured under baseline conditions, and following 10 min stimulation with KCl (60 mM) or KCl plus the EGFR inhibitor AG1478 (1 µM). Values are means ± SE n=4/group; *p<0.05 vs. control KCl. #p<0.05 vs. CH vehicle. τp<0.05 vs. CH KCl.

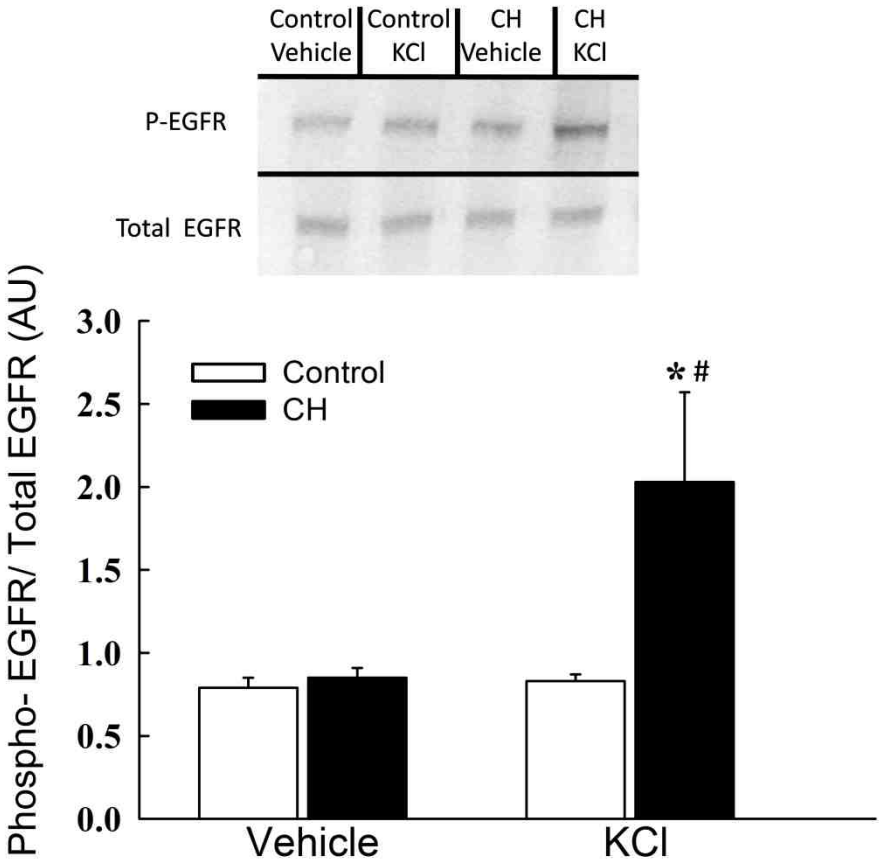

Figure 34. **EGFR phosphorylation is induced by KCl in arteries from CH but not control rats**. Representative Western blots and mean densitometric data for phosphorylated (active) EGFR normalized to total EGFR in pulmonary arterial homogenates from control and CH intrapulmonary arteries. Phosphorylated and total EGFR were measured under baseline and KCl-stimulated (60 mM) conditions. Values are means ± SE n=7/group. *p<0.05 vs. control KCl. #p<0.05 vs. CH vehicle.

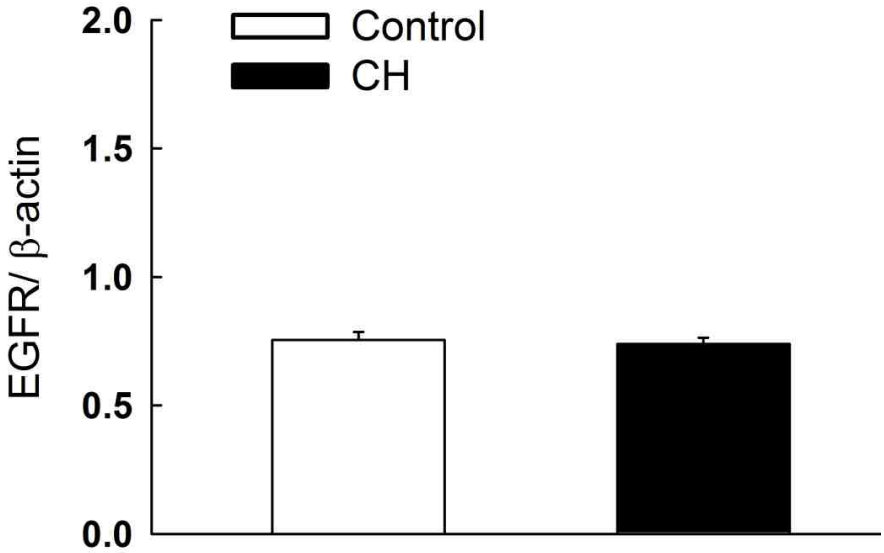

Figure 35. **EGFR expression is not altered by CH**. Mean densitometric data for EGFR in intrapulmonary arteries from normoxic and CH rats normalized to β-actin expression. Values are means ± SE n=14/group; no significant differences were detected.

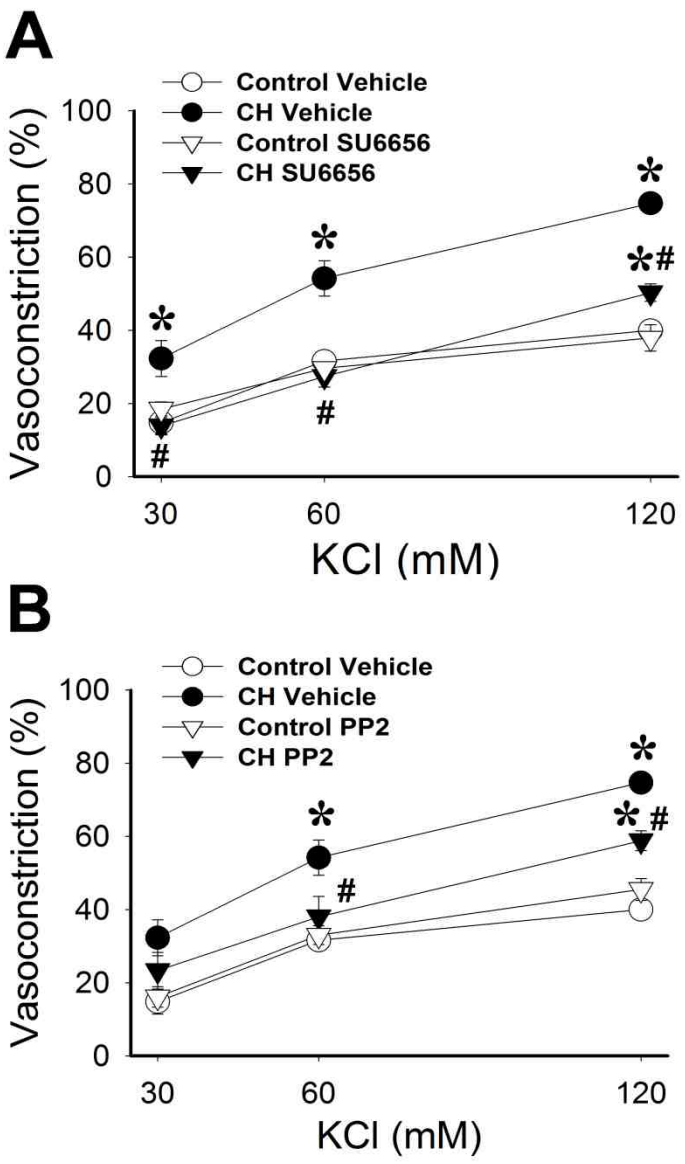

Figure 36. **Enhanced KCl-dependent vasoconstriction and Ca^{2+} sensitization in arteries from CH rats requires Src**. Vasoconstrictor responses to KCl in pressurized, Ca^{2+} permeabilized, endothelial disrupted pulmonary arteries from CH and control rats in the presence of the Src inhibitors SU6656 (10 μM) and PP2 (10 μM). Values are means ± SE n=4-5/group; *p<0.05 vs. control. #p<0.05 vs. CH vehicle.

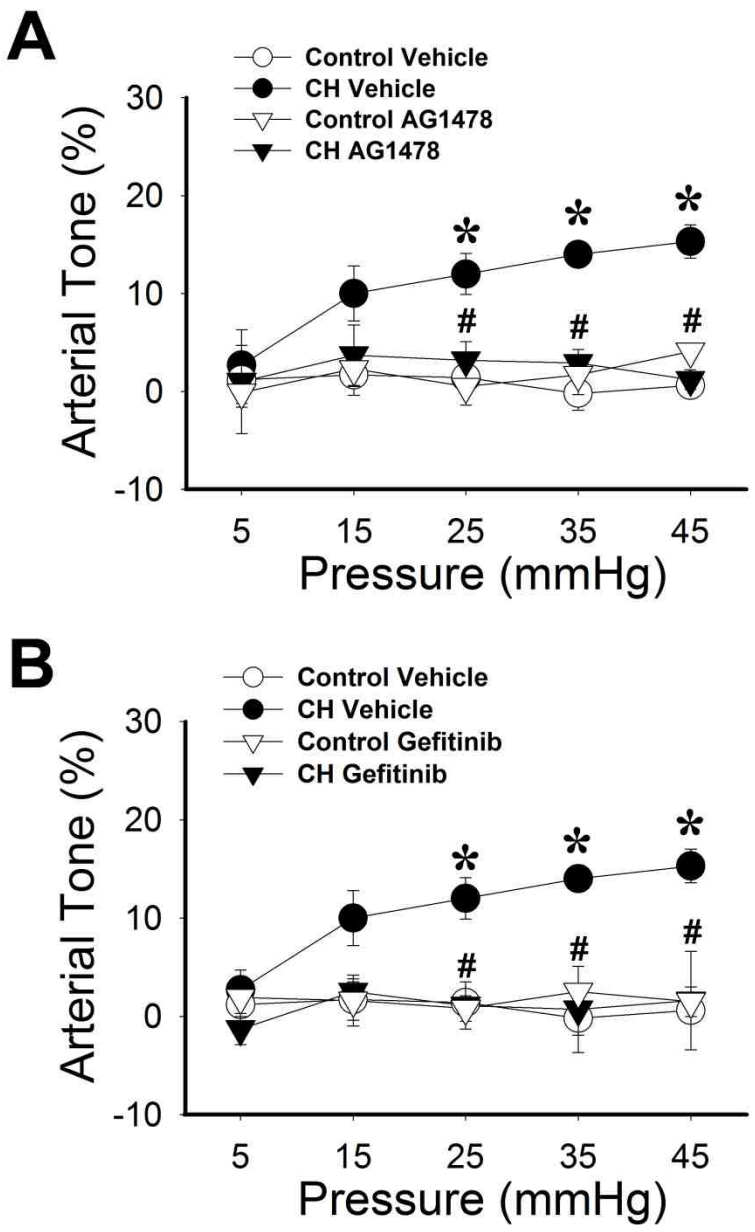

Figure 37. **Enhanced pressure-dependent arterial tone in arteries from CH rats requires EGFR**. Pressure-dependent tone in pressurized, endothelial disrupted pulmonary arteries from CH and control rats in the presence of the EGFR inhibitors AG 1478 (1 μM, A) and gefitinib (50 μM), or their respective vehicles. Values are means ± SE n=4-5/group; *p<0.05 vs. control. #p<0.05 vs. CH vehicle.

in this response by repeating the basal tone protocol in the presence and absence of Src kinase inhibition. We found that inhibition of Src kinases with SU 6656 similarly prevented the development of basal tone (Fig. 38).

Role of EGFR and Src in enhanced ET-1-mediated vasoconstriction following CH

We assessed the contribution of EGFR to enhanced agonist-dependent VSM Ca^{2+} sensitization following CH by examining effects of AG 1478 on ET-1-dependentvasoconstriction in Ca^{2+}-permeabilized arteries. EGFR inhibition attenuated ET-1-dependent vasoconstriction in arteries from CH rats, while having no effect on the arteries from control animals (Fig. 39). Similar to effects of Src kinase inhibition to attenuate CH-induced basal tone and enhanced KCl-dependent vasoconstriction (Figs. 38 and 36 respectively), SU 6656 inhibition also prevented enhanced vasoreactivity to ET-1 resulting in similar responses between groups (Fig. 40).

Basal and ET-1 stimulated ROS production was measured by DHE fluorescence in isolatedCa^{2+}-permeabilized PASMCs from CH and control rats. DHE fluorescence was not different between control and CH cells (Fig 41). ET-1 selectively increased DHE fluorescence in PASMCs from rats exposed to CH, while having no effect in control PASMCs. The EGFR inhibitor, AG 1478, prevented ET-1 induced increases in DHE fluorescence in cells from CH rats resulting in similar fluorescence between groups.

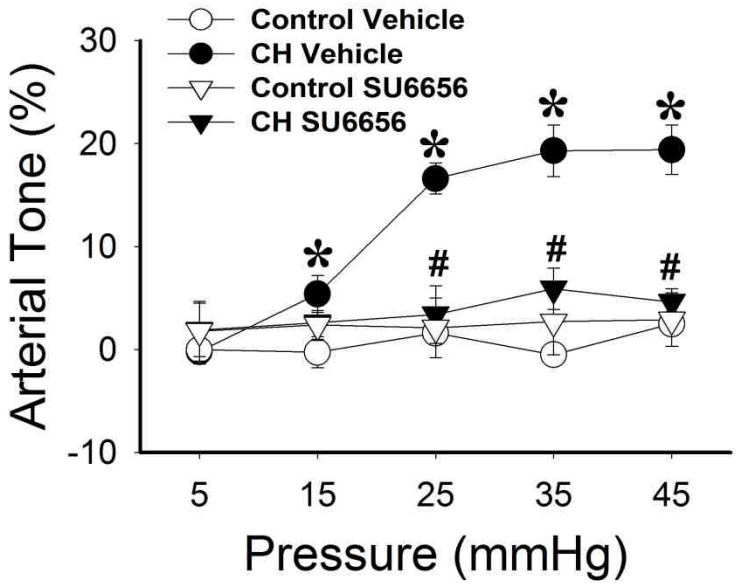

Figure 38. **Src kinases are necessary for CH-dependent basal tone**. Pressure-dependent basal tone in the presence of the Src kinase inhibitor SU 6656 (10 μM) or its vehicle in endothelium-disrupted arteries from CH and control rats. Values are means ± SE n=4/group; *p<0.05 vs. control. #p<0.05 vs. CH vehicle.

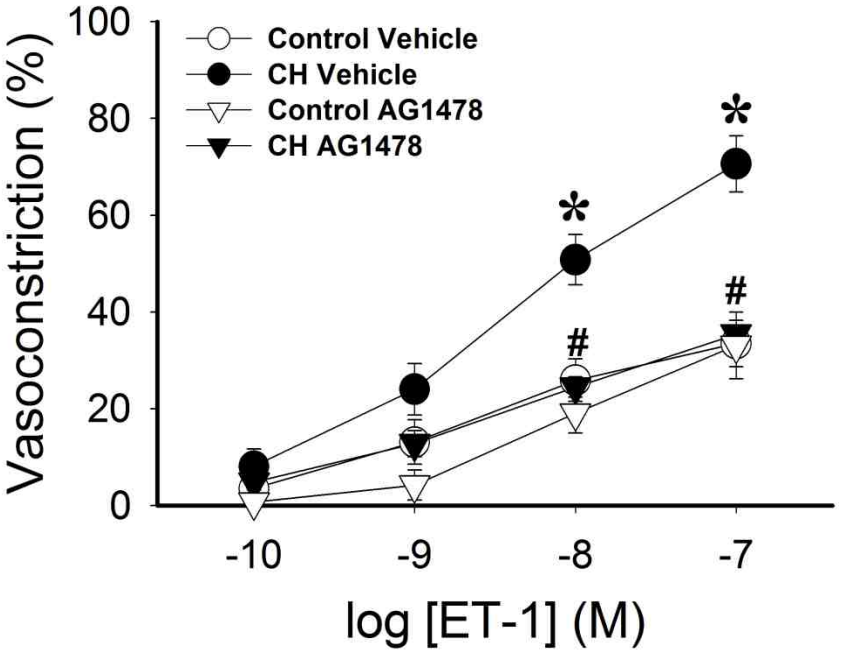

Figure 39. **CH-dependent enhanced vasoconstriction to ET-1 requires EGFR**. Vasoconstrictor responses to ET-1 in pressurized, Ca^{2+} permeabilized, endothelial disrupted pulmonary arteries from CH and control rats in the presence of the specific EGFR inhibitor, AG 1478 (1 µM), or vehicle. Values are means ± SE n=4-6/group; *p<0.05 vs. control. #p<0.05 vs. CH vehicle.

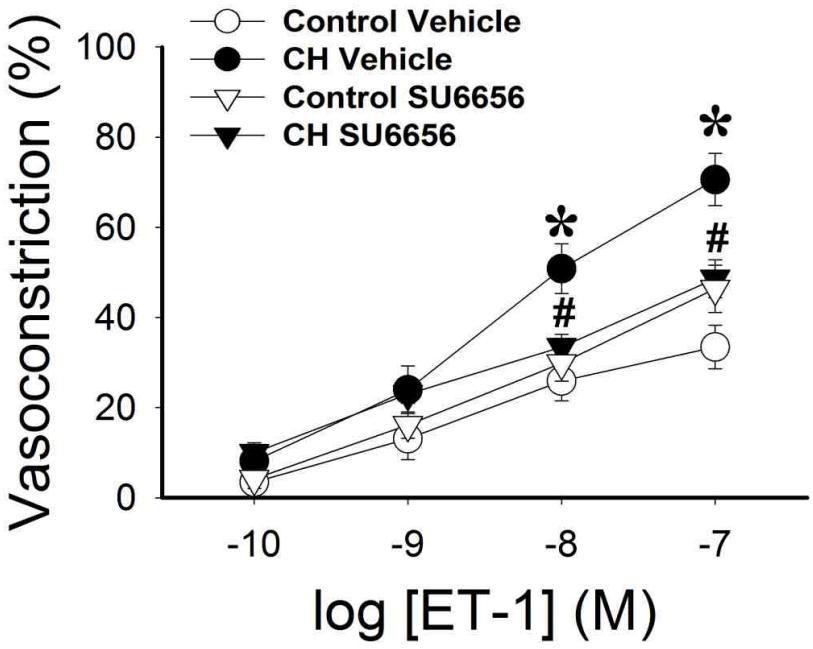

Figure 40. **Src kinases contribute to enhanced ET-1-mediated vasoconstriction and Ca^{2+} sensitization following CH**. Vasoconstrictor responses to ET-1 in pressurized, Ca^{2+} permeabilized, endothelial disrupted pulmonary arteries from CH and control rats in the presence of SU 6656 (10 μM), or its vehicle. Values are means ± SE n=4/group; *p<0.05 vs. control. #p<0.05 vs. CH vehicle.

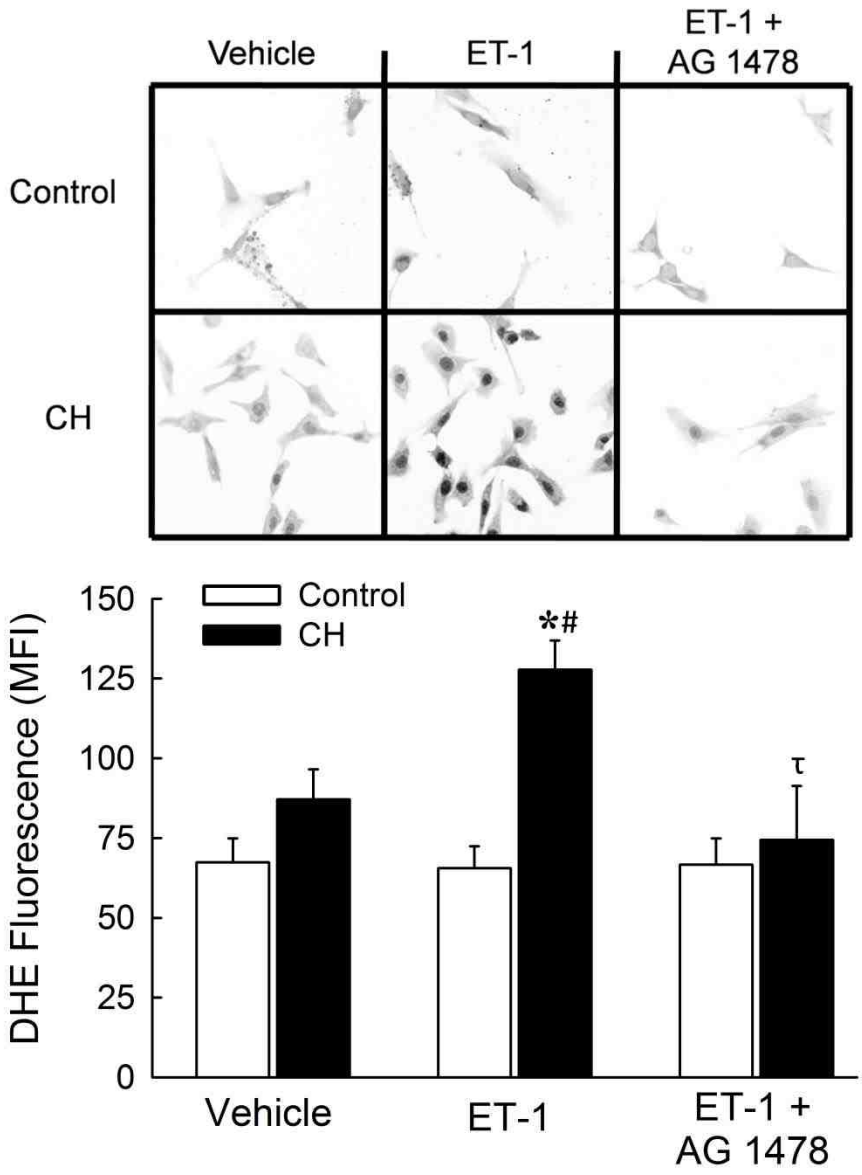

Figure 41. **O_2^- production induced by ET-1 in PASMCs from CH rats requires EGFR**. Digitally inverted representative images and mean fluorescence intensity (MFI) of DHE fluorescence in thresholded images of PASMCs from CH and control rats. Cells were treated with vehicle, ET-1 (10^{-8} M) and ET-1 plus the EGFR inhibitor AG 1478. Values are means ± SE n=4-7/group. *p<0.05 vs. vehicle. #p<0.05 vs. CH vehicle. τp<0.05 vs. CH ET-1.

To further evaluate to role of Src kinases in enhanced vasoconstriction following CH, we measured basal and ET-1 stimulated Src kinase activity in pulmonary arterial homogenates from CH and control rats. No statistically significant differences were detected in basal Src activity (Fig. 42). However, following ET-1 stimulation, Src kinase phosphorylation (indicative of activity) was greater in CH arteries compared to controls. No differences were detected in total Src kinase expression (Fig. 43).

Mechanisms of EGF-Induced Vasoconstriction

To further characterize the role of EGFR in this response, nonpermeabilized pulmonary arteries from CH and control animals were stimulated with increasing concentration of EGF to directly activate EGFR. Interestingly, EGF caused a robust vasoconstriction in arteries from CH rats, while having little effect in control arteries (Fig 44A). There was no significant Ca^{2+} increase associated with the EGF-induced vasoconstriction, suggesting a role for Ca^{2+} sensitization in this response (Fig 44B).

We next sought to determine if EGF causes EGFR dependent constriction in arteries from CH rats through a similar signaling cascade that mediates enhanced reactivity to KCl and ET-1 and facilitates the development of basal tone. Both ROK inhibition (Fig 42A) and NOX 2 inhibition (Fig 42B) prevented vasoconstriction to EGF in pulmonary arteries from CH rats. Furthermore, AG

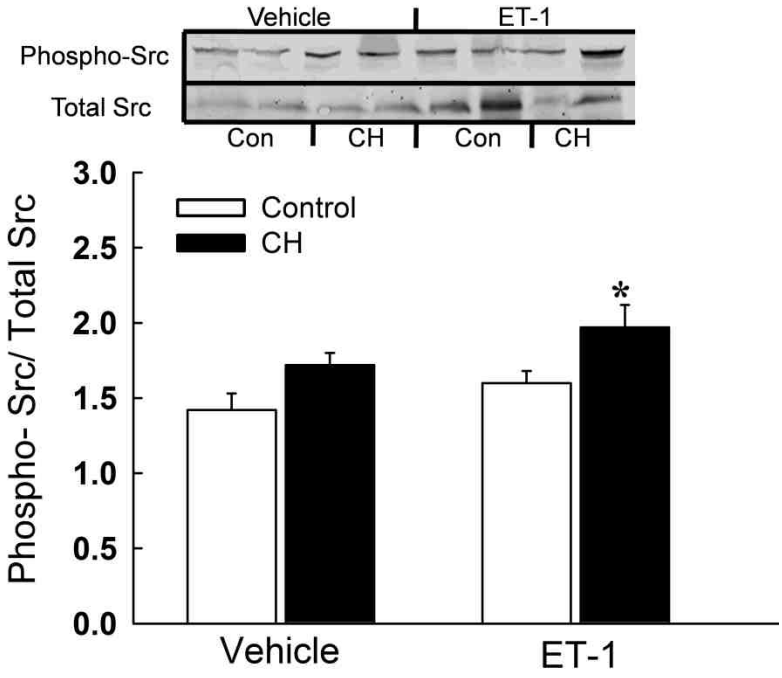

Figure 42. **Src tyrosine 416 phosphorylation is induced by ET-1 in arteries from CH rats**. Representative Western blots and mean densitometric data for phosphorylated (active) Src normalized to total Src in pulmonary arterial homogenates from control and CH intrapulmonary arteries. Phosphorylated and total Src were measured under baseline and KCl-stimulated (60 mM) conditions. Values are means ± SE n=4/group. *p<0.05 vs. control ET-1.

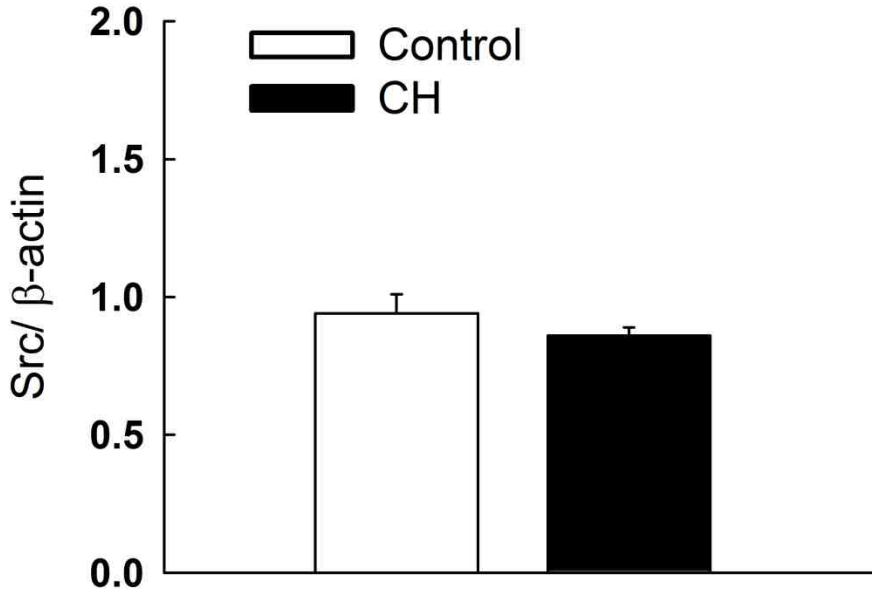

Figure 43. **CH does not alter Src kinase expression is in pulmonary arteries.** Mean densitometric data for Src kinase expression normalized to β-actin expression in intrapulmonary arteries from normoxic and CH rats. Values are means± SE n=8/group; there were no significant differences.

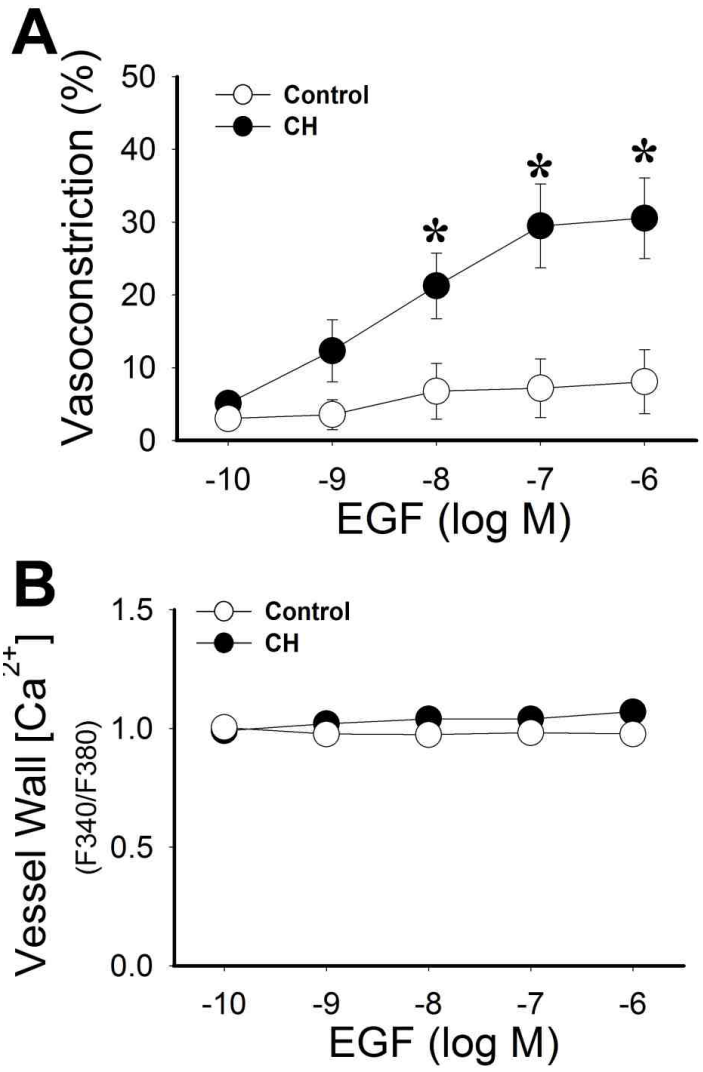

Figure 44. **EGF causes pulmonary vasoconstriction only in arteries from CH rats.** A) Vasoconstrictor and B) vessel wall Ca^{2+} responses to EGF in pressurized, endothelium disrupted pulmonary arteries from CH and control rats. Values are means ± SE n=4-5/group; *p<0.05 vs. control.

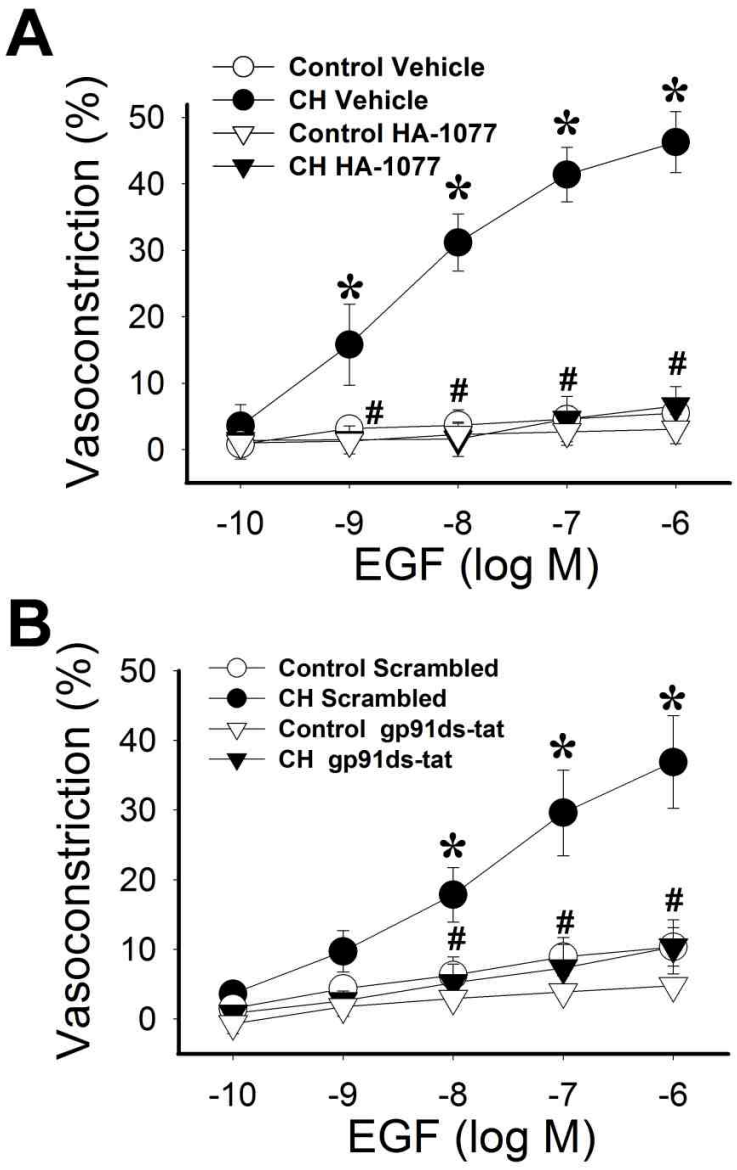

Figure 45. **EGF-induced vasoconstriction of pulmonary arteries from CH rats requires ROK and NOX 2.** Vasoconstriction to EGF in arteries from CH and control rats in the presence of a ROK inhibitor (HA-1077, 10μM;A), the NOX 2 inhibitory peptide (gp91ds-tat, 50 μM; B), or their respective vehicles. All arteries were endothelium-disrupted. Values are means ± SE n=4-5/group; *p<0.05 vs. control. #p<0.05 vs. CH vehicle.

1478 prevented EGF-induced vasoconstriction in arteries from CH rats (Fig. 46A), confirming a role for EGFR in this response. Finally, we wished to examine the role of Src kinases in EGF-induced vasoconstriction in CH arteries to determine if Src kinases signal proximally or distally to EGFR. Src inhibition was without effect on either group of arteries suggesting that Src kinases are not involved in EGF-induced vasoconstriction (Fig. 46B).

Role of matrix metalloproteinases in enhanced pulmonary vasoconstriction following CH

As experimental evidence exists for Src kinase to active EGFR through both MMP-dependent (18; 236; 263) and MMP-independent mechanisms (87; 146; 190; 234), we initially examined vasoconstrictor responses to ET-1 in the presence of a general MMP inhibitor, GM6001, in Ca^{2+} permeabilized pulmonary arteries. We found the MMP inhibition prevented the effect of CH to augment vasoconstriction to ET-1 and further normalized responses between groups (Fig. 47).

As members of the gelatinase family of MMPs are likely mediators of this response (see Introduction page 22), we further investigated the roles of the gelatinases MMP 2 and MMP 9 in enhanced vasoconstriction to ET-1 following CH. MMP 2 inhibition with MMP 2 inhibitor 3 prevented enhanced vasoconstriction to ET-1 in CH arteries and resulted in a similar degree of vasoconstriction in arteries from each group (Fig. 48). Consistent with previous results (124; 131; 240), we observed an effect of CH to increase MMP 2

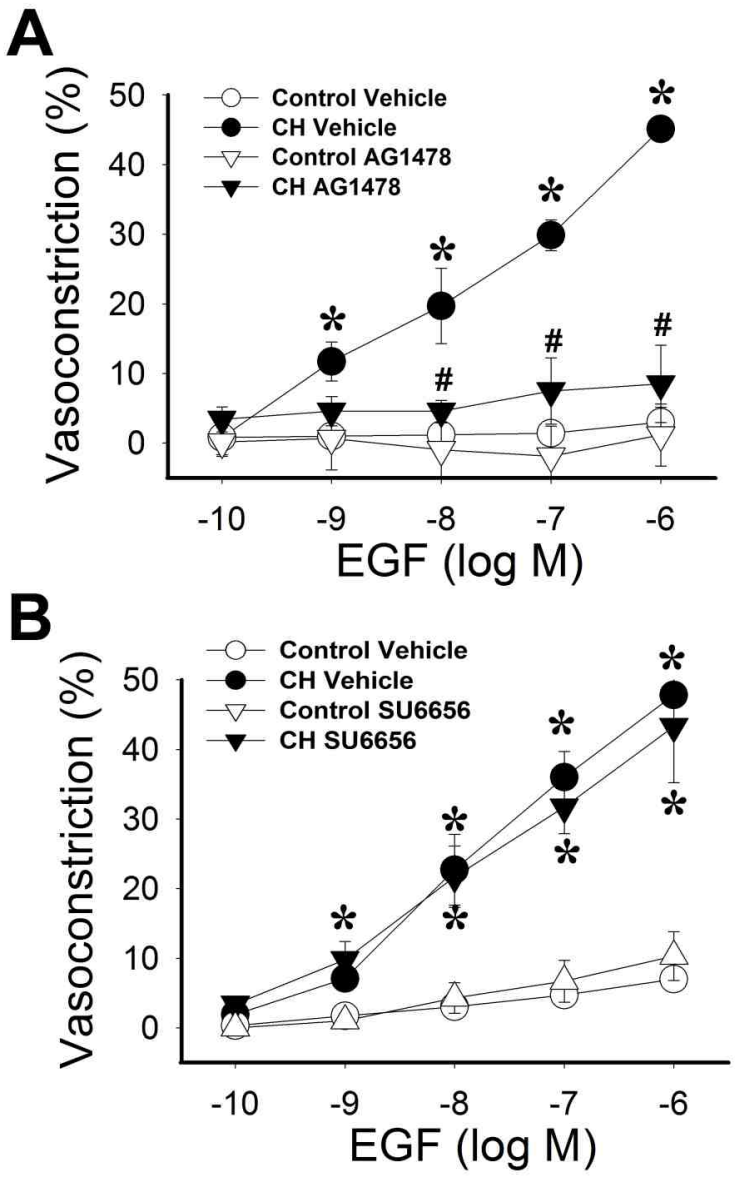

Figure 46. **EGF-dependent vasoconstriction following CH requires EGFR but not Src kinases.** Vasoconstrictor responses to EGF in pressurized, endothelium disrupted pulmonary arteries from CH and control rats. Experiments were performed in the presence or absence of (AG 1478, 1μM;A) and (SU 6656, 10μM; B). Values are means ± SE n=4-5/group; *p<0.05 vs. control. #p<0.05 vs. CH vehicle.

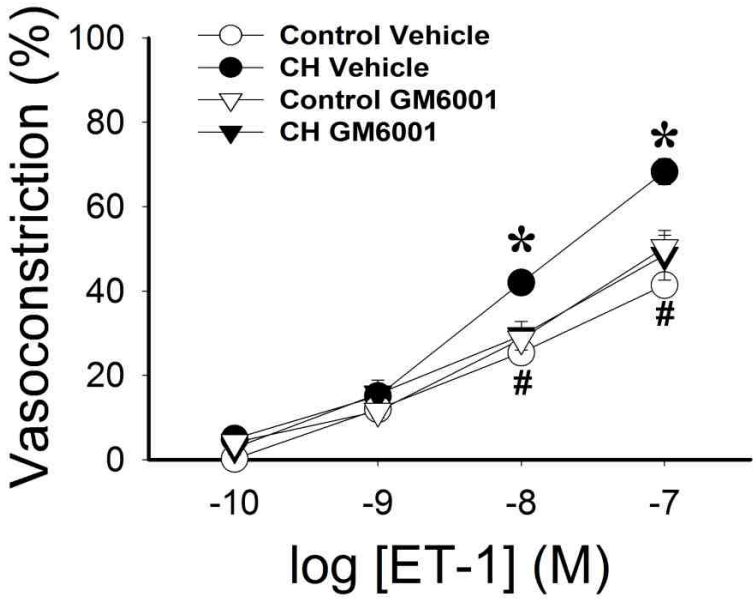

Figure 47. **General MMP inhibition prevents augmented vasoconstriction to ET-1 following CH.** Vasoconstrictor responses to ET-1 in pressurized, Ca^{2+} permeabilized, endothelium disrupted pulmonary arteries from CH and control rats in the presence of GM6001 (15 µM), or vehicle. Values are means ± SE n=4-5/group; *p<0.05 vs. control. #p<0.05 vs. CH vehicle.

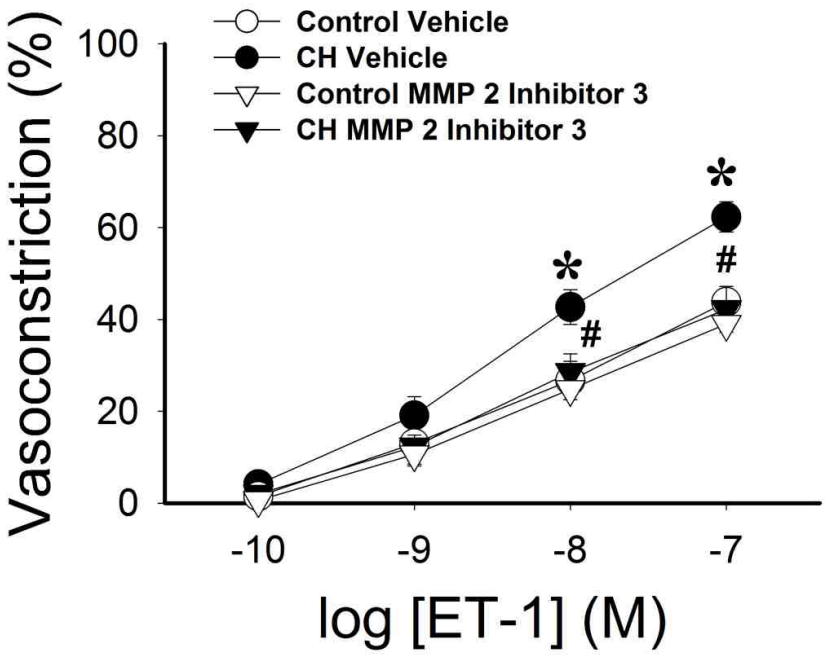

Figure 48. **MMP2 is required from enhanced vasoconstriction to ET-1 following CH.** Vasoconstrictor responses to ET-1 in pressurized, Ca^{2+} permeabilized, endothelial disrupted pulmonary arteries from CH and control rats in the presence of the MMP 2 inhibitor, MMP 2 inhibitor 3 (AP-100, 100 nM), or vehicle. Values are means ± SE n=4/group; *p<0.05 vs. control. #p<0.05 vs. CH vehicle.

expression (Fig. 49). MMP 9 inhibition with MMP 9 inhibitor 2 attenuated vasoconstriction at the highest concentration of ET-1 (Fig. 50), but responses in CH arteries remained augmented compared to control arteries. No significant differences in MMP 9 expression were detected between groups (Fig. 51).

ADAM-17 is also capable of EGF shedding (195), and has an established role in ET-1 signaling (234). We tested the role of ADAM-17 in enhanced ET-1 induced vasoconstriction with the ADAM-17 inhibitor TAPI-1. TAPI-1 slightly attenuated the response to ET-1 at the highest concentration of ET-1 (10^{-7} M), but augmented vasoconstriction to ET-1 following CH persisted (Fig. 52). Furthermore ADAM-17 expression was unaltered following exposure to CH (Fig. 53).

Role of ETR in metabotropic transduction of membrane depolarization and increased intraluminal pressure to enhanced vasoreactivity following CH

We next tested the hypothesis that ETR couple membrane depolarization and vessel wall stretch to EGFR-mediated calcium sensitization and vasoconstriction in arteries from CH rats. However, combined inhibition of ETA and ETB receptors with BQ-123 and BQ-788 (10 μM each) was without effect on either KCl-dependent vasoconstriction (Fig. 54) or basal tone (Fig. 55) in arteries from CH rats.

Contribution of EGFR to CH-induced PH

To evaluate the role of EGFR signaling in the development of CH-induced PH, we treated animals daily for four weeks with an EGFR inhibitor, gefitinib (30 mg/kg/day) or vehicle pills administered orally. Animals exposed to CH had

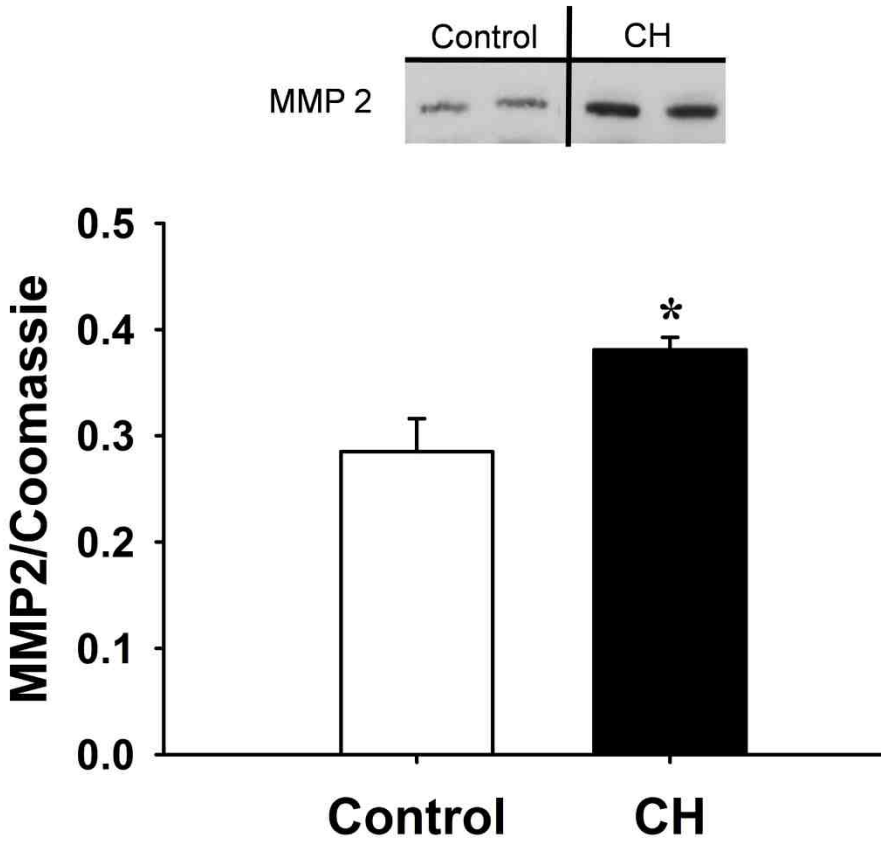

Figure 49. **MMP2 expression is increased in arteries from CH rats.** Western blots and mean densitometric data for MMP 2 in intrapulmonary arteries from normoxic and CH rats. Values are means ± SE n=4/group; *p<0.05 vs. control.

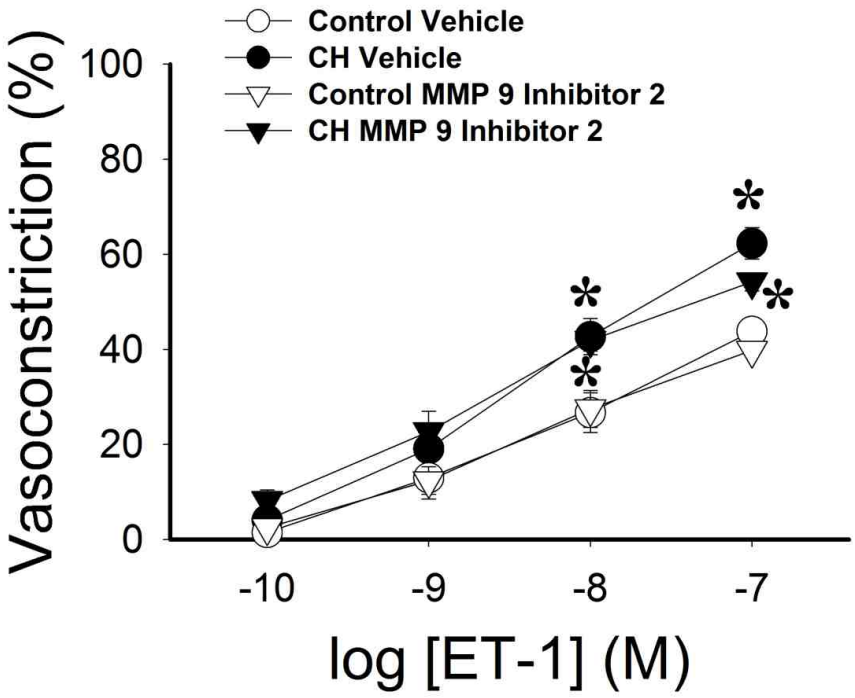

Figure 50. **MMP 9 does not contribute to augmented vasoconstriction to ET-1 following CH.** Vasoconstrictor responses to ET-1 in pressurized, Ca^{2+} permeabilized, endothelium disrupted pulmonary arteries from CH and control rats in the presence of the MMP 9 inhibitor, MMP 9 inhibitor 2 (10 µM), or vehicle. Values are means± SE n=4/group; *p<0.05 vs. control. #p<0.05 vs. CH vehicle.

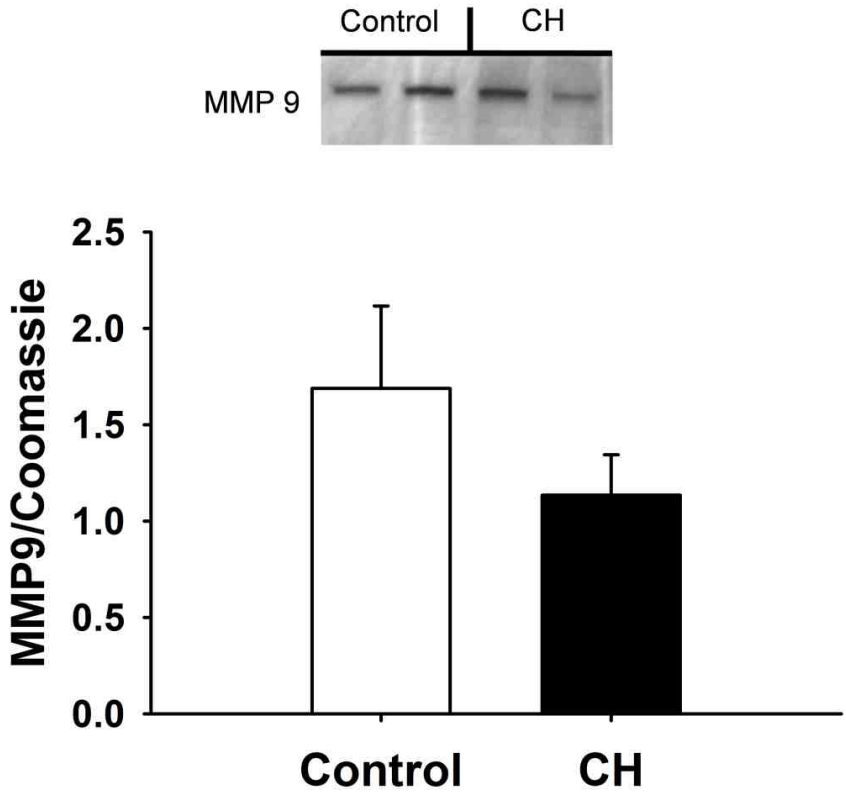

Figure 51. **MMP9 expression is not altered by CH.** Western blots and mean densitometric data for MMP 9 in intrapulmonary arteries from normoxic and CH rats. Values are means ± SE n=4/group; no significant differences were detected.

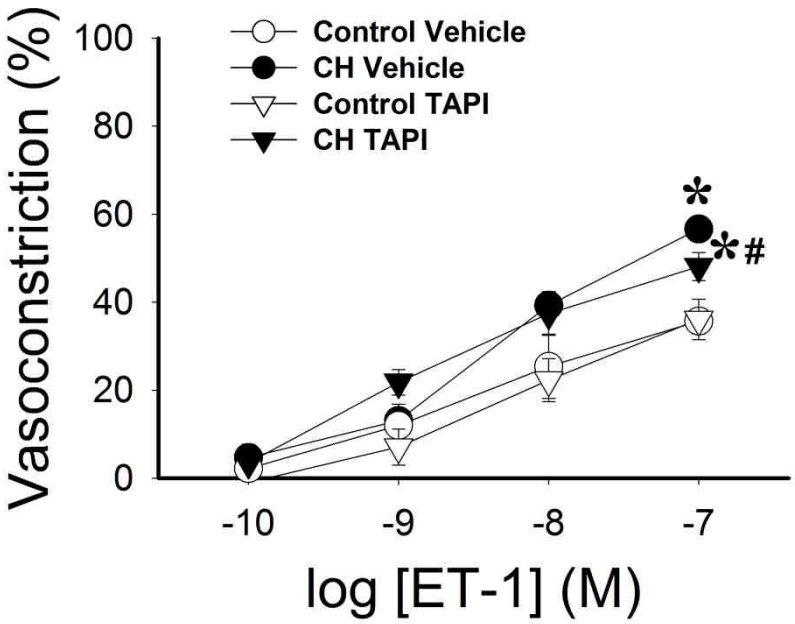

Figure 52. **ADAM-17 inhibition does not prevent augmented vasoconstriction to ET-1 following CH.** Vasoconstrictor responses to ET-1 in pressurized, Ca^{2+} permeabilized, endothelium disrupted pulmonary arteries from CH and control rats in the presence of the ADAM-17 inhibitor, TAPI-1 (10 µM) or vehicle. Values are means ± SE n=4-5/group; *p<0.05 vs. control. #p<0.05 vs. CH vehicle.

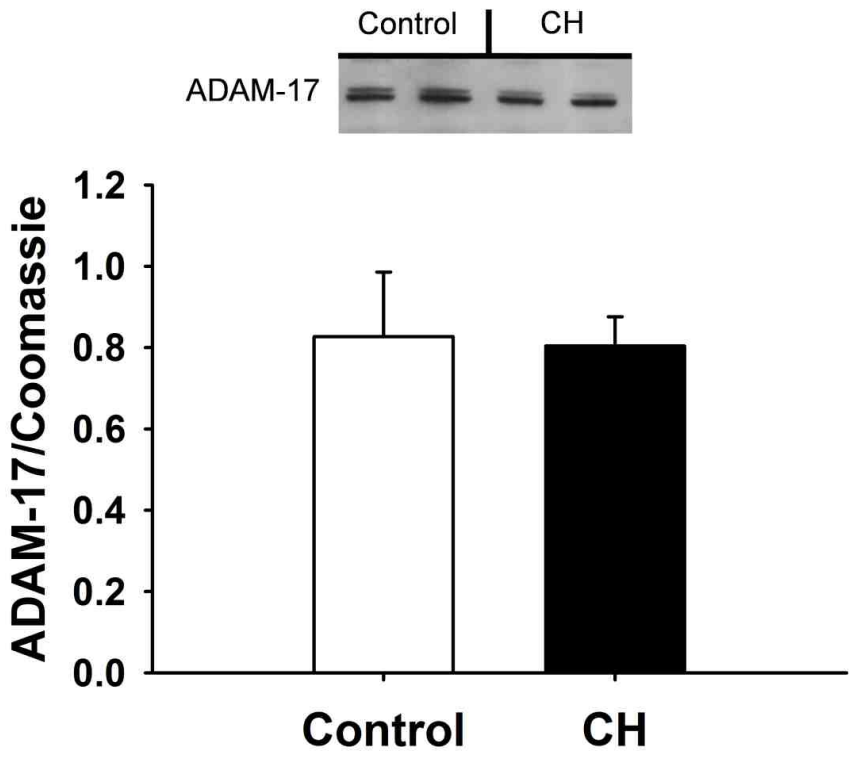

Figure 53. **ADAM-17 expression is not altered by CH.** Western blots and mean densitometric data for ADAM-17 in intrapulmonary arteries from normoxic and CH rats. Values are means ± SE n=4/group; no significant differences were detected.

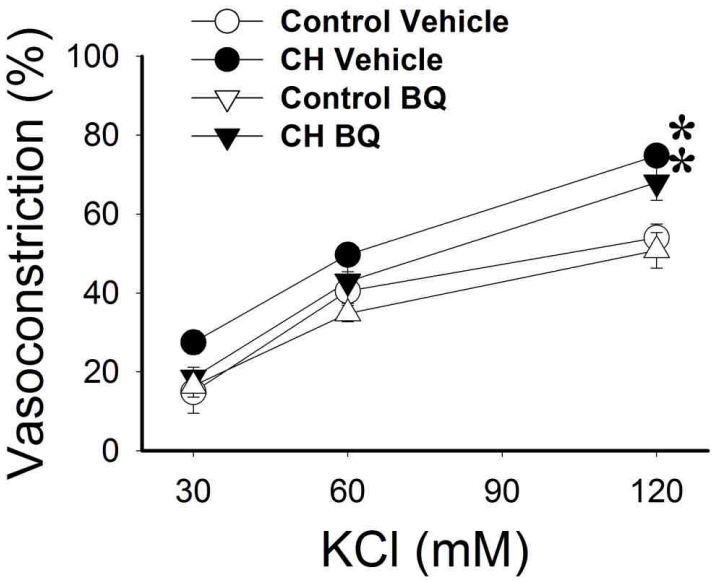

Figure 54. **ETR signaling does not contribute to vasoconstriction to KCl following CH.** Vasoconstrictor responses to KCl in pressurized, Ca^{2+} permeabilized, endothelium disrupted pulmonary arteries from CH and control rats in the presence of BQ 123 and BQ 778 (10 µM each). Values are means ± SE n=4-5/group. *p<0.05 vs. control

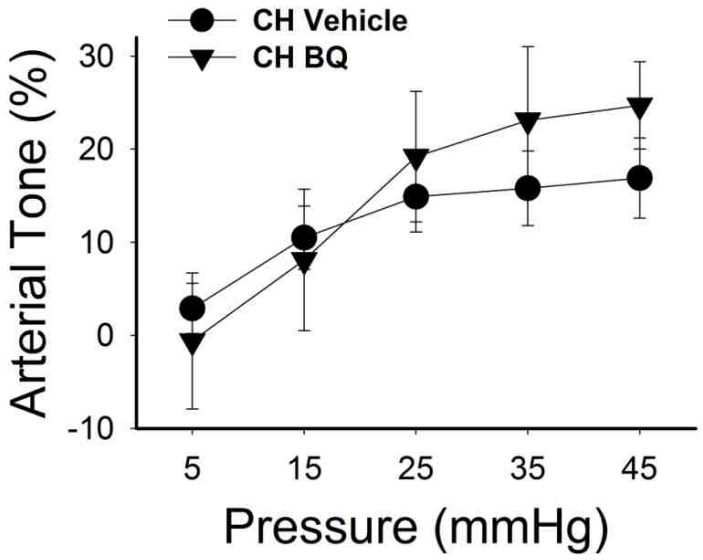

Figure 55. **ETRs do not contribute to CH-dependent basal tone.** Basal arterial tone in small pulmonary arteries from CH rats in the presence or absence of BQ 123 and BQ 778 (10 μM each). Values are means ± SE n=4-5/group. No significant differences.

reduced body weight (BW) compared to normoxic rats (Table 1). Treatment with the EGFR inhibitor had no effect of body weight in either CH or control animals. We additionally measured hematocrit in these animals and observed that CH-dependent polycythemia does not require EGFR (Fig. 56).

Previous studies have implicated EGFR as a contributing factor to monocrotaline-induced vascular remodeling in rats (42). Our results demonstrate that the EGFR inhibitor gefitinib attenuated, but did not prevent vascular remodeling following CH (Fig 57A and 57B). Gefitinib also reduced the increased muscularization of small (<20 μm) pulmonary arteries associated with CH (Fig. 58).

We observed increased RV weight, RV/BW (Table 1), and RV/LV+S ratios (Fig. 59) in CH rats compared to controls in both vehicle and gefitinib treated animals. However, gefitinib treated CH animals displayed a significantly lower RV/LV+S than rats treated with vehicle pills suggesting a role for EGFR in right ventricular hypertrophy. LV+S/BW ratios were not significantly different between groups (Table 1).

In animals treated with vehicle pills, we observed a significant increase in peak right ventricular pressure associated with CH (Fig. 60 A). EGFR inhibition attenuated RVSP in rats exposed to CH, but not controls. However, even in the presence of EGFR inhibition, CH RVSPs were elevated compared to controls.

Table 1. *Body weight (BW) and ventricular weight ratios for animals treated chronically with an EGFR inhibitor.*

Treatment	BW (g)	RV (mg)	LV+S/BW (mg/g)	RV/BW (mg/g)
Control Vehicle	372 ± 4	0.21 ± 0.01	2.03 ± 0.08	0.57 ± 0.02
CH Vehicle	303 ± 4*****	0.33 ± 0.02*****	1.98 ± 0.07	1.08 ± 0.06*****
Control Gefitinib	360 ± 4	0.19 ± 0.01	2.07 ± 0.09	0.52 ± 0.02
CH Gefitinib	306 ± 5*****	0.27 ± 0.02***#**	2.21 ± 0.05	0.87 ± 0.06***#**

Values are means ± SE *n*=5 rats/group. ***** P < 0.05 vs. respective control. # P < 0.05 vs. CH vehicle. n=5/group

RV, right ventricle wt.; T, total ventricle wt.; LV+S, left ventricle plus septum wt.

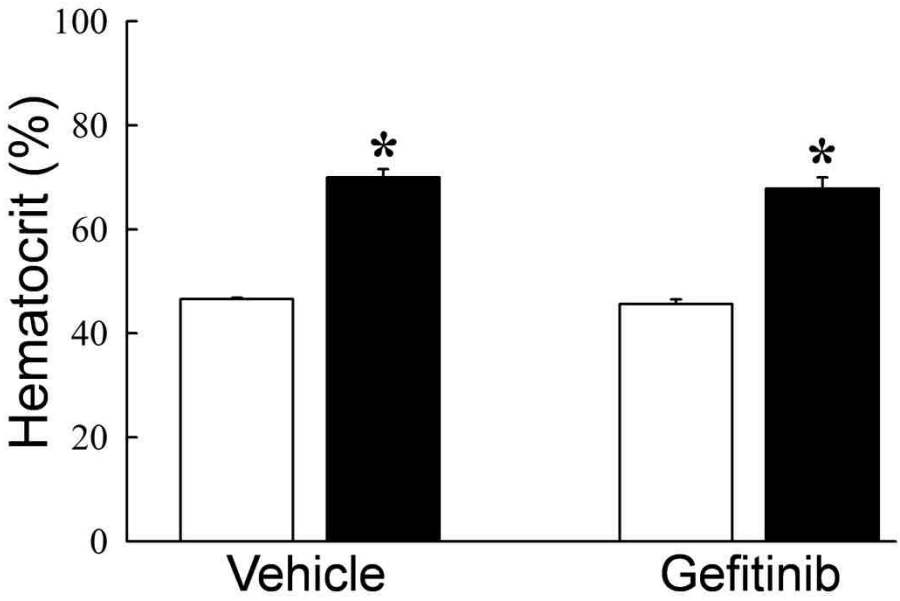

Figure 56. **CH-dependent polycythemia is not mediated by EGFR**. Hematocrit (%) from rats exposed to 4 weeks of CH or normoxia and administered daily gefitinib and vehicle pills. Values are means ± SE n=5/group. *p<0.05 vs. control.

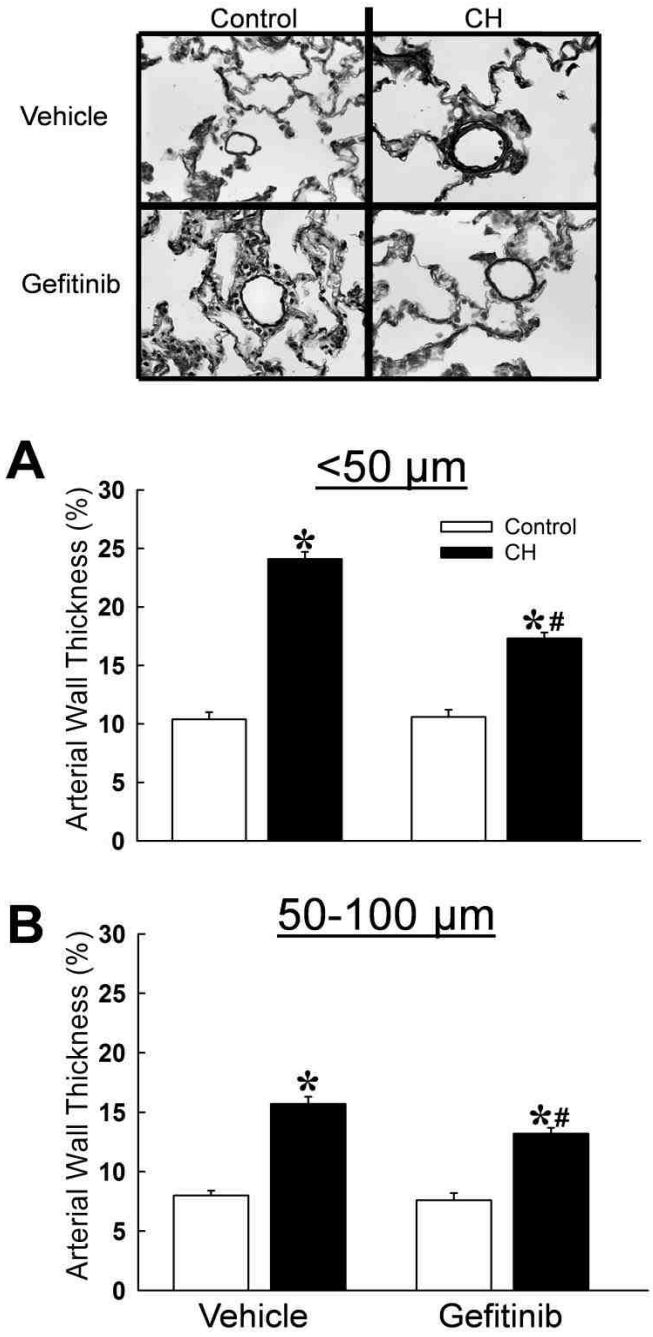

Figure 57. **EGFR contributes to CH-induced pulmonary arterial remodeling.** Representative images and arterial wall thickness (% outer diameter) of pulmonary arteries with diameters of <50 µm (A) and 50-100 µm (B) from CH and control rats administered daily gefitinib (30mg/kg/day) or vehicle pills. Values are mean ± SE n=5/group. *p<0.05 vs. control. #p<0.05 vs. CH vehicle.

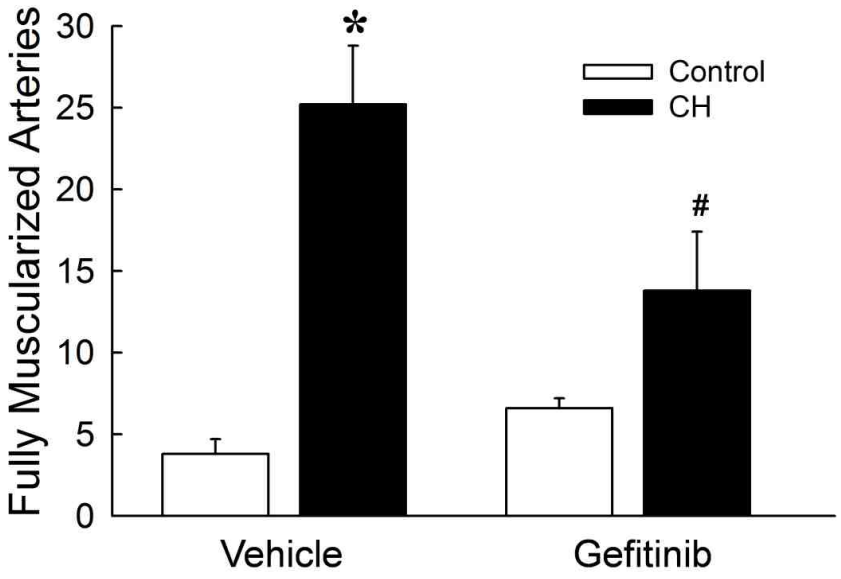

Figure 58. **EGFR contributes to CH-dependent increases in the incidence of fully muscularized small pulmonary arteries.** Numbers of fully muscularized arteries (0-20 µm) from 20 images/section. Values are mean ± SE n=5/group. *p<0.05 vs. control. #p<0.05 vs. CH vehicle.

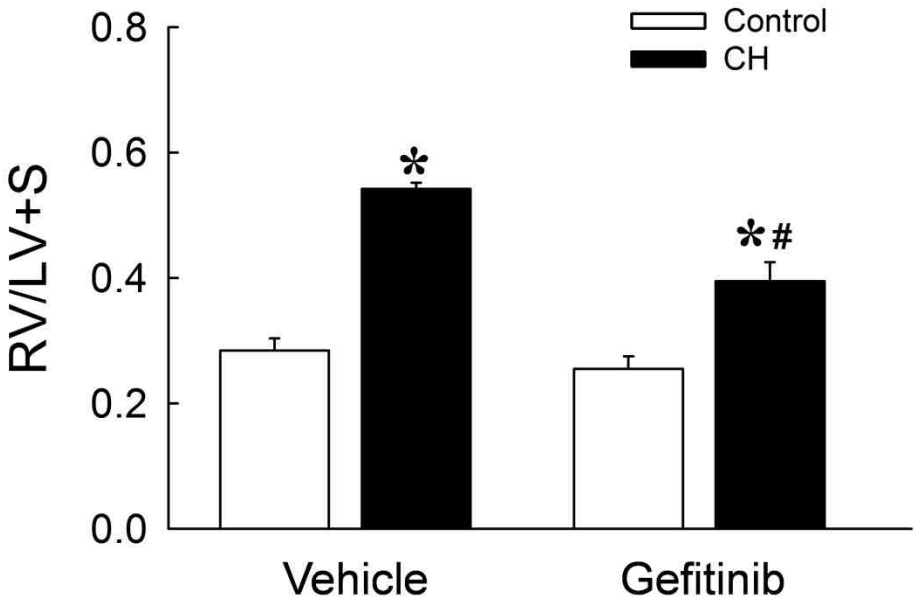

Figure 59. **EGFR contributes to CH-induced right ventricular hypertrophy.** RV/LV+S ratios from CH and control rats treated chronically with the EGFR inhibitor gefitinib (30 mg/kg/day), or vehicle pills. Values are means ± SE n=5/group. *p<0.05 vs. control. #p<0.05 vs. CH vehicle.

Similar findings were observed for mean right ventricular systolic pressures (Fig.60B). Heart rates were not significantly different between groups (control vehicle = 319 ± 7, CH vehicle = 349 ± 6, control gefitinib = 326 ±11, and CH gefitinib = 354 ± 15, n=5/group).

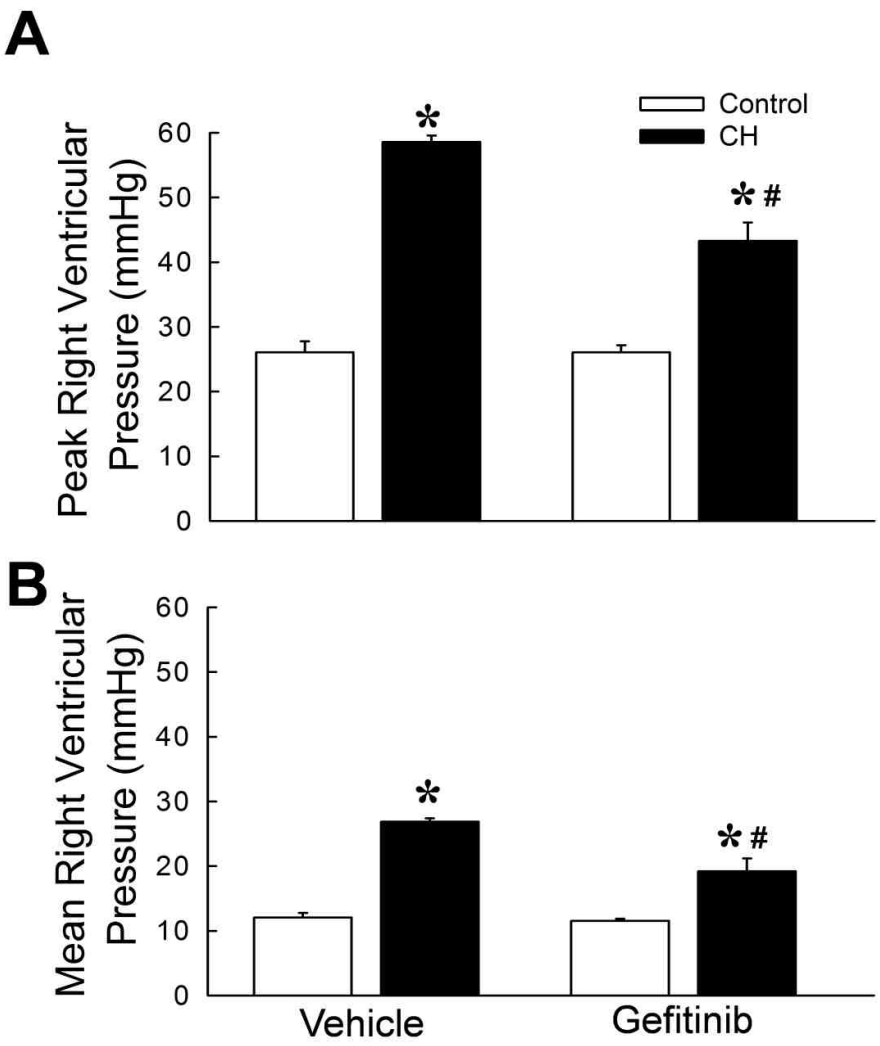

Figure 60. **EGFR contributes to elevated right ventricular systolic pressure following CH.** Peak (A) and mean (B) right ventricular pressures from anesthetized CH and control rats treated chronically with the EGFR inhibitor gefitinib (30 mg/kg/day), or vehicle pills. Values are means ± SE n=4-5/group. *p<0.05 vs. control. #p<0.05 vs. CH vehicle.

Aim 2 Major Findings

- EGFR is required for the development of enhanced vasoconstriction to ET-1 and KCl and pulmonary basal tone following CH (Figs. 31, 37, and 39).

- Depolarization-induced O_2^- generation in pulmonary arteries from CH rats requires EGFR (Fig. 32).

- EGFR activity is increased by KCl in CH arteries, but not controls (Fig. 34).

- Src family tyrosine kinases are necessary for pressure-dependent basal tone, enhanced vasoconstriction to KCl, and augmented vasoreactivity to ET-1 following CH (Figs. 36, 38, and 40).

- Src kinase activity is increased by CH in ET-1 treated arteries, without changes in Src kinase expression (Fig. 42).

- CH induces vasoconstrictor responsiveness to EGF through an EGFR-mediated Ca^{2+} sensitization mechanism involving NOX2 and ROK (Figs. 46 and 47). However, Src kinases do not appear to be involved in this response (Fig. 48).

- MMPS are important mediators of enhanced ETR signaling following CH (Fig. 47). MMP 2, but not MMP 9 or ADAM-17, is required for enhanced vasoconstriction to ET-1 in hypertensive arteries (Figs. 48, 50, and 52).

- ETRs do not function as metabotropic mediators of pressure-dependent or depolarization-induced tone following CH (Figs. 54 and 55).

- EGFR contributes to CH-dependent vascular remodeling (Fig. 57), right ventricular hypertrophy (Fig. 59), and increases in RVSP (Fig. 60).

SPECIFIC AIM 3

Assess the contribution of pressure-dependent and ET-1-induced membrane depolarization to augmented pulmonary vasoconstrictor reactivity following CH.

Hypothesis:

We hypothesize that CH increases vasoconstrictor responsiveness by coupling stretch and ET-1-mediated VSM membrane depolarization to myofilament Ca^{2+} sensitization.

Contribution of membrane depolarization to CH-dependent basal tone.

Increases in intraluminal pressure could result in basal tone via activation of stretch-activated ion channels that results in membrane depolarization. To test the possibility that depolarization contributes to the development of pressure-dependent pulmonary arterial tone, we permeabilized arteries to K^+ with valinomycin in combination with 16 mM extracellular K^+ to clamp membrane potential at ~60 mV [approximate membrane potential of a control artery under baseline conditions (12 mmHg)]. Valinomycin treatment blocked the pressure-dependent depolarization in both CH and control arteries (Fig. 61), and further prevented CH-dependent depolarization at each pressure tested (12 and 35 mmHg). Valinomycin diminished the development of tone in arteries from CH rats (Fig. 62) without altering vessel wall Ca^{2+} in arteries from either group (Fig. 63).

Additional protocols evaluated pressure-dependent responses in nonpermeabilized arteries from each group in the presence or absence of the

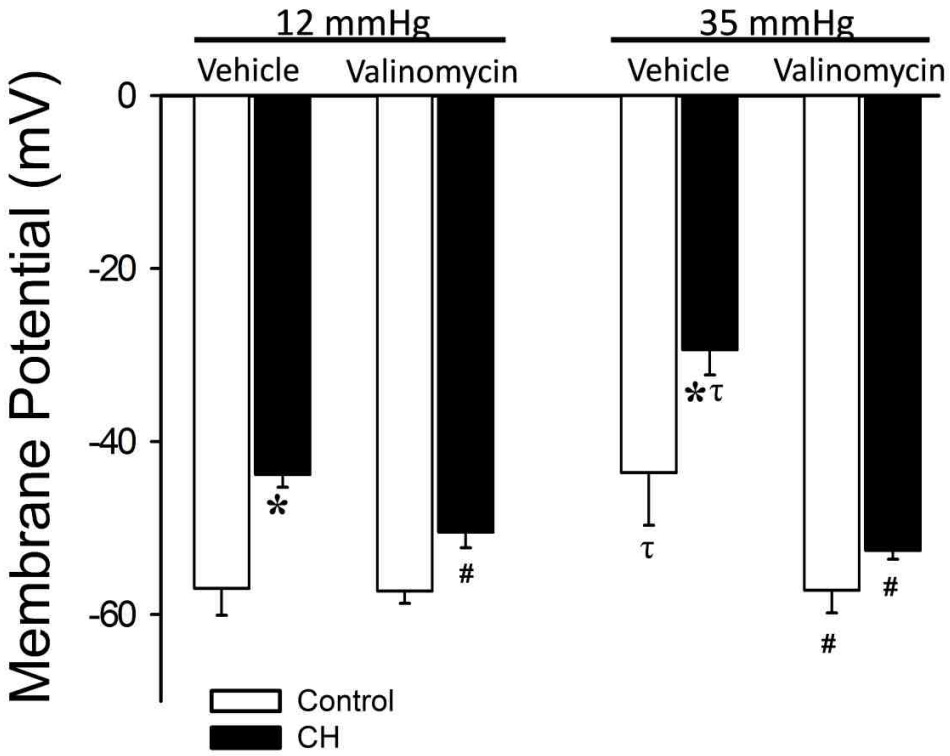

Figure 61. **Valinomycin/16 mM KCl prevents CH-and pressure-dependent membrane depolarization.** Sharp electrode membrane potential measurements in isolated endothelium-disrupted pulmonary arteries from CH and control rats under baseline (12 mmHg) and 35 mmHg pressures. Experiments were performed in the presence/absence of valinomycin/16 mM KCl. Values are means ± SE n=4/group. *p<0.05 vs. control. #p<0.05 vs. CH vehicle 12 mmHg. τp<0.05 35 mmHg vs. 12 mmHg.

K_{ATP} activator pinacidil (100 μM) pinacidil to hyperpolarize VSM membrane potential. Experiments were performed in the presence of the L-type Ca^{2+} channel inhibitor diltiazem to prevent possible effects of pinacidil to reduce vascular smooth muscle Ca^{2+}. Pinacidil caused membrane hyperpolarization in each group, but did not prevent depolarizing influences of either CH or pressure (Fig. 64). Consistent with a role for VSM membrane depolarization in pressure-dependent tone following CH, pinacidil attenuated this response in arteries from CH rats (Fig. 65A) without altering vessel wall Ca^{2+} (Fig. 65B).

Role of membrane depolarization in receptor-mediated vasoconstriction following CH.

ETR stimulation could also lead to membrane depolarization (248). We tested the possibility that membrane depolarization contributes to enhanced vasoconstriction to ET-1 following CH similar to Aim 3.1 using valinomycin and 16 mM KCl to set membrane potential at ~60 mV in Ca^{2+} permeabilized arteries. Resting membrane potential was depolarized in CH arteries compared to controls consistent with our other findings (Figs. 61 and 64). Interestingly, while ET-1 caused a slight depolarization in control arteries (Fig. 66), there was no ET-1 dependent depolarization in the CH arteries. Valinomycin/16 mM KCl prevented these depolarizing effects of CH and ET-1, resulting in similar membrane potential between groups. However, in contrast to effects of valinomycin to prevent pressure-dependent tone in CH arteries (Fig. 62), normalizing membrane potential between groups was without effect on vasoreactivity to ET-1 in vessels from either CH or control arteries (Fig. 67).

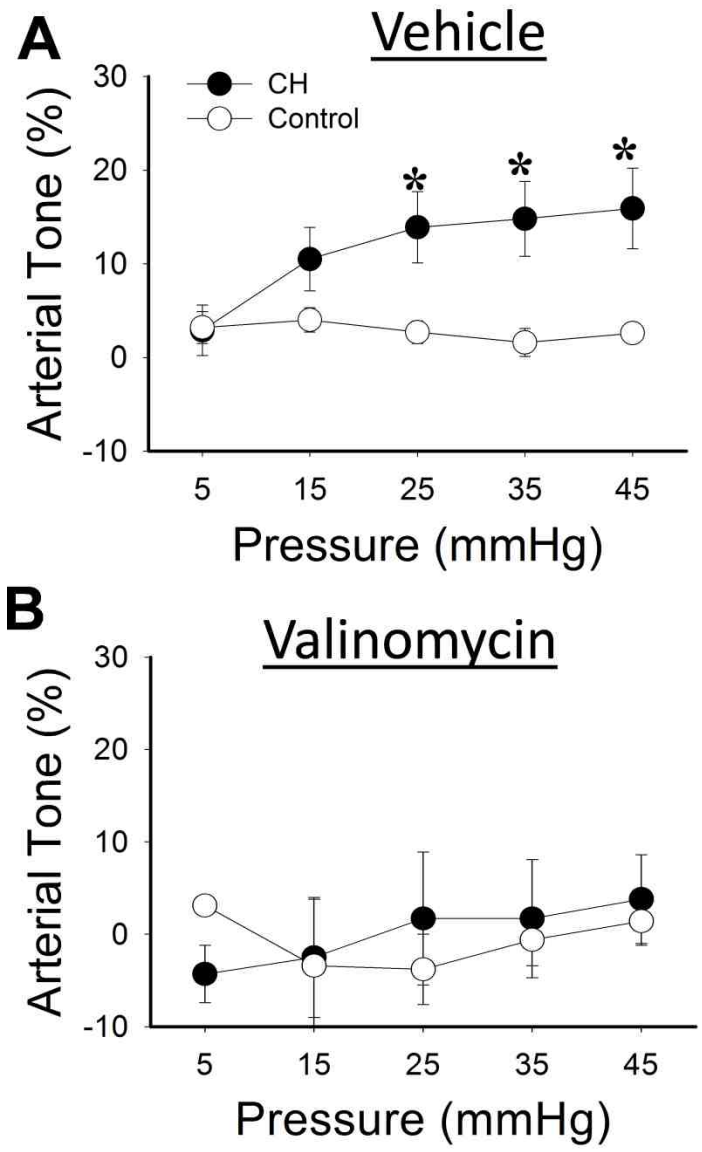

Figure 62. **Membrane depolarization is necessary for CH-dependent basal tone.** Basal tone measurements in isolated endothelium-disrupted pulmonary arteries from CH and control rats. Experiments were performed in the presence/absence of valinomycin/16 mM KCl. Values are means ± SE n=4/group. *p<0.05 vs. control.

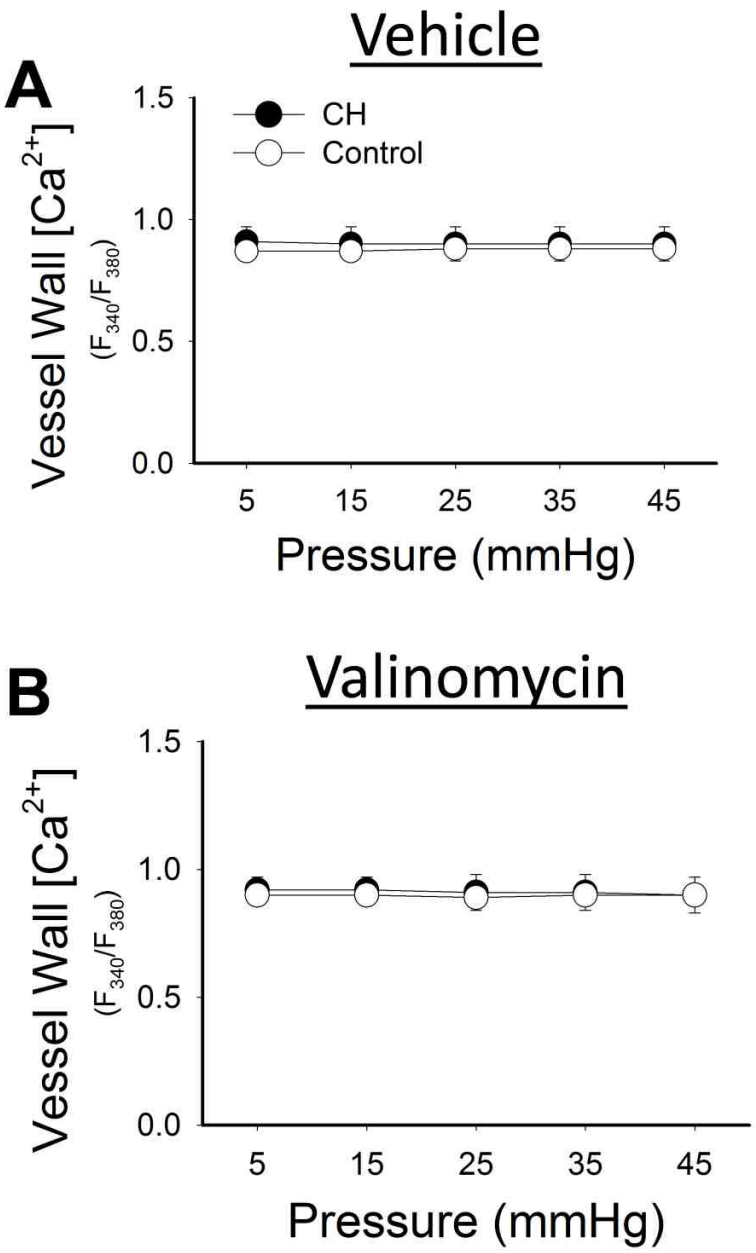

Figure 63. **Vessel wall Ca^{2+} is not altered by valinomycin.** Fura-2 fluorescence measurements in isolated endothelium-disrupted pulmonary arteries from CH and control rats. Experiments were performed in the presence/absence of valinomycin/16 mM KCl. Values are means ± SE n=4/group. No significant differences were detected.

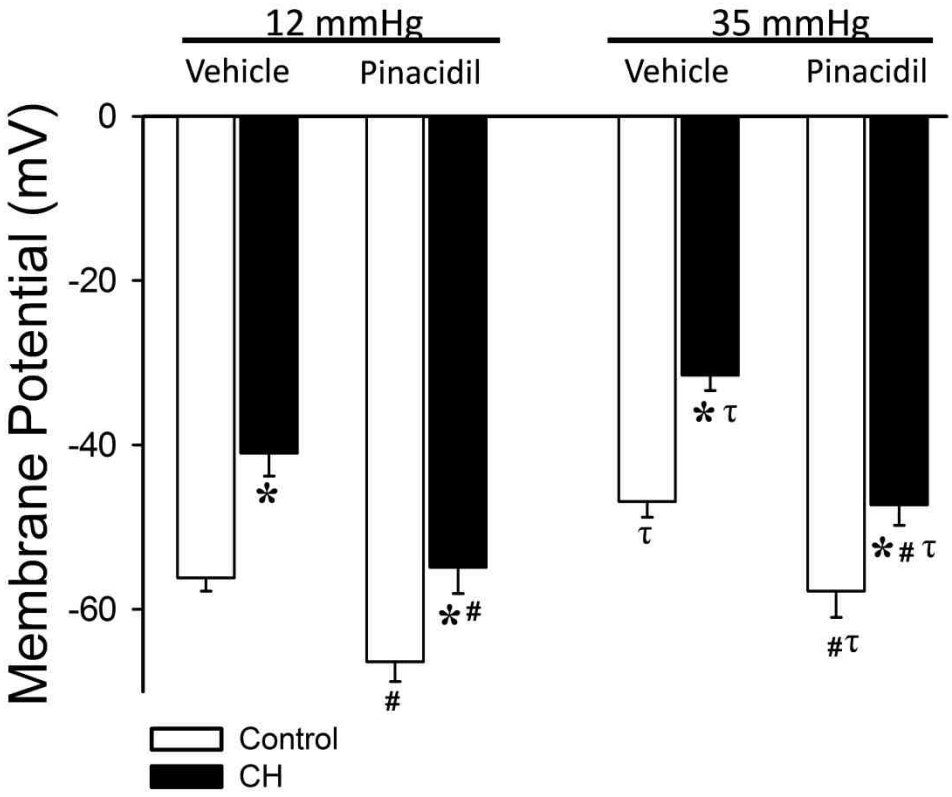

Figure 64. **Pinacidil hyperpolarizes membrane potential in arteries from control and CH rats.** Sharp electrode measurements of membrane potential at 5 and 35 mmHg in endothelium disrupted pulmonary arteries in the presence of diltiazem (50 µM) or diltiazem and pinacidil (100 µM). Values are means ± SE n=4/group. Values are means ± SE n=4/group. *p<0.05 vs. control. #p<0.05 vs. CH vehicle 12 mmHg. τp<0.05 35 mmHg vs. 12 mmHg.

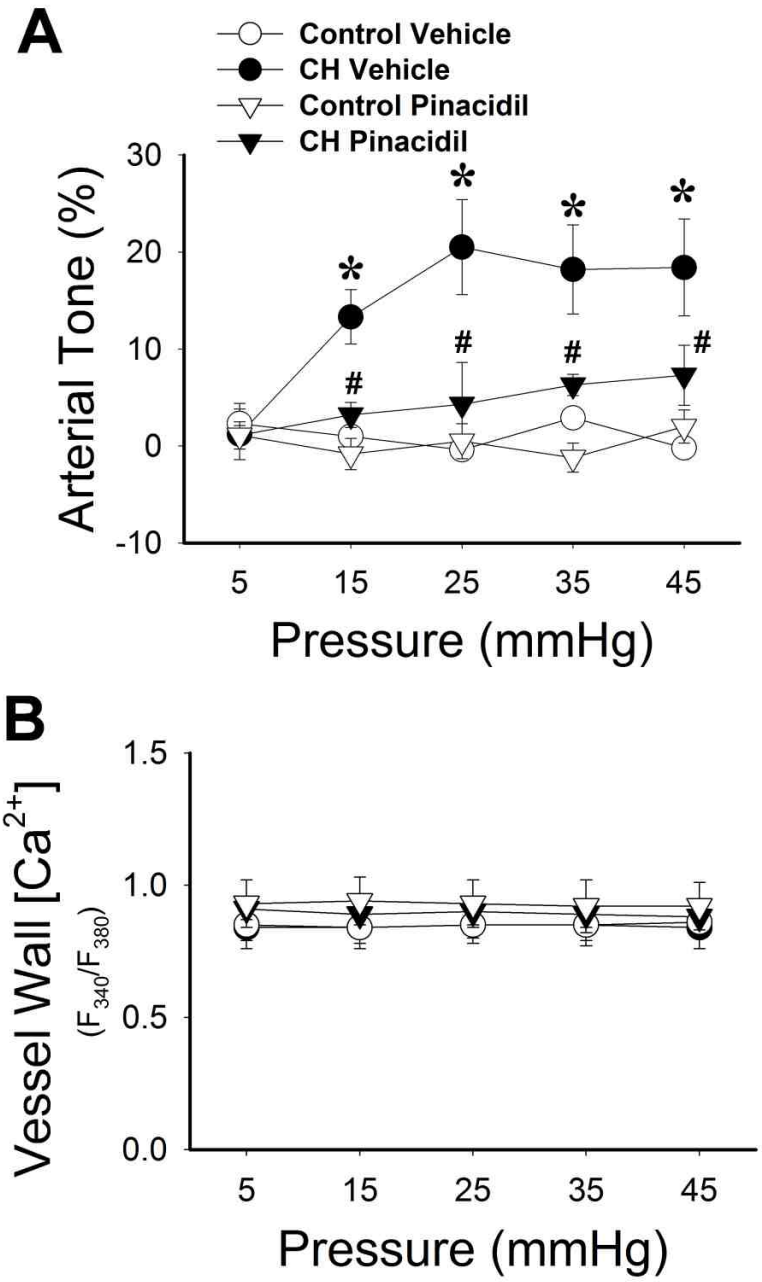

Figure 65. **Membrane depolarization contributes to basal tone following CH.** Pressure dependent tone responses (A) and vessel wall Ca^{2+} (B) in arteries treated with diltiazem (50 µM) or diltiazem and pinacidil (100 µM). Values are means ± SE n=4/group. **p*<0.05 vs. control. #*p*<0.05 vs. CH vehicle.

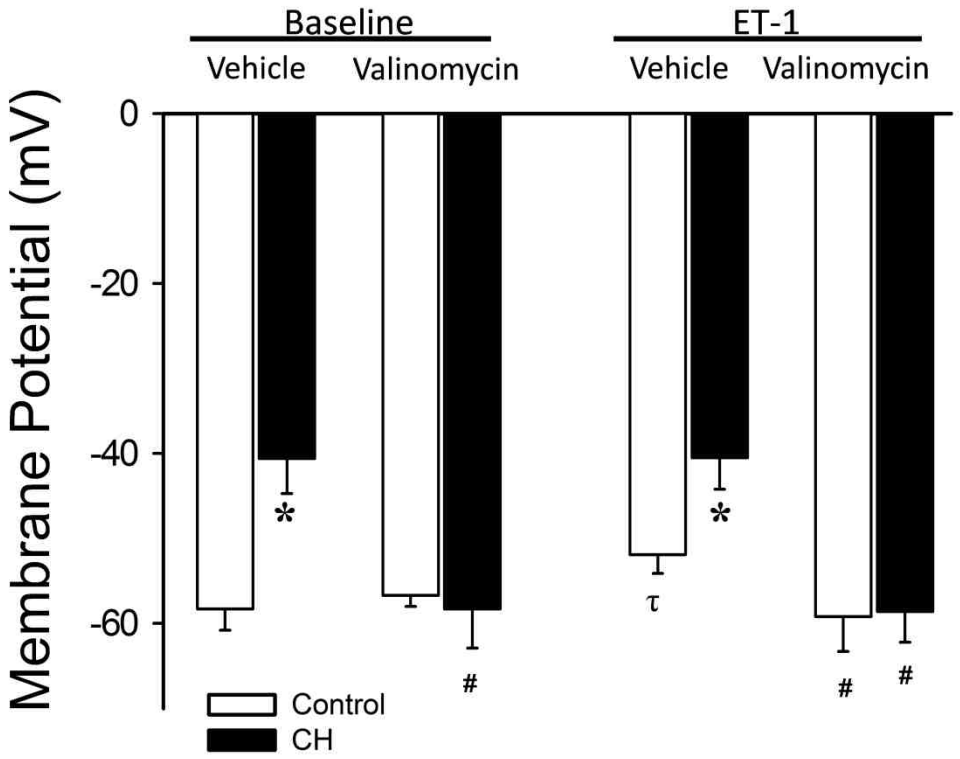

Figure 66. **Valinomycin prevents CH- and ET-1 dependent membrane depolarization.** Sharp electrode measurements of membrane potential in response to ET-1 in pressurized, Ca^{2+} permeabilized, endothelium disrupted pulmonary arteries from CH and control rats in the presence of valinomycin or vehicle. Values are means ± SE n=4-5/group *p<0.05 vs. control. #p<0.05 vs. CH vehicle. τp<0.05 ET-1 vs. 12 vehicle.

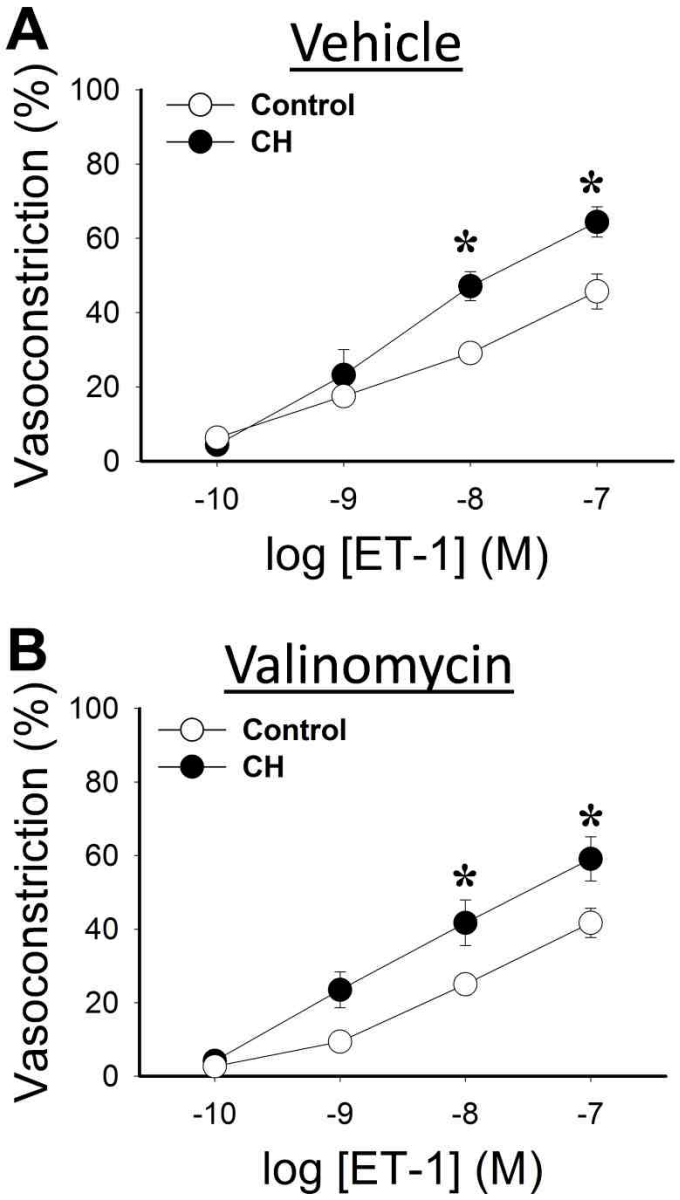

Figure 67. **Augmented ET-1 dependent vasoconstrictor reactivity following CH is not dependent on membrane depolarization.** Vasoconstrictor responses to ET-1 in pressurized, Ca^{2+} permeabilized, endothelium disrupted pulmonary arteries from CH and control rats in the presence of valinomycin or vehicle. Values are means ± SE n=4/group. *p<0.05 vs. control.

Aim 3 Major Findings

- Membrane permeabilization to K^+ prevents CH-induced and pressure-dependent VSM membrane depolarization in small pulmonary arteries (Figs. 61 and 65).

- Membrane depolarization is important for the development of CH-dependent basal tone (Fig. 61).

- ET-1 caused modest depolarization in control arteries, but not in arteries from CH rats (Fig. 66). This response to ET-1 was prevented my membrane permeabilization to K^+.

- Augmented ET-1 dependent vasoconstrictor reactivity following CH is not dependent on membrane depolarization (Fig. 67).

Chapter 4 - Discussion

The overall objective of this project was to determine mechanisms by which CH exposure results in the development of basal pulmonary arterial tone, enhanced vasoconstrictor reactivity and associated PH. The major findings of this project are that following CH: 1) NOX 2-derived ROS contribute to pressure-dependent pulmonary arterial tone and enhanced vasoconstrictor responsiveness to both depolarizing stimuli and ET-1 through myofilament Ca^{2+} sensitization; 2) EGFR is activated by these stimuli and activates Rac1 to mediate these ROS-dependent vasomotor responses; 3) EGFR contributes to CH-induced right ventricular hypertrophy, arterial remodeling and elevated RVSP; 4) Src kinases signal upstream of EGFR to mediate pressure-dependent tone and augmented depolarization- and ET-1-induced pulmonary vasoconstrictor reactivity; 5) MMPs contribute to ligand-dependent EGFR activation in response to these stimuli; and 6) membrane depolarization is required for pressure-dependent basal tone but not enhanced ET-1 mediated vasoconstrictor reactivity. Together, these findings demonstrate a novel signaling pathway in pulmonary VSM involving Src kinases, MMPs, and EGFR-dependent Rac1 activation that mediates NOX 2-induced myofilament Ca^{2+} sensitization, basal pulmonary arterial tone and augmented vasoconstrictor sensitivity following CH. These studies further support an important contribution of EGFR signaling to the development of CH-induced PH.

Exposure to CH increases basal pulmonary arterial tone (27; 177; 304) and augments vasoconstrictor sensitivity to both receptor mediated agonists (10; 109; 182) and depolarizing stimuli (26; 177). Although mechanisms involving

enhanced Ca^{2+} influx may additionally contribute to greater pulmonary vasoreactivity following CH (105; 135; 285), it is clear that myofilament Ca^{2+}sensitization mediated by ROK provides a major contribution to these vasoconstrictor responses (26; 27; 109; 177; 295). Interestingly, the effect of depolarization to activate RhoA in hypertensive pulmonary arteries occurs through a mechanism that is independent of L-type Ca^{2+} channel stimulation or global changes in VSM $[Ca^{2+}]_i$, but dependent on ROS (26). Basal tone and enhanced vasoconstriction to ET-1 following CH are also mediated by myofilament Ca^{2+} sensitization and ROS signaling (27; 109). However, neither the enzymatic source of O_2^-, nor the signaling mechanisms linking depolarization, ETR stimulation, and increases in intraluminal pressure to O_2^- generation had been previously addressed.

ROS ANDNADPH OXIDASE

Endogenous ROS derived from various enzymatic sources and cell types are widely considered to play a critical role in the pathogenesis of various forms of PH, including CH-induced PH (34; 79; 182). The mechanisms by which ROS contribute to PH are multifaceted with roles associated with both enhanced vasoreactivity and vascular remodeling.

O_2^- and H_2O_2 are the primary ROS known to be involved in regulation of pulmonary vascular tone. Our laboratory has previously reported effects of CH to increased pulmonary arterial O_2^- generation (109; 184). Direct effects of both H_2O_2 and O_2^- to promote VSM contraction through various second messenger pathways have been observed (30; 122; 135), while a purported role for H_2O_2 to

exhibit relaxant properties also exists (30). Our research suggests that O_2^- mediates a contractile effect in pulmonary VSM through activation of RhoA leading to ROK-induced myofilament Ca^{2+} sensitization (26; 109).

NADPH oxidases have been implicated in the development of pulmonary hypertension (98; 138; 168), and thus represent a potential source of O_2^- mediatingenhanced vascular tone following CH. In agreement with this possibility is evidence that CH-mediated increases in pulmonary vasoreactivity, ROS production, and PH are attenuated in mice deficient in the catalytic subunit of NOX 2 (138). Additionally, NOX 2 contributes to impaired endothelium-dependent pulmonary vasodilatation in mice (70) and neonatal piglets (68) with CH-induced PH. Furthermore, CH increases NOX-derived ROS production, NOX 1 expression, and $p67^{phox}$ levels in the membrane fraction of small pulmonary arteries from piglets, suggesting elevated NOX 1 activity in neonatal PH (48; 68). NOX 4 gene and protein expression are also elevated following CH exposure in murine pulmonary arteries and lung tissue (11; 168; 182), and are similarly upregulated by CH in cultured human pulmonary endothelial cells (145). However, the contribution of NOX 4 to the development of enhanced vasoconstrictor reactivity remains poorly understood.

Our present findings implicate NOX 2 as a primary source of ROS mediating enhanced pulmonary arterial constriction and Ca^{2+} sensitization following CH (184). A role for NOX in augmented depolarization-induced vasoconstriction following CH is evident by effects of apocynin to attenuate vasoconstrictor responses to KCl in nonpermeabilized arteries and isolated lungs

from CH rats, but not controls (184). This argument is further supported by evidence from Ca^{2+} permeabilized arteries that nonspecific NOX inhibition with apocynin or DPI attenuated both vasoreactivity and O_2^- generation in response to KCl selectively in arteries from CH rats. Furthermore, NOX inhibition prevented KCl-dependent increases in O_2^- production as measured by DHE fluorescence (184). Similar results were observed using the selective NOX 2 inhibitor, gp91ds-tat, which competitively inhibits $p47^{phox}$ binding to the catalytic subunit of NOX 2, and thus prevents assembly of the active enzyme complex (41). This effect of gp91ds-tat does not appear to occur though an alteration of membrane potential, as this inhibitor did not affect membrane potential under baseline conditions or following administration of 60 mM KCl in either CH or control arteries. These data support a distinct contribution of NOX 2-derived O_2^- to enhanced depolarization-induced vasoconstriction independent of changes in global vessel wall $[Ca^{2+}]_i$ following CH. Although, we cannot exclude the possibility that localized, subsarcolemmal Ca^{2+} events contribute to the observed responses, we are confident that, within the sensitivity limits of the system, global $[Ca^{2+}]_i$ is effectively clamped by ionomycin in this preparation. An additional limitation of this system is the inability to selectively measure VSM $[Ca^{2+}]_i$, as other cell types within the vascular wall (*e.g.*, fibroblasts) likely contribute to the fura 2 signal. Experiments with 2 photon microscopy (data not shown), suggest that the majority of the fura 2 signal is localized to the VSM and that fura loading is similar between CH and control arteries, although adventitial remodeling resulting from CH exposure may increase the contribution of this layer to the

overall fura 2 signal. Other cell types may additionally contribute to the DHE signal in studies performed in isolated arteries.

Similar to previous findings (27), we observed the development of basal tone with increasing intraluminal pressure in arteries from pulmonary hypertensive rats, but not controls. We tested the role of NOX in this response using the broad spectrum NOX inhibitor apocynin in nonpermeabilized arteries and found that NOX inhibition prevented the development of tone in arteries from CH rats. Selective NOX 2 inhibition with the gp91ds-tat peptide was also sufficient to prevent the development of basal tone. gp91ds-tat similarly prevented augmented vasoconstrictor reactivity to ET-1 in Ca^{2+} permeabilized arteries. These findings suggest that similar to enhanced depolarization-induced vasoconstriction, NOX 2 serves as the enzymatic source of O_2^- that mediates the development of basal tone and agonist induced vasoconstriction through ROK-dependent Ca^{2+} sensitization.

It is unlikely that greater basal and ET-1 (109) and depolarization (26; 184) stimulated O_2^- production following CH are a function of increased arterial NOX 2 expression. We found no difference in NOX 2 catalytic subunit ($gp91^{phox}$) protein expression between arteries from CH and control rats, consistent with findings by Lui et. al. which demonstrated no change in mRNA levels of gp91phox, p47phox, p67phox, or Rac1 in a hypoxic murine model of pulmonary hypertension (138). The lack of effect of NOX inhibition on vasoreactivity and O_2^- levels in control arteries suggests that CH facilitates a coupling of depolarization, membrane stretch induced through increases in intraluminal pressure, and ETR stimulation

to NOX 2 activation that is not present in the normal pulmonary circulation. Nevertheless, we cannot exclude a possible contribution of altered expression of other components of the NOX 2 complex to this response.

Another factor that may contribute to enhanced NADPH oxidase-derived O_2^- following CH is increased NADPH production. Glucose-6-phosphate dehydrogenase, the rate limiting enzyme in NADPH production, can contribute to coronary artery smooth muscle contraction (83). Reports from Gupte et. al. (84) have demonstrated that acute hypoxia can increase NADPH levels through activation of glucose-6-phosphate dehydrogenase. It remains to be determined it this effect persists with CH, but the increased NADPH substrate may further drive the production of O_2^- following CH.

As NOX 2 expression was unaltered following CH, we sought to determine if alterations in NOX 2 enzyme activation mediate the enhanced vascular tone development following CH. Rac1 is an important mediator of NOX 1 and 2 activation (21; 38), and thus represents a potential signaling factor that links membrane depolarization, intraluminal pressure, and ETR activation to stimulation of NOX 2. Consistent with this possibility is evidence that depolarization activates Rac1 and NOX in endothelial and macula densa cells (32; 142; 158; 254). Here we demonstrate that KCl-mediated membrane depolarization activates Rac1 selectively in arteries from pulmonary hypertensive rats. Our findings that basal and KCl-mediated O_2^- generation and associated vasoconstriction are diminished by NSC 2376 only in CH arteries further suggest that Rac1 activation contributes to both elevated resting O_2^- levels and

depolarization-stimulated O_2^- production and vasoconstriction following CH. Rac1 inhibition also prevented the development of CH-dependent basal tone and enhanced vasoconstriction to ET-1. Combined, these data support a role for Rac1activation as a critical signaling component leading to enhanced VSM Ca^{2+} sensitization and vascular tone following CH.

It is additionally possible that the phosphorylation state of the NOX 2 components $p47^{phox}$ and $p67^{phox}$ is altered by CH, agonist signaling, increases in intraluminal pressure, or membrane depolarization. Phosphorylation of these subunits can also contribute to NOX activation (21; 38; 153). Recent evidence also suggests that catalytic subunit modifications have the potential to alter enzyme activity (264).

EGFR

The present studies additionally support a novel role for EGFR in the development of CH-induced PH. Based on evidence that depolarization leads to EGFR activation in PC12 cells (56; 318) and that membrane stretch stimulates EGFR-dependent NOX activation in mesangial cells (314), we examined a role for EGFR as a proximal mediator of depolarization-induced, Rac1-dependent, NOX 2 activation in CH arteries. A role for EFGR in this response is supported by our present findings that EGFR phosphorylation was induced by a depolarizing stimulus only in CH arteries, and that selective EGFR inhibition prevented effects of CH to augment both depolarization-induced vasoconstriction and vascular O_2^- production. We additionally found that depolarization-mediated Rac1 activation in intrapulmonary arteries from CH rats was prevented by AG

1478, suggesting EGFR signals upstream of Rac1. Unlike responses to Rac1 and NOX 2 inhibition, inhibition of EGFR had no effect to reduce basal ROS production in vessels from CH rats, suggesting that while EGFR is necessary for KCl-mediated O_2^- production, CH elevates basal O_2^- levels through an EGFR-independent mechanism. Further supporting this line of thought is our observation that basal levels of phosphorylated EGFR were unaltered following exposure to CH.

We examined the role of EGFR in the development of pressure-induced tone in arteries from CH rats. Both tested EGFR inhibitors prevented the development of pressure-dependent tone in pulmonary arteries from CH animals. EGFR inhibition also prevented the enhanced vasoreactivity to ET-1 in CH arteries. Combined these findings suggest that enhanced vascular tone following CH is mediated via EGFR-dependent NOX activation.

In contrast with our experiments in isolated arteries, we did not observe significantly greater ROS production in PASMCs from CH rats compared to controls. However, similar to effects of KCl in isolated arteries, ET-1 led to an increase in ROS in PASMC from CH rats while having no effect in controls. This ET-1-dependent ROS production was prevented by EGFR inhibition, further supporting a role for EGFR in enhanced ROS-dependent vasoconstriction and Ca^{2+} sensitization to ET-1 following CH. Although we cannot exclude the possibility that other vascular cells contribute to this signaling pathway *in vivo*, these findings in PASMC suggest that the cellular players in this response are located in pulmonary VSM.

While previous studies have observed a role for EGFR in monocrotaline-induced pulmonary hypertension (42; 162), the role of this receptor in mediating CH-induced PH in rats had not previously been examined. We observed right ventricular hypertrophy and elevated peak RVSPs in CH animals compared to controls, both indicative of the development of PH. Daily treatment of animals with an EGFR inhibitor, gefitinib (30mg/kg/day), attenuated both these indices of PH. EGFR inhibition did not prevent CH-dependent or polycythemia, indicating that EGFR does not play a role in this responses. Indeed there is no known role for EGFR in HIF-1α-dependent erythropoiesis. Our findings contrast those in mice where chronic EGFR inhibition did not significantly attenuate CH-dependent RV hypertrophy, vascular remodeling, or increases in RVSP (42). One potential explanation for the discrepancy between these findings is species differences. Dahal and colleagues additionally found that EGFR expression was not altered in lungs from idiopathic pulmonary hypertensive patients or animal models of pulmonary hypertension (42), and they concluded that EGFR inhibition does not likely have significant therapeutic potential. However, this study did not examine EGFR activity, and our studies support a novel role for posttranslational modifications of EGFR, not changes in expression, to mediate enhanced vasoconstriction following CH.

EGFR has previously been implicated in pulmonary vascular remodeling in both neonatal (247) and monocrotaline models of PH (42). We found that EGFR inhibition attenuated the vascular remodeling in CH-induced PH and decreased the muscularization of small pulmonary arteries. While the

mechanisms that lead to EGFR-induced remodeling remain to be addressed, it is possible that EGFR-dependent gene transcription is involved. NADPH oxidases are enzymatic sources of ROS that contribute to the vascular remodeling component of PH (11). Therefore in addition to mediation of enhanced vascular tone development following CH, enhanced EGFR/NOX signaling in lungs from CH animals also contributes to the vascular remodeling component of CH-dependent PH.

To further characterize EGFR signaling following CH, we applied increasing concentrations of EGF to isolated pulmonary arteries. Interestingly, we observed vasoconstriction only in arteries from CH rats that was not associated with a significant increase in vessel wall $[Ca^{2+}]_i$. Prevention of this response with an EGFR inhibitor confirms that the effect of EGF in vessels from CH rats is mediated through EGFR. This vasoconstriction was additionally dependent on ROK and NOX 2 similar to the development of basal tone and enhanced vasoconstriction following CH (184). These results suggest that an alternative signaling pathway involving Src-dependent EGFR activation, unique to the hypertensive pulmonary circulation, is unmasked or evoked by CH exposure. It is possible that oxidative stress following CH facilitates this pathway through oxidation of cysteine residues on EGFR leading to enzyme activation (71; 277). However, it is additionally possible that CH alters the composition of lipid signaling domains to permit EGFR signaling, as discussed in the following section.

While PKC-dependent NOX activation is an additional mechanism of O_2^- generation (58), previous experiments from our laboratory demonstrated that enhanced Ca^{2+} sensitization and vasoconstriction following CH are not attenuated by general PKC inhibition (26; 109). Other HER family members, besides EGFR (HER1), could also potentially contribute to this response. HER2 has been shown to form signaling complexes with EGFR (292; 317), and dimerization with HER3 and HER4 can also occur (194). Therefore, CH may facilitate coupling of these other HER family members with EGFR to mediate enhanced vasoconstriction, although this possibility remains to be tested.

Signal Regulation by Lipid Domains

Regulation of EGFR by lipid rafts serves as an additional target for investigation. Caveolin-1 (cav-1) is a critical structural component of lipid domains known as caveolae. This protein contains an intracellular scaffolding domain that additionally regulates the activity of various signaling pathways (36; 40; 134). Cav-1 phosphorylation facilitates EGFR (312) and NOX (314) activation in response to membrane stretch and depolarization in mesangial cells, while cav-1 has been implicated as a key regulator of metalloproteinase-dependent EGFR transactivation (271). Our preliminary studies suggest a role for cav-1 dysfunction in enhanced depolarization-induced vasoconstriction following CH (Supplemental Figure 1, Appendix B) as a peptide consisting of the cav-1 scaffolding domain (AP-Cav) was able to prevent augmented vasoconstrictor reactivity to KCl following CH (187). Decreases in cav-1 protein have been observed in humans with idiopathic PH and several models of PH (8;

33; 101; 316), although Patel and colleagues found increased VSM expression of cav-1 in idiopathic pulmonary arterial hypertension (202). Preliminary findings from our laboratory demonstrated no effect of CH on either pulmonary arterial cav-1 expression (assessed by Western blotting) or caveolae number (assessed by electron microscopic analysis of lung sections) in rats (187). Therefore, cav-1 dysfunction in this setting is not likely a result altered expression, but rather a change in cav-1 function that facilitates EGFR/NOX activation following CH.

Cholesterol is a key regulator of cav-1 expression and function (86; 171). Preliminary findings by our group suggest that VSM membrane cholesterol is decreased following CH (186). Interestingly, we found that EGF induced vasoconstriction in CH arteries was attenuated by pretreatment with supplemental cholesterol (Supplemental Figure 2), while enhanced vasoconstriction to EGF was unmasked in control arteries treated with methyl-β-cyclodextrin to reduce membrane cholesterol (Supplemental Figure 2). Although supplemental cholesterol also diminished vasoconstriction to KCl in Ca^{2+} permeabilized pulmonary arteries from CH rats, enhanced vasoconstrictor reactivity was not observed in arteries from control animals with reduced membrane cholesterol (186). These findings suggest that the pathway linking EGFR signaling to NOX-dependent ROS production is inhibited by cholesterol in control arteries, and that decreased cholesterol in hypertensive animals facilitates the activation of an EGFR/NOX 2 signaling axis. Furthermore, our findings that vasoconstriction to EGF but not enhanced vasoconstriction to KCl can be unmasked by cholesterol depletion in control arteries suggest that CH

additionally facilitates signaling upstream of EGFR involving Src kinases and MMPs.

Future studies will be necessary to elucidate that relative contribution of membrane cholesterol and cav-1 to enhanced pulmonary vasoconstriction following CH. Cav-1 has been shown to negatively regulate EGFR activation by angiotensin II in aortic VSM (271), and NOX 1 co-localizes with cav-1 in VSM (90). Recent findings by Chen et. al. implicate a direct role of cav-1 to regulate NOX function (33). Alternatively, other reports suggest a direct role of membrane cholesterol to regulate EGFR function (225). Cholesterol oxidation, potentially through increases in oxidative stress associated with CH, can also result in cav-1 dysfunction (139). Therefore, as opposed to a decrease in total membrane cholesterol, it is possible that an increase in oxidized cholesterol (not detected by filipin fluorescence) facilitates activation of EGFR in arteries from pulmonary hypertensive animals.

SRC FAMILY KINASES

Src family kinases are a large subgroup of non-receptor tyrosine kinases including Src (c-Src), Yes, Fyn, Blk, Lyn, Hck, Yrs, Lck, and Fgr that have similar functions and structures (201). mRNA for all nine of these kinases is expressed in the pulmonary circulation (121). We investigated the hypothesis that Src kinases mediate basal tone and enhanced depolarization and agonist-induced vasoconstriction following CH due to evidence that Src kinases couple these stimuli to EGFR activation (87; 146; 190; 314). Consistent with this hypothesis, we found that Src kinase inhibition prevented pressure-induced tone, as well as

enhanced vasoconstriction to KCl and ET-1 following CH, similar to effects of EGFR, NOX 2 and Rac1 inhibition.

Our finding that Src kinase inhibition did not prevent EGF-induced vasoconstriction in arteries from CH rats supports the hypothesis that Src kinases activate EGFR in response to depolarization, membrane stretch or ET-1 stimulation. We observed no detectable difference in basal Src kinase activity in pulmonary arterial homogenates of CH and control rats. In ET-1 stimulated arteries, however, CH exposure led to an increase in phosphorylated Src kinase at its activation residue, tyrosine 416 (232). Interestingly, Src phosphorylation can also by induced in response to prostaglandin $F_{2\alpha}$ ($PGF_{2\alpha}$) in the pulmonary circulation (121), suggesting that other agonists coupled to GPCRs may also activate Src kinase signaling.

Recent findings by Pullamsetti and colleagues support a novel role for Src family kinases in the development of monocrotaline-induced pulmonary hypertension (210). This study demonstrated that combined Src kinase/ platelet-derived growth factor (PDGF) inhibition prevented vascular remodeling. Our data provide novel insight into the signaling pathway involved in this response, and define the role of Src in the vasoconstrictor component of PH. As Src kinases represent a sizable family of proteins, elucidating the specific Src kinase(s) involved, remains an area for future investigation. A likely candidate is c-Src, since myogenic tone in systemic arteries requires c-Src (173), and c-Src has been linked to depolarization-induced RhoA activation in mesangial cells (314).

Src family kinases are important mediators of transduction of GPCR (147; 246) and mechanical (314) stimuli to EGFR activation. Src kinases can directly activate EGFR via ligand-independent phosphorylation (18; 236; 263). Additionally, Src kinases can also activate EGFR through ectodomain shedding of transmembrane ligands into mature ligands via MMPs (146).

MMPs

Ligands for EGFR are expressed in VSM cells (51; 258). Our findings with a general MMP inhibitor support a role for EGF or another growth factor shed by MMPs to bind to and activate EGFR. Of the selective MMP inhibitors used in this study, only MMP 2 inhibition restored vasoreactivity to ET-1 in CH arteries to the level of controls. Furthermore, we detected increased MMP 2 protein levels in CH arteries compared to controls. Conversely MMP 9 and ADAM-17 inhibition did not normalize vasoconstriction to ET-1 between CH and control arteries, although they did have a modest effect to attenuate pulmonary vasoreactivity to ET-1 in arteries from CH rats.

One limitation of the current study is the limited selectivity of isoform-specific MMP inhibitors due to the structural similarity of these proteins. While MMP-3 can also result in EGFR shedding (266), findings that MMP-3 expression is decreased in pulmonary hypertension (131) suggest that this enzyme is not a critical mediator of this response, although some contribution cannot be ruled out. As MMPs are located in the extracellular space, the isolated vessel preparation employed in this study could lead to the loss of extracellular MMPs. This could provide one explanation for the observed results, and presents the

possibility that alternative MMPs could have a role in this response *in vivo*. For instance, ADAM-17 plays a crucial role in MMP-2 activation resulting in angiotensin II-induced hypertension in the systemic circulation (189).

Hypoxia increases MMP-2 expression in a variety of cell types (2; 167; 305). MMP-14 (MT1-MMP) can activate MMP-2 at the cell surface (265), so potential alterations in MMP-14 activity with CH could also contribute to this pathway. Interestingly, ROS can increase both Src (75; 278) and MMP (274) activity. Therefore, general oxidative stress associated with CH may facilitate this signaling pathway.

Due to their ability to regulated MMPs and ADAMs (22; 77), TIMPs could also be playing a role in this response. TIMPS inhibit MMPs by association and chelating the catalytic zinc cofactor required for metalloproteinase activity (66; 78). Interestingly, increased MMP2 activity in pulmonary arteries from patients with idiopathic pulmonary hypertension has been associated with TIMP imbalance (131). Whether or not TIMPs play a role in the studied responses remains to be established. However, even if they are not involved in this response, they may provide a therapeutic tool in the treatment of PH due to their ability to regulate MMP activity.

SIGNALING PATHWAY INTERACTIONS

Previous reports have demonstrated VSM membrane depolarization associated with increases in intraluminal pressure in pulmonary arteries from both CH and control rats (179), and ET-1-induced depolarization in PASMCs from normotensive rats (248).These studies suggest a potential role for

membrane depolarization to mediate the enhanced vasoconstrictor sensitivity to these stimuli. Consistent with these earlier studies, we found that VSM cells in CH arteries were depolarized compared to controls, and observed pressure-dependent depolarization in arteries from both groups. We tested the possibility that membrane depolarization contributes to pressure-dependent pulmonary arterial basal tone by clamping membrane potential with valinomycin and 16 mM KCl or by hyperpolarizing the membrane potential through activation of K_{ATP} channels with pinacidil. The valinomycin treatment prevented CH- and pressure-dependent depolarization and prevented the development of basal pulmonary arterial tone. These findings suggest that basal tone following CH is mediated through depolarization. Activation of stretch-activated cation channels represents a likely possibility as to how this stretch-induced depolarization occurs. Transient receptor potential channels, for instance, regulate myogenic tone via stretch-dependent depolarization in systemic arteries (298). However, depolarization alone does not account for the effect of CH, as control arteries depolarized with KCl do not demonstrate Src/EGFR/NOX-dependent vasoconstriction. Therefore, while depolarization is an important stimulus mediating basal tone following CH, CH has some other effect that allows for Src/EGFR/NOX activation in response to a depolarizing stimulus. While this change may involve an alteration in lipid signaling domains (186), CH seems to facilitate the coupling of membrane depolarization to Src dependent EGFR activation, a signaling pathway that does not exist in controls. One possibility as

to how this might occur is through metabotropic signaling by voltage sensitive L-type VGCC which can activate ROK (67).

We also examined the role of membrane depolarization in vasoconstrictor responses to ET-1. Whereas we observed no effect of ET-1 to elicit VSM cell depolarization in CH arteries, we did detect a modest depolarizing response to ET-1 in control arteries. This is consistent with findings demonstrating a depolarizing effect of ET-1 in isolated VSM cells from rat pulmonary arteries and no effect of ET-1 to elicit depolarization in PASMCs from CH rats (248). In addition, depolarization does not appear to contribute to ET-1-dependent Ca^{2+} sensitization following CH as vasoconstrictor responses to ET-1 in Ca^{2+} permeabilized arteries from CH rats were elevated compared to control arteries even when membrane potential was maintained at ~-60 mV.

Although the present study provides insights regarding the signaling mechanisms that link vessel wall stretch, membrane depolarization and ETR stimulation to enhanced vasoreactivity following CH, further studies are necessary to elucidate how these various stimuli result in Src kinase activation. As GPCRs are capable of Src kinase activation (148), enhanced vasoconstriction to ET-1 following CH may result from direct activation of Src kinases via ETR.

Due to the ability of GPCRs to activate Src kinases in COS-7 cells (148), and findings that depolarization (141; 154) and mechanical stimuli (113; 161) can activate GPCRs, we wished to determine if metabotropic signaling of ETR couple membrane depolarization and mechanical stimuli mediating basal tone to Src/EGFR/NOX 2 activation. Combined ET_AR and ET_BR inhibition did not

prevent augmented vasoconstriction to KCl in CH arteries, nor was it able to prevent the development of pressure-dependent tone. These results suggest that basal tone and enhanced vasoconstriction to depolarizing stimuli occur independent of ETR activation.

Another potential location of Src signaling is in integrin complexes through detection of membrane stretch (205; 223). Changes in various integrin subunit expression levels have been observed in both CH and monocrotaline-induced PH (282), and mechanical stretch can result in integrin dependent EGFR activation (120).While membrane stretch could directly activate Src kinases through signaling locations such as integrin complexes (205; 223), it is more likely that Src activation occurs through pressure-dependent membrane depolarization. This is supported by our findings that basal tone requires membrane depolarization. The mechanism by which membrane depolarization leads to Src activation is not clear. Potential candidates include metabotropic ion channel signaling (67), G-protein coupled receptors (other than the ET-1 receptor, Fig. 45) (141; 154), and voltage sensitive phosphatases (172).

Interestingly, persistent vasoconstrictor responses to KCl and ET-1 were observed in Ca^{2+} permeabilized arteries from both CH and control rats after inhibition of NOX, Rac1, EGFR, or Src in arteries from both groups. Previous findings have demonstrated that a portion of this remaining ET-1-dependent vasoconstriction is mediated by ROK (109). Our observations that NOX, EGFR, and Src inhibition had no effect in control arteries suggest that ET-1 stimulation can lead to ROK-dependent vasoconstriction through additional mechanisms.

Neither inhibition of ROK and PKC, nor scavenging of O_2^- significantly attenuated the remaining vasoconstriction to KCl (26). Although the mechanism of this residual vasoconstriction is unknown, it is possible that a Ca^{2+}-independent myosin light chain kinase, such as integrin linked kinase (47) or ZIP kinase (181), contributes to this response.

The presence of basal tone in CH but not control arteries could be a confounding factor in our findings. Although little if any tone development occurs in arteries from CH rats at intraluminal pressures of 12 mmHg used for vasoreactivity studies (Fig. 25), it is possible that any drug-induced increases in basal tone could limit subsequent vasoconstrictor responses to KCl or ET-1 due to a ceiling effect (i.e. when vessel diameter approaches the limit of detection). However, vessel diameters were similar between groups in the presence and absence of inhibitors, suggesting that these inhibitors did not produce substantial changes in basal tone (Appendix C). Tone in Ca^{2+} permeabilized arteries (300 nM Ca^{2+}) tended to be greater in vessels from CH rats compared to controls, but there were no apparent effects of inhibitors to alter tone in these arteries (Appendix C).

Approaches that assess organ regulation independent of the whole animal have several limitations. Living organisms are complex functional systems. The present study relied heavily on isolated vessel approaches in endothelium disrupted arteries. *In vivo* there are a variety of other factors, such as NO, AVP, and ET-1, released from the surrounding lung, the endothelium, and sources other than the lung that can alter the level of tone within the pulmonary

circulation. Endothelium-derived ROS contribute to regulation of pulmonary vascular smooth muscle tone (107), and the present study does not examine this source of ROS. Pulmonary arteries in the whole animal are surrounded by the structure of the lung. This structure may limit the distension of arteries (Fig. 7) in response to increases in intraluminal pressure *in vivo*. Additionally, our studies focus on only one branch of the arterial tree, making it somewhat difficult to extrapolate our findings to the whole pulmonary circulation. However, previous findings from our laboratory demonstrate that enhanced vasoreactivity to KCl in isolated saline perfused lungs requires O_2^- and ROK similar to the pathway studied in isolated vessels (26). This supports a role for the present findings in the intact pulmonary circulation.

PHYSIOLOGICAL SIGNIFICANCE

CH, associated with residence at high altitude and chronic obstructive pulmonary diseases, is a pathophysiological stimulus that leads to PH and right heart failure in severe cases of lung disease. Although PH is a multifaceted disease with many contributing factors, increasing evidence suggests that mechanisms of ROK-mediated Ca^{2+} sensitization are important in this disease (177), and that inhibition of this response provides a promising avenue of therapeutic potential in the treatment of PH (12). The ability to understand the signaling pathways that mediate this response may provide the potential for alternative treatments for PH. Findings by this study and others (42; 162) suggest that EGFR inhibition, through attenuations in remodeling and vasoconstriction,

may provide a therapeutic target for the treatment of PH. Src kinases, MMPs, and NOX 2 are also potential drug targets.

Vasoconstriction to other agonists besides ET-1 is augmented following CH. Increased vasoreactivity to $PGF_{2\alpha}$, the thromboxane analogue U-46619, 5-HT, and norepinepherine has been observed in the hypertensive pulmonary circulation (159; 207; 290). CH may also couple these other GPCRs to ROK-dependent Ca^{2+} sensitization via the mechanisms studied. Increased production of several agonists, such as ET-1 (4; 49), 5-HT (63), and thromboxanes (123) in the setting of PH could make this pathway more relevant. Furthermore, any stimuli that evoke membrane depolarization may also be capable of activating this Src/EGFR/NOX pathway. This signaling pathway may also be relevant in the normoxic pulmonary circulation. Vasoconstriction to $PGF_{2\alpha}$ in pulmonary arteries also requires ROK-mediated Ca^{2+} sensitization (121). Interestingly, this vasoconstriction also involved Src kinases.

The basal tone in pulmonary arteries from CH rats observed by this study and previous findings from our laboratory (27) suggest that this response is markedly different compared to systemic vessels. In systemic vessels, myogenic tone is characterized by a passive distention to pressure followed by active constriction mediated by calcium influx (45; 198). In contrast, tone development in the pulmonary circulation is not associated with a secondary constriction, but rather a limiting of the distension that occurs. Where pressure dependent tone in the systemic circulation regulates blood flow in response to changes in blood

pressure (45), the tone in pulmonary arteries appears to be pathological in nature.

Depolarization stimulates ROS production in a variety of cell types including the endothelium, neurons, and macula densa cells (1; 32; 126; 143; 239; 254). A similar Src/EGFR/NOX signaling pathway to the one in the present study has been identified in renal mesangial cells (314). Alterations in Src and EGFR signaling are observed in numerous forms of cancer (117). A wide variety of EGR mutants have been observed in tumors with functional consequences (94; 127). Therefore, the relevance for the findings in the current study are not limited to the pathology of PH, but may have broader implications for regulation of contraction, proliferation and apoptosis in other forms of lung injury, cardiovascular disease, and tumorigenesis associated with hypoxia and oxidative stress.

CONCLUSIONS

In conclusion, we have identified a unique signaling pathway in pulmonary vascular smooth muscle involving Src-dependent, EGFR-induced Rac1 and NOX 2 activation that couples membrane depolarization and ETR stimulation to myofilament Ca^{2+} sensitization and ROK-dependent vasoconstriction (Fig. 68). Increases in intraluminal pressure appear to activate this pathway through stretch-dependent membrane depolarization. Furthermore, whereas this signaling pathway does not exist in the normotensive pulmonary circulation, it is induced by long-term hypoxia, and may provide a basis for understanding mechanisms of VSM Ca^{2+} sensitization and vasoconstriction that contribute to

CH-induced PH. Finally, our studies in animals treated chronically with an EGFR inhibitor support a novel role for EGFR in the development of CH-induced PH.

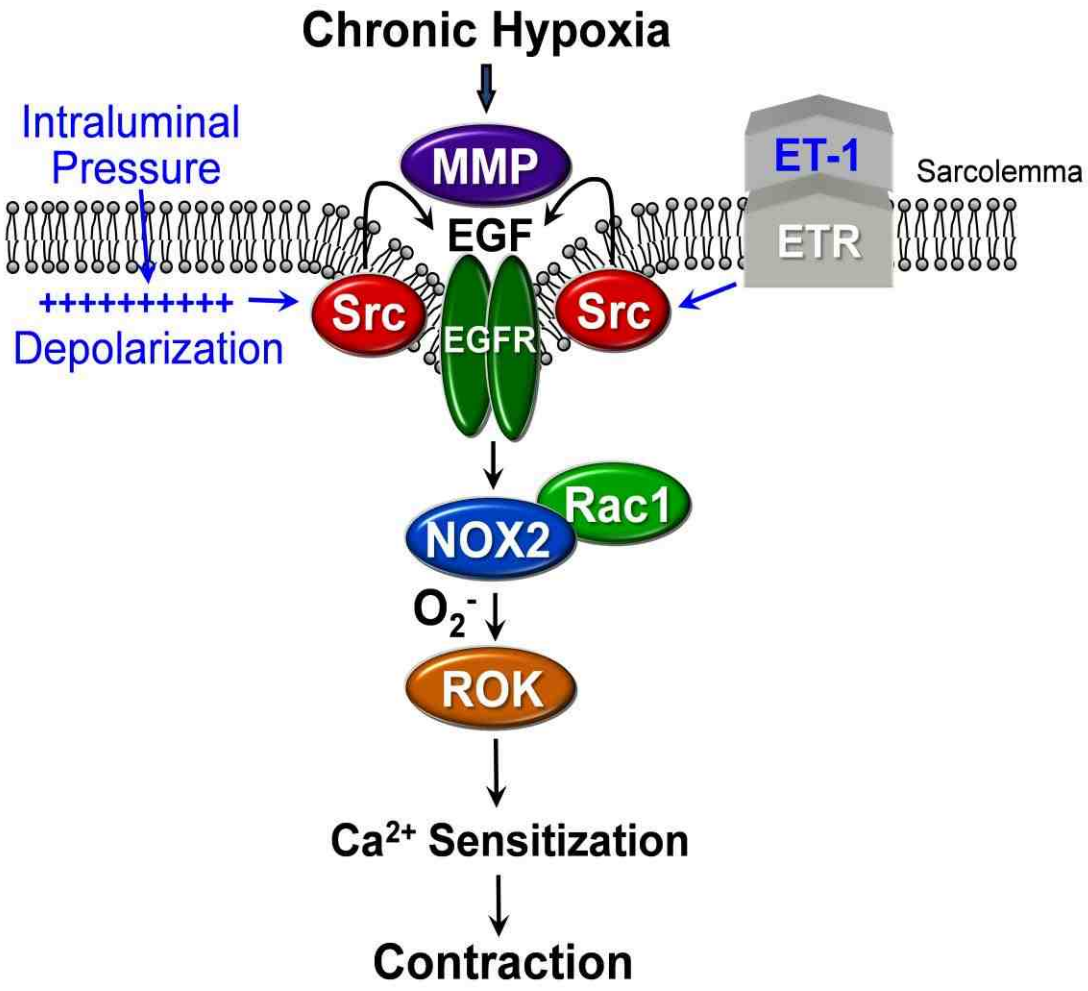

Figure 68: Diagram of Src/EGFR/NOX 2 signaling pathway in VSM of pulmonary arteries following CH. This pathway is elicited by increases in intraluminal pressure, membrane depolarization, and ETR stimulation.

APPENDIX A- Abbreviations and Acronyms

a disintegrin and a metalloproteinase = ADAM

acetylcholine = ACh

caveolin-1 = cav-1

chronic hypoxia = CH

chronic obstructive pulmonary diseases = COPD

diacylglycerol = DAG

dihydroethidium = DHE

endoplasmic reticulum = ER

endothelial nitric oxide synthase = eNOS

endothelin-1 = ET-1

endothelin receptors = ETR

epidermal growth factor = EGF

epidermal growth factor receptor = EGFR

G-protein-coupled receptor = GPCR

hypoxia inducible factor = HIF

hypoxic pulmonary vasoconstriction = HPV

hydrogen peroxide = H_2O_2

inhibitor = INH

inner diameter = ID

inositol trisphosphate = IP_3

left ventricle = LV

matrix metalloproteinase = MMP

myosin light chain = MLC

myosin light chain kinase = MLCK

myosin light chain phosphatase = MLCP

NADPH oxidase = NOX

nitric oxide = NO

peroxynitrite = $ONOO^-$

phosphatidylinositol 4,5-bisphosphate = PIP_2

phospholipase C = PLC

physiological saline solution = PSS

polyethylene glycol = PEG

prostaglandin $F_{2\alpha}$ = $PGF_{2\alpha}$

pulmonary artery smooth muscle cell = PASMC

pulmonary hypertension = PH

reactive oxygen species = ROS

receptor-operated Ca^{2+} entry = ROCE

right ventricle = RV

right ventricular systolic pressure = RVSP

Rho kinase = ROK

sarcoplasmic reticulum = SR

sarcoplasmic endoplasmic reticulum Ca^{2+} ATPase = SERCA

septum = S

serotonin = 5-HT

Src homology domain = SH

store-operated Ca^{2+} entry = SOCE

superoxide anion = O_2^-

superoxide dismutase = SOD

tissue inhibitor of metalloproteinase = TIMP

transient receptor potential canonical = TRPC

vascular smooth muscle = VSM

voltage gated Ca^{2+} channels = VGCC

xanthine oxidase = XO

APPENDIX B- Supplemental Data

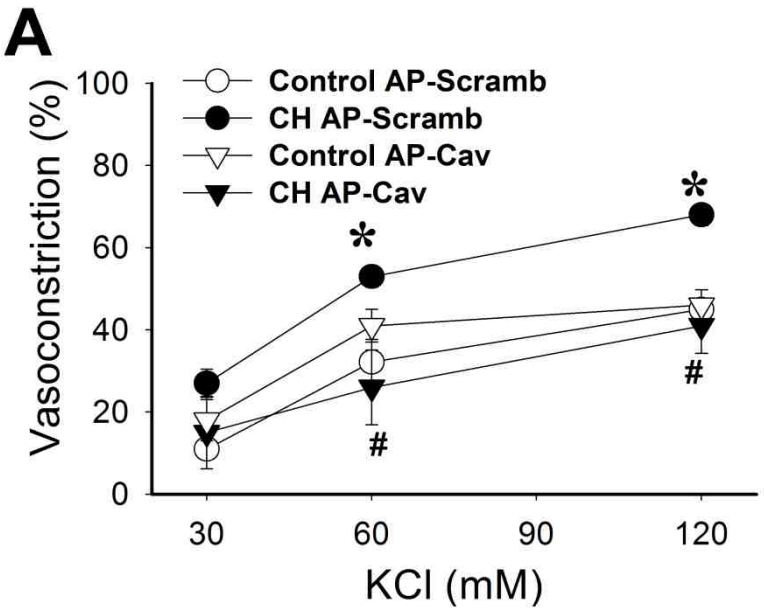

Supplemental Figure 1. **AP-Cav prevents enhanced vasoconstriction to KCl following CH.** Vasoconstrictor responses to KCl in pressurized, Ca^{2+} permeabilized, endothelial disrupted pulmonary arteries from CH and control rats in the presence of AP-Cav or its scrambled control peptide (50 µM). Values are means ± SE n=5-6/group. *p<0.05 vs. control AP-Scramb. #P< 0.05 CH AP-Scramb.

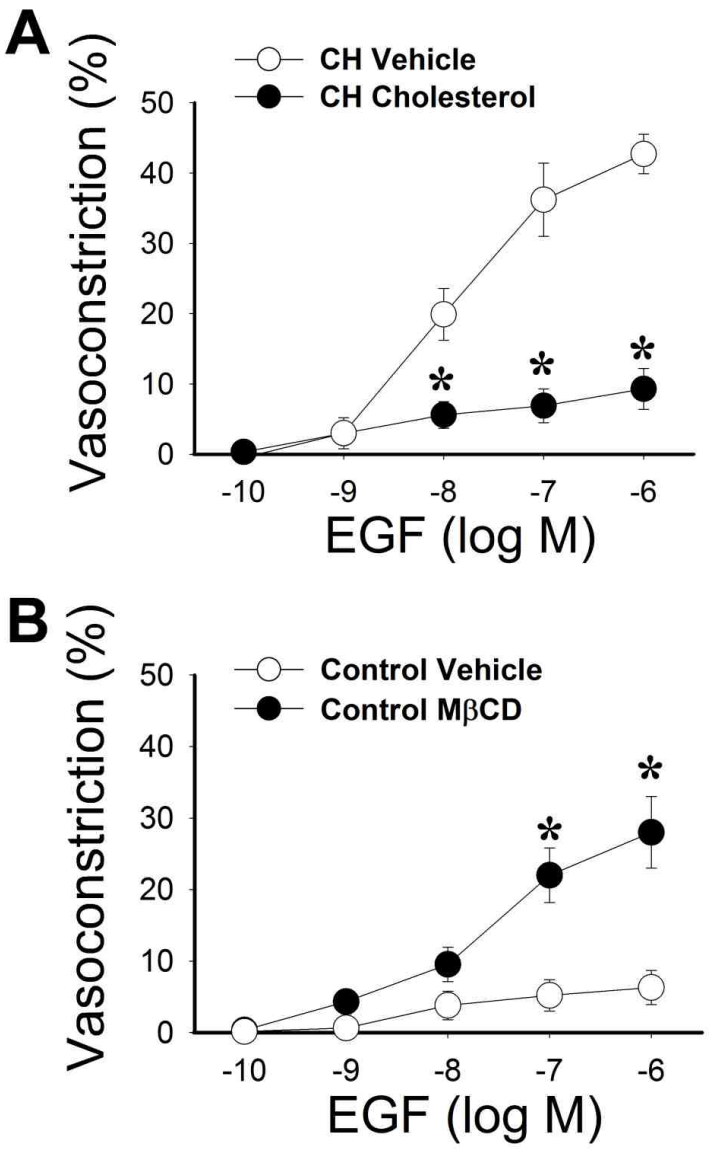

Supplemental Figure 2. **Membrane cholesterol prevents EGF-dependent vasoconstriction.** Vasoconstrictor responses to EGF in pressurized, Ca^{2+} permeabilized, endothelial disrupted pulmonary arteries from CH and control rats in the presence of supplemental cholesterol or MβCD. Values are means ± SE n=4/group. *p<0.05 vs. vehicle.

APPENDIX C- Baseline Arterial Diameters

Baseline inner diameters for isolated vessel experiments in arteries stimulated with KCl, increases in intraluminal pressure (Tone), ET-1, or EGF treated with various inhibitors (INH) and tone (%) at 300 nM Ca^{2+} in Ca^{2+} permeabilized arteries. Values are means ± SE.

Figure/Agonist	Group	Baseline Diameter (μm)	Tone (300 nM Ca^{2+})
Fig. 12	Control Vehicle	176 ± 19	NA
KCl	CH Vehicle	173 ± 22	NA
	Control Apocynin	164 ± 9	NA
	CH Apocynin	143 ± 13	NA
Fig. 13A	Control Vehicle	176 ± 9	1.3
KCl	CH Vehicle	151 ± 9	4.0
	Control Apocynin	154 ± 7	0.6
	CH Apocynin	160 ± 15	4.9
Fig. 13B	Control Vehicle	176 ± 9	1.3
KCl	CH Vehicle	151 ± 9	4.0
	Control DPI	160 ± 13	1.6
	CH DPI	135 ± 7	4.3
Fig. 14	Control scrambled	156 ± 9	0.7
KCl	CH scrambled	172 ± 16	3.0
	Control gp91ds-tat	155 ± 7	1.5
	CH gp91ds-tat	144 ± 4	4.5
Fig. 18A	Control Vehicle	144 ± 15	1.7
KCl	CH Vehicle	160 ± 5	5.1
	Control SOD	151 ± 22	-0.4
	CH SOD	128 ± 21	3.3

Figure/Agonist	Group	Baseline Diameter	Tone (300 nM Ca^{2+})
Fig. 18B	Control Vehicle	144 ± 15	1.7
KCl	CH Vehicle	160 ± 5	5.1
	Control Catalase	167 ± 9	1.4
	CH Catalase	176 ± 8	7.9
Fig. 19	Control Vehicle	169 ± 24	1.9
KCl	CH Vehicle	154 ± 11	4.0
	Control NSC 23766	153 ± 20	2.4
	CH NSC 23766	182 ± 11	5.0
Fig. 23	Control Vehicle	136 ± 9	NA
Tone	CH Vehicle	124 ± 5	NA
	Control Apocynin	138 ± 10	NA
	CH Apocynin	146 ± 13	NA
Fig. 24	Control scrambled	152 ± 17	NA
Tone	CH scrambled	139 ± 9	NA
	Control gp91ds-tat	149 ± 8	NA
	CH gp91ds-tat	156 ± 14	NA
Fig. 25	Control Vehicle	159 ± 10	NA
Tone	CH Vehicle	143 ± 10	NA
	Control NSC 23766	135 ± 10	NA
	CH NSC 23766	151 ± 10	NA

Figure/Agonist	Group	Baseline Diameter	Tone (300 nM Ca^{2+})
Fig. 26A	Control Vehicle	150 ± 14	NA
Tone	CH Vehicle	165 ± 11	NA
	Control SOD	125 ± 8	NA
	CH SOD	138 ± 24	NA
Fig. 26B	Control Vehicle	150 ± 14	NA
Tone	CH Vehicle	165 ± 11	NA
	Control Catalase	149 ± 4	NA
	CH Catalase	156 ± 14	NA
Fig. 28	Control scrambled	188 ± 13	-0.3
ET-1	CH scrambled	167 ± 13	5.0
	Control gp91ds-tat	138 ± 10	1.4
	CH gp91ds-tat	159 ± 11	4.9
Fig. 29	Control Vehicle	155 ± 10	1.1
ET-1	CH Vehicle	164 ± 10	3.8
	Control NSC 23766	173 ± 13	2.4
	CH NSC 23766	145 ± 16	3.5
Fig. 31	Control Vehicle	169 ± 24	1.9
KCl	CH Vehicle	154 ± 11	4.0
	Control AG1478	162 ± 16	1.3
	CH AG1478	162 ± 11	5.7

Figure/Agonist	Group	Baseline Diameter	Tone (300 nM Ca^{2+})
Fig. 36A	Control Vehicle	180 ± 10	2.2
KCl	CH Vehicle	177 ± 6	4.9
	Control SU6656	164 ± 12	2.0
	CH SU6656	165 ± 15	3.7
Fig. 36B	Control Vehicle	180 ± 10	2.2
KCl	CH Vehicle	177 ± 6	4.9
	Control PP2	157 ± 11	2.0
	CH PP2	155 ± 13	3.6
Fig. 37A	Control Vehicle	163 ± 10	NA
Tone	CH Vehicle	152 ± 10	NA
	Control AG1478	174 ± 19	NA
	CH AG1478	150 ± 16	NA
Fig. 37B	Control Vehicle	163 ± 10	NA
Tone	CH Vehicle	152 ± 10	NA
	Control Gefitinib	166 ± 17	NA
	CH Gefitinib	145 ± 21	NA
Fig. 38	Control Vehicle	159 ± 13	NA
Tone	CH Vehicle	143 ± 9	NA
	Control SU6656	131 ± 4	NA
	CH SU6656	153 ± 10	NA

Figure/Agonist	Group	Baseline Diameter	Tone (300 nM Ca^{2+})
Fig. 39	Control Vehicle	142 ± 16	2.8
ET-1	CH Vehicle	161 ± 16	6.2
	Control AG1478	152 ± 11	2.4
	CH AG1478	159 ± 15	3.5
Fig. 40	Control Vehicle	142 ± 16	2.8
ET-1	CH Vehicle	161 ± 16	6.2
	Control SU6656	152 ± 21	2.5
	CH SU6656	159 ± 15	4.2
Fig. 44	Control Vehicle	173 ± 15	NA
EGF	CH Vehicle	172 ± 12	NA
Fig. 45A	Control Vehicle	173 ± 15	NA
EGF	CH Vehicle	172 ± 12	NA
	Control HA-1077	138 ± 9	NA
	CH HA-1077	154 ± 16	NA
Fig. 45B	Control Vehicle	143 ± 15	NA
EGF	CH Vehicle	146 ± 13	NA
	Control gp91ds-tat	143 ± 21	NA
	CH gp91ds-tat	162 ± 16	NA

Figure/Agonist	Group	Baseline Diameter	Tone (300 nM Ca^{2+})
Fig. 46A	Control Vehicle	152 ± 10	NA
EGF	CH Vehicle	157 ± 19	NA
	Control AG1478	153 ± 17	NA
	CH AG1478	147 ± 16	NA
Fig. 46B	Control Vehicle	136 ± 14	NA
EGF	CH Vehicle	173 ± 5	NA
	Control SU6656	148 ± 17	NA
	CH SU6656	145 ± 10	NA
Fig. 47	Control Vehicle	144 ± 10	2.9
ET-1	CH Vehicle	180 ± 8	5.4
	Control GM6001	161 ± 12	2.1
	CH GM6001	174 ± 12	6.0
Fig. 48	Control Vehicle	155 ± 17	0.6
ET-1	CH Vehicle	158 ± 11	5.0
	Control MMP2 INH3	167 ± 16	0.5
	CH MMP2 INH3	160 ± 12	4.2
Fig. 50	Control Vehicle	155 ± 17	0.7
ET-1	CH Vehicle	158 ± 11	5.0
	Control MMP9 INH2	161 ± 14	1.2
	CH MMP9 INH2	176 ± 5	4.4

Figure/Agonist	Group	Baseline Diameter	Tone (300 nM Ca^{2+})
Fig. 52	Control Vehicle	156 ± 6	2.5
ET-1	CH Vehicle	165 ± 14	3.4
	Control TAPI	160 ± 16	1.5
	CH TAPI	150 ± 21	4.3
Fig. 54	Control Vehicle	133 ± 13	2.5
KCl	CH Vehicle	185 ± 12	4.2
	Control BQ	169 ± 7	1.6
	CH BQ	163 ± 10	4.8
Fig. 55	CH Vehicle	139 ± 8	NA
Tone	CH BQ	148 ± 19	NA
Fig. 62	Control Vehicle	136 ± 10	NA
Tone	CH Vehicle	124 ± 5	NA
	Control Valinomycin	152 ± 19	NA
	CH Valinomycin	153 ± 7	NA
Fig. 65	Control Vehicle	145 ± 14	NA
Tone	CH Vehicle	148 ± 7	NA
	Control Pinacidil	161 ± 19	NA
	CH Pinacidil	161 ± 12	NA
Fig. 67	Control Vehicle	160 ± 9	0.1
ET-1	CH Vehicle	174 ± 17	1.6
	Control Valinomycin	174 ± 6	1.2
	CH Valinomycin	168 ± 11	7.0

REFERENCES

1. **Al-Mehdi A, Zhao G, Dodia C, Tozawa K, Costa K, Muzykantov V, Ross C, Blecha F, Dinauer M and Fisher AB**. Endothelial NADPH oxidase as the source of oxidants in the lungs exposed to ischemia or high K+. *Circ Res* 83: 730-737, 1998.

2. **Alfonso-Jaume M, Bergman M, Mahimkar R, Cheng S, Jin Z, Karliner J and Lovett DH**. Cardiac ischemia-reperfusion injury induces matrix metalloproteinase-2 expression through the AP-1 components FosB and JunB. *Am J Physiol Heart Circ Physiol* 291: H1838-H1846, 2006.

3. **Altun-Gultekin Z and Wagner J**. Src, Ras, and Rac mediate the migratory response elicited by NGF and PMA in PC12 cells. *Neurosci Res* 44: 308-327, 1996.

4. **Ambalavanan N, Li P, Bulger A, Murphy-Uldritch J, Oparil S and Chen Y**. Endothelin-1 mediates hypoxia-induced increases in vascular collagen in the newborn mouse lung. *Pediatr Res* 61: 4447-4452, 2007.

5. **Amin A, Abd Elmageed Z, Partyka M and Matrougui K**. Mechanisms of myogenic tone of coronary arteriole: Role of down stream signaling of the EGFR tyrosine kinase. *Microvascular Research* 81: 135-142, 2011.

6. **Archer S, Marsboom G, Kim G, Zhang H, Toth P, Svensson E, Dyck J, Gomberg-Maitland M, Thebaud B, Husain A, Cipriani N and Rehman J**. Epigenetic attenuation of mitochondtiral superoxide dismutase 2 in pulmonary arterial hypertensioh: a basis for

excessive cell proliferation and a new therapeutic target. *Circulation* 121: 2661-2670, 2010.

7. **Asakura M, Kitakaze M, Takashima S, Liao Y, Ishikura F, Yoshinaka T, Ohmoto H, Node K, Yoshino K, Ishiguro H, Asanuma H, Sanada S, Matsumura Y, Takeda H, Beppu S, Tada M, Hori M and Higashiyama S**. Cardiac hypertrophy is inhibited by antagonism of ADAM12 procession og HB-EGF: metalloproteinase inhibitors as a new therapy. *Nat Med* 8: 35-40, 2002.

8. **Austin E, Ma L, LeDuc C, Rosenzweig E, Borczuk A, Phillips J, Palomero T, Sumazin P, Kim H, Talati M, West J, Loyd J and Chung W**. Whole exome sequencing to identify a novel gene (caveolin-1) associated with human pulmonary arterial hypertension. *Circ Cardiovasc Genet* 5: 336-343, 2012.

9. **Austin E, Rock M, Mosse C, Vnencak-Jones C, Yoder S, Robbins I, Loyd J and Meyrick B**. T lymphocyte subset abnormalities in the blood and lung in pulmonary arterial hypertension. *Respir Med* 104: 454-462, 2010.

10. **Barman SA**. Vasoconstrictor effect of endothelin-1 on hypertensive pulmonary arterial smooth muxcle involves Rho-kinase and protein kinase C. *Am J Physiol Lung Cell Mol Physiol* 293: L472-L479, 2007.

11. **Barman SA, Chen F, Su Y, Dimitropoulou C, Wang Y, Catravas J, Han W, Orfi L, Szanti-Kis C, Szabadkai I, Barbutis N, Rafikov R, Black S, Jonigk D, Giannis A, Asmis R, Stepp D, Ramesh G and Fulton D**. NADPH oxidase 4 is expressed in pulmonary artery adventitia

and contributes to hypertensive vascular remodeling. *Arterioscler Throm Vasc Biol* 34: 1704-1715, 2014.

12. **Barman SA, Zielinski J and White R**. RhoA/Rho-kinase signaling: a therapeutic target in pulmonary hypertension. *Vasc Health Risk Manag* 5: 663-671, 2009.

13. **Batzer A, Rotlin D, Urena J, Skolnik E and Schlessinger J**. Hierarchy of binding sites for Grb2 and Shc on the epidermal growth factor receptor. *Mol Biol Cell* 14: 5192-5201, 1994.

14. **Bayliss W**. On the local reaction of the arterial wall to changes of internal presure. *J Physiol* 28: 220-231, 1902.

15. **Berk B, Brock T, Webb RC, Taubman M, Atkinson W and Gimbrone M**. Epidermal growth factor, a vascular smooth muscle mitogen induces rat aortic contraction. *J Clin Invest* 75: 1083-1086, 1985.

16. **Bierer R, Nitta C, Codianni S, de Frutos S, Dominguez-Bautista J, Howard T, Resta T and Bosc L**. NFATc3 is required for chronic hypoxia-induced pulmonary hypertension in adult and neonatal mice. *Am J Physiol Lung Cell Mol Physiol* 301: L872-L880, 2011.

17. **Billaud M, Marthan R, Savineau J and Guibert C**. Vascular smooth muscle modulates endothelial control of vasoreactivity via reactive oxygent spedies production through myoendothelial communications. *PLoS One* 4: e6432, 2009.

18. **Biscardi J, Maa M, Tice D, Cox M, Leu T and Parsons S**. c-Src-mediated phosphorylation of the epidermal grwoth factor receptor on Tyr845 and Tyr1101 is associated with modulation of receptor function. *J Biol Chem* 274: 8335-8343, 1999.

19. **Bobik A, Grooms A, Millar J, Mitchell A and Grinpukel S**. Growth factor activity of endothelin on vascular smooth muscle. *Am J Physiol Cell Physiol* 258: C408-C415, 1990.

20. **Boggon T and Eck M**. Structure and regulation of SRC family kinases. *Oncogene* 23: 7918-7928, 2004.

21. **Brandes RP and Kreuzer J**. Vascular NADPH oxidases: molecular mechanisms of activation. *Cardiovascular Research* 65: 16-27, 2004.

22. **Brew K, Dinakarpandian D and Nagase H**. Tissue inhibitors of metalloproteinases: evolution, structure and function. *Biochem Biophys* 1477: 267-283, 2000.

23. **Bromann P, Kokaya H and Courtneidge S**. The interplay between Src family kinases and receptor tyrosine kinases. *Oncogene* 23: 7928-7946, 2004.

24. **Brooke M, Etheridge S, Kaplan N, Simpson C, O'Toole E, Ishida-Yamamoto A, Marches O, Getsios S and Kelsell D**. iRHOM2-dependent regulation of ADAM 17 in cutaneous disease and epidermal barrier function. *Hum Mol Genet* 23: 4046-4076, 2014.

25. **Broome M and Hunter T**. Requirement for c-Src catalytic activity and the SH3 domain in platelet-derived growth factor BB and epidermal growth factor mitogenic signaling. *J Biol Chem* 271: 16798-16806, 1996.

26. **Broughton BR, Jernigan NL, Norton CE, Walker BR and Resta TC**. Chronic hypoxia augments depolarization-induced Ca^{2+} sensitization in pulmonary vascular smooth muscle through superoxide-dependent stimulation of RhoA. *Am J Physiol Lung Cell Mol Physiol* 298: L232-L242, 2010.

27. **Broughton BR, Walker BR and Resta TC**. Chronic hypoxia induces Rho kinase-dependent myogenic tone in small pulmonary arteries. *Am J Physiol Lung Cell Mol Physiol* 294: L797-L806, 2008.

28. **Bruick R and McKnight SL**. A conserved family of prolyl-4-hydroxylases that modify HIF. *Science* 294: 1337-1340, 2001.

29. **Bunn H, Gu J, Huang L, Park J and Zhu H**. Erythropoietin: a model system for studying oxygen-dependent gene regulation. *Exp Biol* 201: 1197-1201, 1998.

30. **Burke TM and Wolin MS**. Hydrogen peroxide elicits pulmonary arterial relaxation and guanylate cyclase activation. *Am J Physiol* 252: H721-H732, 1987.

31. **Charbonneau M, Harper K, Grondin F, Pelmus M, McDonald P and Dubois C**. Hypoxia-inducible factor mediates hypoxic and tumor necrosis factor a-induced increases in

tumor necrosis factor a converting enzyme/ADAM17 expression by synovial cells. *J Biol Chem* 282: 33714-33724, 2007.

32. **Chatterjee S, Browning EA, Hong N, Debolt K, Sorokina EM, Liu W, Birnbaum MJ and Fisher AB**. Membrane depolarization is the trigger for PI3K/Akt activation and leads to the generation of ROS. *Am J Physiol Heart Circ Physiol* 302: H105-H114, 2012.

33. **Chen F, Barman SA, Yu Y, Haigh S, Wang Y, Dou H, Bagi Z, Han W, Su Y and Fulton D**. Caveolin-1 is a negative regulator of NADPH oxidase-derived reactive oxygen species. *Free Radic Biol Med* 73: 201-213, 2014.

34. **Chen MJ, Chiang LY and Lai YL**. Reactive oxygen species and substance P in monocrotaline-induced pulmonary hypertension. *Toxicol Appl Pharmacol* 171: 165-173, 2001.

35. **Chen Y, Pouyssegur J, Courtneidge S and Van Obberghen-Schilling E**. Activation of Src family kinase activity by the G protein-coupled thrombin receptor in growth responsive fibroblasts. *J Biol Chem* 269: 27372-27377, 1994.

36. **Chen Z, Bakhshi F, Shajahan A, Sharma T, Mao M, Trane A, Bernatchez P, van Nieuw Amerongen G, Bonini M, Skidgel R, Malik A and Minshall R**. Nitric oxide-dependent Src activation and resultant caveolin-1 phosphorylation. *Mol Biol Cell* 23: 1388-1398, 2012.

37. **Cheng G, Xiurong L, Xiangzhen L and Songbin F**. IL-17 stimulates migration of carotid artery vascular smooth muscle cells in an MMP-9 dependent manner via p38 MAPK and ERK1/2-dependent NF-κB and AP-1 activation. *Cell Mol Neurobiol* 29: 1161-1158, 2009.

38. **Clempus RE and Griendling KK**. Reactive oxygen species signaling in vascular smooth muscle cells. *Cardiovascular Research* 71: 216-225, 2006.

39. **Cooper J and Howell B**. The when and how of Src regulation. *Cell* 73: 1051-1054, 1993.

40. **Couet J, Sargiacomo M and Lisanti MP**. Interaction of a receptror tyrosine kinase, EGF-R, with caveolins. Caveolin binding negatively regulates tyrosine and serine/threonine kinase activities. *J Biol Chem* 272: 30429-30438, 1997.

41. **Csanyi G, Cifuentes-Pagano E, Ghouleh IA, Ranayhossaini DJ, Egena L, Lopes LR, Jackson HM, Kelly EE and Pagano PJ**. Nox2 B-loop peptide, Nox2ds, specifically inhibits the NADPH oxidase NOX 2. *Free Radical Biology and Medicine* 51: 1116-1125, 2011.

42. **Dahal BK, Cornitescu T, Tretyn A, Pullamsetti SS, Kosanovic D, Dunitrascu R, Ghofrani HA, Weissmann N, Voswinckel R, Banat G, Seeger W, Grimminger F and Schermuly RT**. Role of epidermal growth factor inhibition in experimental pulmonary hypertension. *Am J Respir Crit Care Med* 181: 158-167, 2010.

43. **Davie N, Haleen S, Upton P, Polak J, Yacoub M, Morrell N and Wharton J**. ET(A) and ET(B) receptors modulate the proliferatin of human pulmonary artery smooth muscle cells. *Am J Respir Crit Care Med* 165: 398-405, 2002.

44. **Davis M and Hill M**. Signaling mechanism underlying the vascular myogenic response. *Physiol Rev* 79: 387-423, 199.

45. **Davis M and Hill M**. Signaling mechanisms underlying the vascular myogenic response. *Physiol Rev* 79: 387-423, 1999.

46. **DeMarco V, Habibi J, Whaley-Connell A, Schneider R, Bosanquet J, Hayden M, Delcour K, Cooper S, Andresen B, Sowers J and Dellsperger K**. Oxidative stress contributes to pulmonary hypertension in the transgenic (mRen2)27 rat. *Am J Physiol Heart Circ Physiol* 294: H2659-H2668, 2008.

47. **Deng J, Van Lierop J, Sutherland C and Walsh M**. Ca2+-independent smooth muscle contraction. A novel function for integrin-linked kinase. *J Biol Chem* 276: 16365-16373, 2001.

48. **Dennis KE, Aschner JL, Milatovic D, Shmidt JW, Aschner M, Kaplowitz MR, Zhang Y and Fike CD**. NADPH oxidases and reactive oxygen species at different stages of chronic hypoxia-induced pulmonary hypertension in newborn piglets. *Am J Physiol Lung Cell Mol Physiol* 297: L596-L607, 2009.

49. **DiCarlo V, Chen S, Meng Q, Durand J, Yano M, Chen Y and Oparil S**. ETA-receptor antagonist prevents and reverses chronic hypoxia-induced pulmonary hypertension in rat. *Am J Physiol Lung Cell Mol Physiol* 269: L690-L697, 1995.

50. **Dikalov S, Dikalova A, Bikineyeva A, Schmidt H, Harrison D and Griendling KK**. Distinct roles of Nox1 and Nox4 in basal and angiotensin II-stimulated superoxide and hydrogen peroxide production. *Free Radical Biology and Medicine* 45: 1340-1351, 2008.

51. **Dreux A, Lamb D, Modjtahedi H and Fems G**. The epidermal growth factor receptors and their family of ligands: Their putative role in atherogenesis. *Atherosclerosis* 2006: 38-53, 2006.

52. **Dufour A, Sampson N, Li J, Rizzo R, DeLeon J, Zhi J, Jaber N, Lui E, Zucker S and Cao J**. Small-molecule anticancer compounds selectively target the homopexin domain of matrix metalloproteinase-9. *Cancer Res* 71: 4977-4986, 2011.

53. **Dziadek M and Johnstone L**. Biochemical properties and cellular localization of STIM proteins. *Cell Calcium* 42: 123-132, 2007.

54. **Ebert B and Bunn H**. Regulation of the erythropeietin gene. *Blood* 94: 1864-1877, 1999.

55. **Eddahibi S, Raffestin B, Tayarani Y, Carville C and Adnot S**. Hypoxia/reoxygenation impairs NO-mediated vasodilation in rat lungs. *Am J Physiol Lung Cell Mol Physiol* 271: L441-L449, 1996.

56. **Egea J, Espinet C and Comella JX**. Calmodulin modulates mitogen-activated protein kinase activation in response to membrane depolarization in PC12 cells. *J Neurochem* 70: 2554-2564, 1998.

57. **Eichinger MR and Walker BR**. Nitric oxide and cGMP do not affect fluid flux in isolated rat lungs. *J Appl Physiol* 80: 69-76, 1996.

58. **El Benna J, Faust R, Johnson J and Babior B**. Phosphorylation of the respiratory burst oxidase subunit p47phox as determined by two-dimensional phophopeptide mapping. Phophorylation by protein kinase C, protein kinase A, and a mitogen activated protein kinase. *J Biol Chem* 271: 6374-6378, 1996.

59. **El-Adway MS, Ansari HR, Fil D, Tilley SL and Mustafa SJ**. NADPH oxidase pathway is involved in aortic contraction induced by A3 adenosine receptor in mice. *Journal of Pharmacology and Experimental Therapeutics* 338: 711-717, 2011.

60. **Elmedal B, de Dam M, Mulvany M and Simonsen U**. The superoxide dismutase mimetic, tempol, blunts right ventricular hypertrophy in chronic hypoxic rats. *Br J Pharmacol* 141: 105-113, 2004.

61. **Esteve J, Launay J, Kellermann O and Maroteaux L**. Functions of serotinin in hypoxic pulmonary vascular remodeling. *Cell Biochem Biophys* 47: 33-44, 2007.

62. **Fan G, Shumay E, Malbon C and Wang H**. c-Src tyrosine kinase binds the beta 2-adrenergic receptor via phospho-Tyr-350, phosphorylates G-protein-linked receptor kinase 2, and mediates agonist-induced receptor desensitization. *J Biol Chem* 276: 13240-13247, 2001.

63. **Fanburg B and Lee S**. A new role for an old molecule:seratonin as a mitogen. *Am J Physiol Lung Cell Mol Physiol* 272: L795-L373, 1997.

64. **Faraci F and Didion S**. Vascular protection: superoxide dismutase isoforms in the vessel wall. *Arterioscler Throm Vasc Biol* 24: 1367-1373, 2004.

65. **Feng J, Ito M, Ichikawa K, Isaka N, Nishikawa M, Hartshorne D and Nakano T**. Inhibitory phosphorylation site for Rho-associated kinase on smooth muscle myosin phosphatase. *J Biol Chem* 274: 37385-3390, 1999.

66. **Fernandez-Catalan C, Bode W, Huber R, Turk D, Calvete J, Lichte A, Tschesche H and Maskos K**. Crystal structure of the complex formed by the membrane type 1-matrix metalloproteinase with the tissure inhibitor of metalloproteinases-2, the soluble progelatinase a receptor. *EMBO J* 17: 5238-5248, 1998.

67. **Fernandez-Tenorio M, Porras-Gonzalez C, Castellana A, Del Valle-Rodriguez A, Lopez-Barneo J and Urena J**. Metabotropic regulation of RhoA/Rho-associated kinase by L-type Ca2+ channels: new mechanism for depolarization-evoked mammalian arterial contraction. *Circ Res* 108: 1348-1357, 2011.

68. **Fike CD, Dikalova A, Slaughter J, Kaplowitz MR, Zhang Y and Aschner M**. Reactive oxygen species reducing strategies improve pulmonary arterial responses to nitric oxide in piglets with chronic hypoxia-induced pulmonary hypertension. *Antioxid Redox Signal* 18: 1727-1738, 2013.

69. **Fike CD, Slaughter J, Kaplowitz MR, Zhang Y and Aschner JL**. Reactive oxygen species from NADPH oxidase contribute to altered pulmonary vascular responses in piglets with chronic hypoxia-induced pulmonary hypertension. *Am J Physiol Lung Cell Mol Physiol* 295: L881-L888, 2008.

70. **Fresquet F, Pourageaud F, Leblais V, Brandes RP, Savineau J, Marthan R and Muller B**. Role of reactive oxygen species and gp91phox in endothelial dysfunction of pulmonary arteries induced by chronic hypoxia. *Br J Pharmacol* 148: 714-723, 2006.

71. **Frijhoff J, Dagnell M, Augsten M, Beltrami E, Giorgio M and Ostman A**. The mitochondrial reactive oxygen species regulator p66Shc controls PDGF-induced signaling and migratin through protein tyrosine phosphatase oxidation. *Free Radic Biol Med* 68: 268-277, 2014.

72. **Frisdal E, Gest V, Vieillard-Baron A, Lavame M, Lepetit H, Eddahibi S, Lafuma C, Harf A, Adnot S and d'Ortho M**. Gelatinase expression in pulmonary arteries during experimental pulmonary hypertension. *Eur Respir J* 18: 838-845, 2001.

73. **Fujio H, Nakamura K, Matsubara H, Kusan K, Miyaji K, Nagase S, Ikeda T, Ogawa A, Ohta-Ogo K, Miura A, Miyazaki M, Date H and Ohe T**. Carvedilol inhibits proliferation of cultured pulmonary artery smooth muscle cells of patients with idiopathic pulmonary arterial hypertension. *J Cardiovasc Pharmacol* 47: 250-255, 2006.

74. **Gay B, Suarez S, Weber C, Rahuel J, Fabbro D, Furet P, Caravatti G and Schoepfer J**. Effect of potent and selective inhibitors of the Grb2 SH2 domain on cell motility. *J Biol Chem* 274: 23311-23315, 1999.

75. **Giannoni E, Taddei M and Chiarugi P**. Src redox regulation: again in the front line. *Free Radic Biol Med* 49: 516-527, 2010.

76. **Golovina V, Platoshyn O, Bailey C, Wang J, Limsuwan A, Sweeney M, Rubin L and Yuan J**. Upregulated TRP and enhanced capacitative Ca(2+) entry in human pulmonary artery myoctes during proliferation. *Am J Physiol Heart Circ Physiol* 280: H746-H755, 2001.

77. **Gomez D, Alonso D, Yoshiji H and Thorgeirsson U**. Tissue inhibitors of metalloproteinases: structure, regulation and biological functions. *Eur J Cell Biol* 74: 111-112, 1997.

78. **Gomis-Ruth F, Maskos K, Betz M, Bergner A, Huber R, Suzuki K, Yoshida N, Nagase H, Brew K, Bourenkos G, Bartunik H and Bode W**. Mechanism of inhibition of the human matrix metalloproteinase stromelysin-1 by TIMP-1. *Nature (Lond)* 389: 77-81, 1997.

79. **Gonzalez Bosc LV, Resta TC, Walker BR and Kanagy NL**. Mechanisms of intermittent hypoxia induced hypertension. *Journal of Cellular and Molecular Medicine* 14: 3-17, 2010.

80. **Greenberg B and Kishiyama S**. Endothelium-dependent and -independent responses to severe hypoxia in rat pulmonary artery. *Am J Physiol* 265: H1712-H1720, 1993.

81. **Grobe A, Wells S, Benavidez E, Oishi P, Azakie A, Fineman J and Black S**. Increased oxidatve stress in lambs with increased pulmonary blood flow and pulmonary hypertension:role of NADPH oxidase and endothelial NO synthase. *Am J Physiol Lung Cell Mol Physiol* 290: L1069-L1077, 2006.

82. **Gschwind A, Zwick E, Prenzel N, Leserer M and Ullrich A**. Cell communication networks:epidermal growth factor receptor transactivation as the paradigm for interrreceptor signal transmission. *Oncogene* 20: 1594-1600, 2001.

83. **Gupte R, Ata H, Rawat D, Abe M, Taylor M, Ochi R and Gupte SA**. Glucose-6-phosphate dehydrogenase is a regulator of vascular smooth muscle contraction. *Antioxid Redox Signal* 14: 543-558, 2011.

84. **Gupte R, Rawat D, Chettimada S, Cioffi DL, Wolin MS, Gerthoffer W, McMurtry I and Gupte SA**. Activation of glucose-6-phosphate dehydrogenase promotes acute hypoxic pulmonary artery contraction. *J Biol Chem* 285: 19561-19571, 2000.

85. **Haase VH**. Regulation of erythropoiesis by hypoxia-inducible factors. *Blood Reviews* 27: 53, 2013.

86. **Hailstones D, Sleer L, Parton R and Stanley K**. Regulation of caveolin and caveolae by cholesterol in MDCK cells. *J Lipid Res* 39: 369-379, 1998.

87. **Hao L, Du M, Lopez-Campistrous A and Fernandez-Patron C**. Agonist induced activation of matrix matalloproteinase-7 promotes vasoconstriction through epidermal growth factor-receptor pathway. *Circ Res* 94: 68-76, 2004.

88. **Hassoun P, Yu F, Shedd A, Zylueta J, Thannickal V, Lanzillo J and Fanburg B**. Regulation of endothelial cell xanthine dehrogenase xanthine oxidase gene expression by oxygen tension. *Am J Physiol* 266: L163-L171, 1994.

89. **Heget J, Novotna J, Bibova J, Pobysilova V, Vankova M and Hampl V**. Metalloproteinase inhibition by Batimastat attenuates pulmonary hypertension in chronically hypoxic rats. *Am J Physiol Lung Cell Mol Physiol* 285: L199-L208, 2003.

90. **Hilenski LL, Clempus RE, Quinn MT, Lambeth JD and Griendling KK**. Distinct subcellular localizations of Nox 1 and Nox 4 in vascular smooth muscle cells. *Arterioscler Throm Vasc Biol* 24: 667-673, 2004.

91. **Hoshikawa Y, Ono S, Suzuki S, Tanita T, Chida M, Song C, Noda M, Tabata T, Voelkel NF and Fujimura S**. Generation of oxidative stress contributes to the development of pulmonary hypertension induced by hypoxia. *J Appl Physiol* 90: 1299-1306, 2001.

92. **Hoyert D and Xu J**. Deaths: Preliminary data for 2011. *In: National vital statistics reports Hyattsville, MD: National Center for Health Statistics* 2012.

93. **Hu J, Discher D, Bishopric N and Webster K**. Hypoxia regulates expression of the ET-1 gene through aproximal Hif1 binding site on the antisense strand. *Biochem Biophys Res Commun* 245: 894-899, 1998.

94. **Huang H, Nagane M, Klingbeil C, Lin H, Nishikawa R, Ji X, Huang C, Gill G, Wiley H and Cayenee W**. The enhanced tumorigenic activity of a mutant epidermal growth factor receptor common in human cancers is mediated by threshold levels of constitutive tyrosine phosphorylation and unattenuated signaling. *J Biol Chem* 272: 2927-2935, 1997.

95. **Huang L, Gu J, Schau M and Bunn H1**. Regulation of hypoxia-inducible factor 1á is mediated by an O_2-dependent degradation domain via the ubiquitin-proteasome pathway. *Proc Natl Acad Sci USA* 95: 7992, 1998.

96. **Hyvelin J, Howell J, Nichol A, Costeollo C, Preston R and McLoughlin P**. Inhibition of Rho-kinase attenuates hypoxia-induced angiogenesis in the pulmonary circulation. *Circ Res* 97: 185-191, 2005.

97. **Iqbal M, Cawthon D, Wideman R and Bottje W**. Lung mitochondrial dysfunctin in pulmonary hypertension syndrome. II. Oxidative stress and inability to improve function with repeated addition of adenosine diphosphate. *Poult Sci* 80: 656-665, 2001.

98. **Ismail S, Sturrock A, Wu B, Cahill B, Norman K, Huecksteadt T, Sanders K, Kennedy T and Hoidal J**. NOX4 mediates hypoxia-induced proliferation of human pulmonary artery smooth muscle cells:the role of autocrine production of transforming growth factor-

{beta}1 and insulin-like growth factor binding protien-3. *Am J Physiol Lung Cell Mol Physiol* 296: L489-L499, 2009.

99. **Ivan M, Kondo K, Yang H, Kim W, Valiando J, Ohh M, Salic A, Asara J, Lane W and Kaelin W**. HIFá targeted for VHL-mediated destruction by proline hydoxylation:implication for O_2 sensing. *Science* 292: 464-468, 2001.

100. **Jaakkola P, Mole D, Tian Y, Wilson M, Gielbert J, Gaskell S, Kriegsheim A, Hebestreit H, Mukherji M, Schofield C and Waxwell P**. Targeting of HIF-á to the von Hippel-Lindauubiquitulation complex by O_2-mediated regulated prolyl hydoxylation. *Science* 292: 468-472, 2001.

101. **Jasmin J, Mercier I, Dupuis J, Tanowitz H and Lisanti MP**. Short-term administration of a cell-permeable caveolin-1 peptide prevents the development of monocrotaline-induced pulmonary hypertension and right ventricular hypertrophy. *Circulation* 114: 912-920, 2006.

102. **Jelkmann W**. Regulation of erythropoetin production. *J Physiol* 589: 1251-1258, 2010.

103. **Jernigan NL, Broughton BR, Walker BR and Resta TC**. Impaired NO-dependent inhibition of store- and receptor-operated calcium entry in pulmonary vascular smooth muscle after chronic hypoxia. *Am J Physiol Lung Cell Mol Physiol* 290: L517-L525, 2006.

104. **Jernigan NL, Herbert L, Walker BR and Resta TC**. ASIC1 contributes to pulmonary vasculat smooth muscle store-operated Ca(2+) entry. *Am J Physiol Lung Cell Mol Physiol* 297: L271-L285, 2009.

105. **Jernigan NL, Herbert L, Walker BR and Resta TC**. Chronic hypoxia upregulares pulmonary arterial ASIC1:A novel mechanism of enhanced store-operated Ca2+ enty and receptor dependent vasoconstriction. *Am J Physiol Cell Physiol* 302: C931-C940, 2012.

106. **Jernigan NL and Resta TC**. Chronic hypoxia attenuates cGMP-dependent pulmonary vasodilation. *Am J Physiol Lung Cell Mol Physiol* 282: L1366-L1375, 2002.

107. **Jernigan NL, Resta TC and Walker BR**. Contribution of oxygen radicals to altered NO-dependent pulmonary vasodilation in acute and chronic hypoxia. *Am J Physiol Lung Cell Mol Physiol* 286: L947-L955, 2004.

108. **Jernigan NL, Walker BR and Resta TC**. Chronic hypoxia augments protein kinase G-mediated Ca2+ desensitization in pulmonary vascular smooth muscle through inhibition of RhoA/Rho kinase signaling. *Am J Physiol Lung Cell Mol Physiol* 287: L1220-L1229, 2004.

109. **Jernigan NL, Walker BR and Resta TC**. Reactive oxygen species mediate RhoA/Rho kinase-induced Ca^{2+} sensitization in pulmonary vascular smooth muscle following chronic hypoxia. *Am J Physiol Lung Cell Mol Physiol* 295: L515-L529, 2008.

110. **Jousset H, Frieden M and Dmaurex N**. STIM1 knockdown reveals that store operated Ca2+ channel located close to the sarco/endoplasmic Ca2+ ATPases (SERCA) pumps silently refill the endoplasmic reticulum. *Biol Chem* 282: 11456-11464, 2007.

111. **Kakiashvili E, Dan Q, Vandermeer M, Zhang Y, Waheed F, Pharm M and Szaszi K**. The epidermal growth factor recptor mediates tumor necrosis factor-alpha-induced activation of ERK/GEF-H1/RhoA pathway in tubular epithelium. *J Biol Chem* 286: 9268-9279, 2011.

112. **Kamezaki F, Tasaki H, Yamashita K, Tsutsui M, Kiode S, Nakata S, Tanimoto A, Okazaki M, Sasaguri Y, Adachi T and Otsuji Y**. Gene transfer of extracellular superoxide dismutase ameliorates pulmonary hypertension in rats. *Am J Respir Crit Care Med* 177: 219-226, 2008.

113. **Kauffenstein G, Laher I, Matrougui K, Guerineau N and Henrion D**. Emerging role of G-protein-coupled receptors in microvascular myogenic tone. *Cardiovascular Research* 95: 223-232, 2012.

114. **Kawano Y, Yoshimura T and Kaibuchi K**. Smooth muscle contraction by small GTPase Rho. *Nagoya J Med Sci* 65: 1-8, 2002.

115. **Khalil R, Lajoie C, Resnick M and Morgan K**. Ca(2+)-independent isoforms of protein kinase C differentially translocate in smooth muscle. *Am J Physiol* 263: C714-C719, 2014.

116. **Killilea D, Hester R, Balczon R, Babal R and Gillespie M**. Free radical production in hypoxic pulmonary artery smooth muscle cells. *Am J Physiol Lung Cell Mol Physiol* 279: L408-L412, 2000.

117. **Kim H and Muller W**. The role of the epidermal growth factor receptror family in mammary tumorigenesis and metastisis. *Exp Cell Res* 253: 78-87, 1999.

118. **Kitazawa T, Ikebe N and Eto M**. Reconstitution of protein kinase C-induced contractile Ca2+ sensitization in triton X-100-demembraned rabbit arterial smooth muscle. *J Physiol* 520: 139-152, 1999.

119. **Kizub I, Strielkov I, Shaifta Y, Becker S, Prieto-Llorot J, Snetkov V, Soloviev A, Aaronson P and Ward J**. Gap junctions support the sustained phase of hypoxic pulmonary vasoconstriction by facilitating calcium sensitization. *Cardiovascular Research* 99: 401-411, 2013.

120. **Knies Y, Bernd A, Kaufmann R, Bereiter-Hahn J and Kippenberger S**. Mechanical stretch induces clustering of β1-integrins and facilitates adhesion. *Exp Dermatol* 15: 347-355, 2006.

121. **Knock G, Shaifta Y, Snetkov V, Vowles B, Drndarski S, Ward J and Aaronson P**. Interaction between Src family kinases and rho-kinase induced Ca2+-sensitization of rat pulmonary artery. *Cardiovascular Research* 77: 570-579, 2008.

122. **Knock G, Snetkov V, Shaifta Y, Connolly M, Dmdarski S, Noah A, Pourmahram G, Becker S, Aaronson P and Ward J**. Superoxide constricts rat pulmonary arteries via Rho-kinase mediated Ca^{2+} sensitization. *Free Radical Biology and Medicine* 46: 633-642, 2009.

123. **Ko F**. Low affinity thromboxane receptor mediates proliferiation in cultured vasculular smooth muscle cellls of rats. *Arterioscler Throm Vasc Biol* 17: 1274-1282, 1997.

124. **Koo H, Kim K and Hong Y**. Gene expressions of nitric oxide synthase and matrix metalloproteinase-2 in monocrotaline induced pulmonary hypertension in rats after bosentan treatment. *Korean Circ J* 41: 83-92, 2011.

125. **Kramer R, Roberts E, Strifler B and Johnstone E**. Thrombin induces activation of p38 MAP kinase in human platelets. *J Biol Chem* 270: 27395-27398, 1995.

126. **Kronz F, Sohn HY, Keller M, Gloe T, Bolz S, Becker B and Pohl U**. Depolarization of endothelial cells enhances platelet aggregation through oxidative inactivation of endothelial NTPDase. *Arterioscler Throm Vasc Biol* 22: 2003-2009, 2002.

127. **Kuan C, Wikstrand C and Bigner D**. EGF mutant receptor vII as a molecular target in cancer therapy. *Endocr Relat Cancer* 8: 83-96, 2001.

128. **Kwan Y, To K, Lau W and Tsang S**. Comparison of the vascular relaxant effects of ATP-dependent K+ channel openers on aorta and pulmonary artery isolated from spontaneously hypertensive and Wistar-Kyoto rats. *Eur J Pharmacol* 365: 251, 1999.

129. **Le Cras TD, Hardie W, Fagan KA, Whitsett J and Korfhagen T**. Disrupted pulmonary vascular development and pulmonary hypertension in transgenic mice overexpressing transforming growth factor-alpha. *Am J Physiol Lung Cell Mol Physiol* 285: L1046-L1054, 2003.

130. **Leach R, Robertson T, Tword C and Ward J**. Hypoxic vasoconstriction in rat pulmonary and mesenteric arteries. *Am J Physiol* 266: L223-L231, 1994.

131. **Lepetit H, Eddahibi S, Fadel E, Frisdal E, Munaut C, Noel A, Humbert M, Adnot S, d'Ortho M and Lafuma C**. Smooth muscle cell matrix metalloproteinases in idiopathic pulmonary arterial hypertension. *Eur Respir J* 25: 834-842, 2005.

132. **Li H, Elton T, Chen Y and Oparil S**. Increased endothelin receptor gene expression in hypoxic rat lung. *Am J Physiol* 266: L553-L560, 1994.

133. **Li H, Witte K, August M, Brausch I, Godtel-Armbrust U, Habermeier A, Closs E, Oelze M, Munzel T and Fosterman U**. Reversal of endothelial nitric oxide synthase uncuopling and up-regulation of endothelial nitric oxide synthase expression lowers blood pressure in hypertensive rats. *J Am Coll Cardiol* 47: 2536-2544, 2006.

134. **Li S, Couet J and Lisanti MP**. Src tyrosine kinases, Gα subunits, and H-Ras share a common membrane anchored scaffolding protein, caveolin. Caveolin binding nefatively refulates the auto-actinvation of Src tyrosine kinases. *J Biol Chem* 271: 29182-29190, 1996.

135. **Lin MJ, Leung GP, Zhang WM, Yang XR, Yip KP, Tse CM and Sham JS**. Chronic hypoxia-induced upregulation of store-operated and receptor-operated Ca2+ channels in pulmonary arterial smooth muscle cells: a novel mechanism of hypoxic pulmonary hypertension. *Circ Res* 95: 496-505, 2004.

136. **Lin MJ, Yang XR, Cao Y and Sham JS**. hydrogen peroxide-induced Ca2+ mobilization in pulmonary arterial smooth muscle cells. *Am J Physiol Lung Cell Mol Physiol* 292: L1598-L1608, 2007.

137. **Liu J, Liao Z, Camden J, Griffin K, Barrad R, Santiago-Perez L, Gonzalez F, Seye C, Weisman G and Erb L**. Src homology 3 binding sites in the P2Y2 nucleotied receptor interact with Src and regulate activities of Src, poline-rich tyrosine kinase 2, and growth factor receoptors. *J Biol Chem* 279: 8212-8218, 2004.

138. **Liu JQ, Zelko IN, Erbynn EM, Sham JS and Folz RJ**. Hypoxic pulmonary hypertension: role of superoxide and NADPH oxidase (gp91phox). *Am J Physiol Lung Cell Mol Physiol* 290: L2-L10, 2006.

139. **Liu P, Wang P, Michaely P, Zhu M and Anderson R**. Presence of oxidized cholesterol in caveolae uncouples active platelet-derived growth factor receptors from tyrosine kinase substrates. *J Biol Chem* 275: 31648-31654, 2000.

140. **Liu Q, Sham JS, Shimoda LA and Sylvester JT**. Hypoxic constriction of porcine distal pulmonary arteries:endothelium and endothelin dependence. *Am J Physiol Lung Cell Mol Physiol* 280: L856-L865, 2001.

141. **Liu Q, Zheng Y, Korde A, Yadav V, Rathore R, Wess J and Wang Y**. Membrane depolarization causes a direct activation of G protein-coupled receptors leading to local Ca2+ release in smooth muscle. *Proc Natl Acad Sci USA* 106: 11418-11423, 2009.

142. **Liu R, Garvin J, Ren Y, Pagano P and Carretero O**. Depolarization of the macula densa induces superoxide production via NAD(P)H oxidase. *Am J Physiol Renal Physiol* 292: F1867-F1872, 2007.

143. **Liu R and Juncos LA**. GTPase-Rac enhances depolarization induced superoxide production by the macula densa during tubuloglomerular feedback. *Am J Physiol Regul Integr Comp Physiol* 298: R453-R458, 2010.

144. **Lu W, Wang J, Peng G, Shimoda LA and Sylvester JT**. Knockdown of stromal interaction molecule 1 attenuates store operated Ca2+ entry and Ca2+ responses to acute hypoxia in pulmonary arterial smooth muscle. *Am J Physiol Lung Cell Mol Physiol* 297: L17-L25, 2009.

145. **Lu X, Murphy T, Nanes M and art CM**. PPAR {gamma} regulates hypoxia-induced Nox4 expression in human pulmonary artery smooth muscle cells through NF-{kappa}B. *Am J Physiol Lung Cell Mol Physiol* 299: L559-L566, 2010.

146. **Lucchesi P, Sabri A, Belmadani S and Matrougui K**. Involvement of metalloproteinases 2/9 in epidermal growth factor receptor transactivation in pressure-induced myogenic tone in mouse mesenteric resistance arteries. *Circulation* 110: 3587-3593, 2004.

147. **Luttrell D and Luttrell L**. Not so strange bedfellows: G-protein-coupled receptors and Src family kinases. *Oncogene* 23: 7969-7978, 2004.

148. **Luttrell L, Hawes B, van Biesen T, Luttrell D, Lansing T and Lefkowitz R**. Role of c-Src tyrosinge kinase in G protein-coupled receptor- and /Gbetagamga subunit-mediated activation activation of mitogen-activated protein kinases. *J Biol Chem* 271: 19443-19450, 1996.

149. **Ma H, Peng Z, Hiragun T, Iwaki S, Gilfillan A and Beaven M**. Canonical transient receptor potential 5 channel in conjunction with Orai1 and STIM1 allows Ca2+ entry, optimal influx of Ca2+, and degranulation in rat mast cell line. *J Immunol* 180: 2233-2239, 2008.

150. **Ma Y, Huang H, Ali S, Lowry W and Huang X**. Src tyrosine kinase is a novel direct effector of G proteins. *Cell* 102: 635-646, 2000.

151. **MacNee W, Wathen C, Hannan W, Flenley D and Muir A**. Effects of pirbuterol and sodium nitroprusside on pulmonary haemodynamics in hypoxic cor pulmonale. *Br Med J* 287: 1169-1172, 1983.

152. **Madden J, Vadula M and Kurup V**. Effects of hypoxia and other vasoactive agents on pulmonary and cerebral artery smooth muscle cells. *Am J Physiol* 263: L384-L393, 1992.

153. **Manea A**. NADPH oxidase-derived reactive oxygen species: involvement in vascular physiology and pathology. *Cell Tissue Res* 342: 325-339, 2010.

154. **Martinez-Pinna J, Gurung I, Mahaut-Smith M and Morales A**. Direct voltage control of endogenous lysophosphatidic acid G-protein-coupled receptors in Xenopus oocytes. *J Physiol* 588: 1683-1693, 2010.

155. **Matsubra T and Ziff M**. Superoxide anion release by human endothelial cells: synergism between a phorbol ester and a colcium ionophore. *J Cell Physiol* 127: 207-210, 1986.

156. **Matsui K, Takano Y, Yu Z, Hi J, Stetler-Stevenson W, Travis W and Ferrans V**. Immunohistochemical study of endothelin-1 and matrix metalloproteinases in plexogenic pulmonary arteriopathy. *Pathol Res Pract* 198: 403-412, 2002.

157. **Matsuno K, Yamanda H, Iwata K, Jin D, Katsuyama M, Matsuki M, Takai S, Yaminishi K, Miyazaki M, Matsubara H and Yabe-Nishimura C**. Nox 1 is involved in angiotensin II-mediated hypertension: a study in Nox 1-deficient mice. *Circulation* 112: 2677-2685, 2005.

158. **Matsuzaki I, Chatterjee S, Debolt K, Manevich Y, Zhang Q and Fisher AB**. Membrane Depolarization and NADPH oxidase activation in aortic endothelium during ischemia reflect altered mechanotransduction. *Am J Physiol Heart Circ Physiol* 288: H336-H343, 2005.

159. **McMurtry IF, Petrun MD and Reeves JT**. Lungs from chronically hypoxic rats have decreased pressor response to acute hypoxia. *Am J Physiol* 235: H104-H109, 1978.

160. **McNamara PJ, Murthy P, Kantores C, Teixeira L, Engelberts D, van Vliet T, Kavanagh BP and Jankov RP**. Acute vasodilator effects of Rho-kinase inhibitors in neonatal rats with pulmonary hypertension unresponsive to nitric oxide. *Am J Physiol Lung Cell Mol Physiol* 294: L205-L213, 2008.

161. **Mederos y Schnitzler M, Storch U, Meibers S, Nurwakagari P, Breit A, Essin K, Gollasch M and Gudermann T**. Gq-coupled receptors as mechanosensors mediating myogenic vasoconstriction. *EMBO J* 27: 3092-30103, 2008.

162. **Merklinger S, Jones P, Martinez E and Rabinovitch M**. Epidermal growth factor receptor blockade mediates smooth muscle cell apoptosis and improves survival in rats with pulmonary hypertension. *Circ Res* 112: 423-431, 2005.

163. **Meyrick B and Reid L**. The effect of continued hypoxia on rat pulmonary arterial circulation. *Lab Invest* 38: 188-200, 1978.

164. **Meyrick B and Reid L**. Endothelial and subintimal changes in rat hilar pulmonary artery during recovery from hypoxia. A quantitative ultrastructural study. *Lab Invest* 42: 603-615, 1980.

165. **Michelakis E, Hampl V, Nsair A, Wu X, Harry G, Haromy A, Gurtu R and Archer S**. Diversity in mitochondrial function explains differences in vascular oxygen sensing. *Circ Res* 90: 1307-1315, 2002.

166. **Mineo C, Gill G and Anderson R**. Regulated migration of epidermal growth factor receptor from caveolae. *J Biol Chem* 274: 30636-30643, 1999.

167. **Misra S, Fu A, Misra K, Shergil U, Leof E and Mukhopadhyay D**. Hypoxia-induced phenotypic switch of fibroblast to myofibroblasts through a matrix metalloproteinase2/tissue inhibitor of metalloproteinases-mediated pathway:implications for venous neointimal hyperplasia in hemodialysis access. *J Vasc Interv Radiol* 21: 896-902, 2010.

168. **Mittal M, Roth M, Konig P, Hofmann E, Dony E, Goyal P, Selbitz AC, Schermuly RT, Ghofrani HA, Kwapiszewska G, Kummer W, Klepetko W, Hoda MA, Fink L, Hanze J, Seeger W, Grimminger F, Schmidt H and Weissmann N**. Hypoxia-dependent regulation of nonphagocytic NADPH oxidase subunit NOX4 in the pulmonary vasculature. *Circ Res* 101: 258-267, 2007.

169. **Mohazzab K, Kaminski P and Wolin MS**. NADH oxidoreductase is a major source of superoxide anion in bovine coronary endothelium. *Am J Physiol* 266: H2568-H2572, 1994.

170. **Moinard J, Manier G, Pillet O and Castaing Y**. Effect of inhaled nitric oxide on hemodynamics and VA/Q inequalities in patients with chronic obstructive pulmonary disease. *Am J Respir Crit Care Med* 149: 1482-1487, 1994.

171. **Murata M, Peranen J, Schreiner R, Wieland F, Kurzchalia T and Simons K**. VIP21/ caveolin is a cholesterol-binding protein. *Proc Natl Acad Sci USA* 92: 10339-10343, 1995.

172. **Murata Y, Iwasaki H, Sasaki M, Inaba K and Okamura Y**. Phosphoinositide phosphatase activity coupled to an intrinsic voltage sensor. *Nature* 435: 1239-1243, 2005.

173. **Murphy T, Spurrell B and Hill M**. Cellular signalling in arteriolar myogenic constriction: involvement of tyrosine phosphorylation pathways. *Clin Exp Pharmacol Physiol* 29: 612-619, 2002.

174. **Myhre G, Toruner M, Abraham S and Egan L**. Metalloproteinase disintegrin-mediated ectodomain shedding of EGFR ligands, promotes intestinal epithelial restitution. *Am J Physiol Gastrointest Liver Physiol* 287: G1213-G1219, 2004.

175. **Nada S, Okada M, MacAuley A, Cooper J and Nakagawa H**. Cloning of a complementary DNA for a protein-tyrosine kinase that specifically phosphorylates a negative regulatory site of p60 c-src. *Nature* 351: 69-72, 1991.

176. **Nagaoka T, Fagan KA, Gebb SA, Morris KG, Suzuki T, Shimokawa H, McMurtry IF and Oka M**. Inhaled Rho kinase inhibitors are potent and selective vasodilators in rat pulmonary hypertension. *Am J Respir Crit Care Med* 171: 494-499, 2005.

177. **Nagaoka T, Morio Y, Casanova N, Bauer N, Gebb SA, McMurtry IF and Oka M**. Rho/ Rho kinase signaling mediates increased basal pulmonary vascular tone in chronically hypoxic rats. *Am J Physiol Lung Cell Mol Physiol* 287: L665-L672, 2004.

178. **Nagase H and Woessner J**. Matrix metalloproteinases. *J Biol Chem* 274: 21491-21494, 1999.

179. **Naik J, Earley S, Resta TC and Walker BR**. Pressure-induced smooth muscle cell depolarization in pulmonary arteries from control and chronically hypoxic rats. *Am J Physiol Lung Cell Mol Physiol* 98: 1119-1114, 2005.

180. **Nguyen A, Montezano A, Burger D and Touyz R**. Angiotensin II, NADPH oxidase, and redox signaling in the vasculature. *Antioxid Redox Signal* 19: 1110-1120, 2013.

181. **Niiro N and Ikebe M**. Zipper-interacting protein kinase induces Ca2+ free smooth muscle contraction via myosin light chain phosphorylation. *J Biol Chem* 276: 29567-29574, 2001.

182. **Nisbet RE, Graves AS, Kleinhenz DJ, Rupnow HL, Reed AL, Fan TH, Mitchell PO, Sutliff RL and Hart CM**. The role of NADPH oxidase in chronic intermittent hypoxia-induced pulmonary hypertension in mice. *Am J Respir Cell Mol Biol* 40: 601-609, 2009.

183. **Nitta C, Osmond D, Herbert L, Beasley B, Resta TC, Walker BR and Jernigan NL**. Role of ASIC1 in the development of chronic hypoxia-induced pulmonary hypertension. *Am J Physiol Heart Circ Physiol* 306: H41-H52, 2014.

184. **Norton CE, Broughton BR, Jernigan NL, Walker BR and Resta TC**. Enhanced depolarization-induced pulmonary vasoconstriction following chronic hypoxia requires EGFR-dependent activation of NAD(P)H Oxidase 2. *Antioxid Redox Signal* 18: 1777-1788, 2013.

185. **Norton CE, Jernigan NL, Kanagy NL, Walker BR and Resta TC**. Intermittent Hypoxia Augments Pulmonary Vascular Smooth Muscle Reactivity to NO: Regulation by Reactive Oxygen Species. *J Appl Physiol* 111: 980-988, 2011.

186. **Norton CE, Naik J, Walker BR and Resta TC**. Decreased membrane cholesterol facilitates depolarization induced Ca2+ sensitization in pulmonary vascular smooth muscle following chronic hypoxia. *FASEB Journal* 26: 873.14, 2012.

187. **Norton CE, Walker BR and Resta TC**. Role of caveolin-1 in membrane depolarization induced Ca2+ sensitization in pulmonary vascular smooth mucled following chronic hypoxia. *FASEB Journal* 25: 1034.5, 2011.

188. **Nozik-Grayck E and Stenmark KR**. Role of reactive oxygen species in chronic hypoxia-induced pulmonary hypertension and vascular remodeling. *Adv Exp Med Biol* 618: 101-112, 2007.

189. **Odenbach J, Wang X, Cooper S, Chow F, Oka T, Lopaschuk G, Kassiri Z and Fernandez-Patron C**. MMP-2 mediates angiotensin II-induced hypertension under the transcriptional contrrol of MMP-7 and TACE. *Hypertension* 57: 123-130, 2010.

190. **Ohtsu H, Dempsey P, Frank G, Bailoiu E, Higuchi S and Suzuki H**. ADAM17 mediates epidermal growth factor receptor transactivation and vascular smooth muscle cell hypertrophy induced by angiotensin II. *Arterioscler Throm Vasc Biol* 26: e133-e137, 2006.

191. **Oikawa H, Maesawa C, Tatemichi Y, Nishinari Y, Nishiya M, Mizugai H, Ikeda A, Oikawa K, Takikawa Y and Masuda T**. A disintegrin and metalloproteinase 17 (ADAM17) mediates epidermal growth factor receptor transactivation by angiotensin II on hepatic stelate cells. *Life Sci* 97: 137-144, 2014.

192. **Oka M, Hasunuma K, Webb SA, Stelzner TJ, Rodman DM and McMurtry IF**. EDRF suppresses an unidentified vasoconstrictor mechanism in hypertensive rat lungs. *Am J Physiol Lung Cell Mol Physiol* 264: L587-L597, 1993.

193. **Okamoto T, Akuta T, Tamura R, van Der Vliet A and Akaike T**. Molecular mechanism for activatio and regulation of matrix matalloproteinases during bacterial infections and respiratory inflammation. *J Biol Chem* 385: 997-1006, 2004.

194. **Olayloye M, Neve R, Lane H and Hyne N**. The ErbB signaling network:receptor hererodimerizatin in development and cancer. *EMBO J* 19: 3159-3167, 2000.

195. **Ongusaha P, Kwak J, Zwible A, Macip S, Higashiyama S, Taniguchi N, Fang L and Lee S**. HB-EGF is a potent inducer of tumor growth and angiogenesis. *Cancer Res* 64: 5283-5290, 2004.

196. **Oparil S, Chen S, Meng Q, Elton T, Yano M and Chen Y**. Endothelin-A receptor antagonist prevents acute hypoxia-induced pulmonary hypertension in the rat. *Am J Physiol* 268: L95-L100, 1995.

197. **Ormiston M, Chang C, Long L, Soon E, Jones D, Machado R, Reacy C, Toshner M, Campbell K, Riding A, Southwood M, Pepke-Zaba J, Exley A, Trembath R, Colucci F, Wills M, Trowsdale J and Morrell N**. Impaired natural killer cell phenotype and function in indiopathic and heritable pulmonary arterial hypertension. *Circulation* 28: 1099-1109, 2012.

198. **Osol G, Brekke J, McElroy-Yaggy K and Gokina N**. in vitro arterial myogenic behavior. *Am J Physiol Heart Circ Physiol* 283: H2260-H2267, 2002.

199. **Packer L**. *Educational Methods in Enzymology*. San Diego, CA: Academic Press, 2002,

200. **Parekh A and Putney J**. Store-operated calcium channels. *Physiol Rev* 85: 757-810, 2005.

201. **Parsons S and Parsons J**. Src family kinases, key regulators of signal transduction. *Oncogene* 23: 7906-7909, 2004.

202. **Patel H, Zhang S, Murray F, Suda R, Head B, Yokoyama Y, Swaney J, Niesman I, Schermuly RT, Pullamsetti SS, Thistlewaite P, Miyanohara A, Farquhar M, Yuan J and Insel P**. Increased smooth muscle cell expression of caveolin-1 and caveolae contribute to the pathophysiology of idiopathic pulmonary arterial hypertension. *FASEB Journal* 21: 2970-2979, 2007.

203. **Perros F, Dorfmuller P, Montani D, Hammad H, Waelput W, Girerd B, Raymond N, Mercier O, Mussot S, Cohen-Kaninsky S, Humbert M and Lambrecht B**. Pulmonary

lymphoid neogenesis in idiopathid pulmonary arterial hypertension. *Am J Respir Crit Care Med* 185: 311-321, 2012.

204. **Perros F, Dorfmuller P, Souza R, Durand-Gasselin I, Mussot S, Mazmanian M, Herve P, Emilie D, Simonneau G and Humbert M**. Dendtritic cell recruitment in lesion of human and experimental pulmonary hypertension. *Eur Respir J* 29: 462-468, 2007.

205. **Playford M and Schaller M**. The interplay between SRC and integrins in normal and tumor biology. *Oncogene* 23: 7928-7946, 2004.

206. **Plomaritas D, Herbert L, Yellowhair T, Resta TC, Gonzalez Bosc LV, Walker BR and Jernigan NL**. Chronic hypoxia limits H_2O_2-induced inhibition of ASIC-1-dependent store-operated calcium entry in pulmonary arterial smooth muscle. *Am J Physiol Lung Cell Mol Physiol* 307: L419-L430, 2014.

207. **Porcelli R and Bergman M**. Effects of chronic hypoxia on pulmonary vascular responsees to biogenic amines. *J Appl Physiol* 55: 534-540, 1983.

208. **Prenzel N, Zwick E, Daub H, Leserer M, Abraham R, Wallasch C and Ullrich A**. EGF receptor transactivation by G-protein-coupled receptorrs requires metalloproteinase cleavage of proHB-EGF. *Nature* 402: 884-888, 1999.

209. **Pugh C, O'Rourke J, Nagao M, Gleadle J and Ratcliffe P**. Activation of hypoxia-inducible factor-1; definition of regulatory domains within the á subunit. *J Biol Chem* 272: 11205-11214, 1997.

210. **Pullamsetti S, Berghausen E, Dabral S, Tretyn A, Butrous E, Savai T, Butrous G, Dahal BK, Brandes RP, Ghofrani HA, Weissmann N, Grimminger F, Seeger W, Rosenkranz S and Schermuly RT**. Role of Src tyrosine kinases in experimental pulmonary hypertension. *Arterioscler Throm Vasc Biol* 32: 1354-1365, 2012.

211. **Puyraimond A, Weitzman J, Babiole E and Menashi S**. Examining the relationship between the gelatinolytic balance and the invasive capacity of endothelial cells. *J Cell Sci* 112: 1283-1290, 1999.

212. **Raffestin B, Adnot S, Eddhibi S, Macquin-Mavier I, Braquet P and Chabrier P**. Pulmonary vascular response to endothelin in rats. *J Appl Physiol* 70: 567-574, 1991.

213. **Rajavashisth T, Xu X, Jovinge S, Meisel S, Xu X, Chai N, Fishbein M, Kaul S, Cercek B, Sharifi B and Shah P**. Membrane type 1 matrix metalloproteinase expression in human atherosclerotic plaques: evidence for activation by proinflammatory mediators. *Circulation* 99: 3103-3109, 1999.

214. **Ramiro-Diaz J, Nitta C, Maston L, Codianni S, Giermakowska W, Resta TC and Gozalez-Bosc L**. NFAT is required for spontaneous pulmonary hypertension in superoxide dismutase 1 knockout. *Am J Physiol Lung Cell Mol Physiol* 304: L613-L625, 2013.

215. **Rathore R, Zheng Y, Niu C, Liu Q, Korde A, Ho Y and Wang Y**. Hypoxia activates NADPH oxidase to increase [ROS](i) and [Ca(2+)](i) through the mitochondrial ROS-PKCvarepsilon signaling axis in pulmonary artery smooth muscle cells. *Free Radical Biology and Medicine* 45: 1223-1231, 2008.

216. **Reeve H, Michelakis E, Nelson D, Weir E and Archer S**. Alterations in a redox oxygen sensing mechanism in chronic hypoxia. *J Appl Physiol* 90: 2249-2256, 2001.

217. **Resta TC, Chicoine LG, Omdahl JL and Walker BR**. Maintained upregulation of pulmonary eNOS gene and protein expression during recovery from chronic hypoxia. *Am J Physiol* 276: H699-H708, 1999.

218. **Resta TC, Gonzales RJ, Dail WG, Sanders TC and Walker BR**. Selective upregulation of arterial endothelial nitric oxide synthase in pulmonary hypertension. *Am J Physiol* 272: H806-H813, 1997.

219. **Resta TC, Kanagy NL and Walker BR**. Estradiol-induced attenuation of pulmonary hypertension is not associated with altered eNOS expression. *Am J Physiol Lung Cell Mol Physiol* 280: L88-L97, 2001.

220. **Resta TC and Walker BR**. Chronic hypoxia selectively augments endothelium-dependent pulmonary arterial vasodilation. *Am J Physiol* 270: H888-H896, 1996.

221. **Rey FE, Cifuentes ME, Kiarash MT and Pagano PJ**. Novel Competitive Inhibitor of NAD(P)H Oxidase Assembly Attenuates Vascular O_2^- and Systolic Blood Pressure in Mice. *Circ Res* 89: 408-414, 2001.

222. **Rey FE, Cifuentes M, Kiarash M, Quinn M and Pagano PJ**. Novel competitive inhibitor of NAD(P)H oxidase assembly attenuates vascular superoxide and sytolic blood pressure in nice. *Circ Res* 89: 408-414, 2001.

223. **Reynolds A and Roczniak-Ferguson A**. Emerging roles for p120-catenin in cell adhesion and cancer. *Oncogene* 23: 7947-7956, 2004.

224. **Rhee S, Kang S, Netto L, Seo M and Stadtman E**. A family of novel peroxidases, peroxiredoxins. *Biofactors* 10: 207-209, 1999.

225. **Ringerike T, Blystad F, Levy F, Madshus I and Stang E**. Cholesterol is important in control of EGF receptor kinase activity but EGF receptors are not concentrated in caveolae. *J Cell Sci* 115: 1331-1340, 2002.

226. **Risinger G, Updike D, Bullen E, Tomasek J and Howard E**. TGF-beta suppresses the upregulation of MMP-2 by vascular smooth muscle cellls in response to PDGF-BB. *Am J Physiol Cell Physiol* 298: C191-C201, 2010.

227. **Robertson T, Aaronson P and Ward J**. Ca2+ sensitization during sustained hypoxic pulmonary vasoconstriction is endothelium dependent. *Am J Physiol Lung Cell Mol Physiol* 284: L1121-L1126, 2003.

228. **Robertson T, Hague D, Aaronson P and Ward J**. Voltage-independent calcium entry in hypoxic pulmoary vasoconstriction of intrapulmonary arteries of the rat. *J Physiol* 525: 669-680, 2000.

229. **Rodriguez D, Morrison C and Overall C**. Matrix metalloproteinases: what do they not do? New substrates and biological roles identified by murine models and proteomics. *Biochem Biophys* 1803: 39-54, 2010.

230. **Rose F, Grimminger F, Appel J, Heller M, Pies V, Weissmann N, Fink L, Schmidt S, Krick S, Camenisch G, Gassmann M, Seeger W and Hanze J**. Hypoxic pulmonary artery fibroblasts trigger proliferation of vascular smooth muscle cells: role of hypoxia-inducible transcription factors. *FASEB Journal* 16: 1660-1661, 2002.

231. **Rosello A, Nuti E and Orlandi E**. New N-arylsulfonyl-N-alkoxyaminoacetohydroxamic acids as selective inhibitors of gelatinase A (MMP-2). *Bioorg Med Chem* 12: 2441-2450, 2004.

232. **Roskoski R**. Src kinase regulation by phosphorylation and dephosphorylation. *Biochem Biophys Res Commun* 331: 1-14, 2005.

233. **Rubanyi C and Vanhoutte P**. Superoxide anions and hyperoxia inactive endothelium-derived relaxing factor. *Am J Physiol* 250: H822-H827, 1986.

234. **Sanderson M, Abbott C, Tada H, Seno M, Dempsey P and Dunbar A**. Hydrogen peroxide and ET-1 are novel activators of betacellulin ectodomain shedding. *J Biol Chem* 99: 609-623, 2006.

235. **Sato K, Morio Y, Morris KG, Rodman DM and McMurtry I**. Mechanism of hypoxic pulmonary vasoconstriction involvs ET(A) receptor-mediated inhibition of K(ATP) channel. *Am J Physiol Lung Cell Mol Physiol* 278: L434-L442, 2000.

236. **Sato K and Sato A**. c-Src phosphorylates epidermal growth factor receptor on tyrosine 845. *Biochem Biophys Res Commun* 215: 1078-1087, 1995.

237. **Sato K, Webb SA, Tucker A, Rabinovitch M, O'Brien R, McMurtry IF and Stelzner T**. Factors influencing the indiopathic development of pulmonary hypertension in the fawn hooded rat. *Ther American review of respiratory disease* 145: 793-797, 1992.

238. **Savail R, Pullamsetti S, Kolbe J, Bieniek E, Fink L, Scheed A, Ritter C, Dahal BK, Vater A, Klussmannn S, Ghofrani H, Weissmann N, Klepetko W, Banat G, Seeger W, Grimminger F and Schermuly RT**. Immune/inflammatory cell involvement in the pathology of idiopathic pulmonary arterieal hypertension. *Am J Respir Crit Care Med* 186: 897-908, 2012.

239. **Saybasili H, Yuksel M, Haklar G and Yalcin A**. Depolarization-induced superoxide radical formation in rat hippocampal slices. *Nerochem Res* 27: 473-476, 2002.

240. **Schermuly RT, Dony E, Ghofrani HA, Pullamsetti S, Savail R, Roth M, Sydykov A, Lai YL, Weissmann N, Seeger W and Grimminger F**. Reversal of experimental pulmonary hypertension by PDGF inhibition. *J Clin Invest* 115: 2811-2821, 2005.

241. **Schermuly RT, Kreisselmeier K, Ghofrani HA, Samidurai A, Pullamsetti S, Weissmann N, Schudt C, Ermert M, Seeger W and Grimminger F**. Antiremodeling effects of iloprost and the dual-selective phosphodiesterase 3/4 inhibitor tolafentrine in chronic experimental pulmonary hypertension. *Circ Res* 94: 1101-1108, 2004.

242. **Schermuly RT, Kreisselmeier K, Ghofrani H, Yilmaz H, Butrous G, Ermert M, Weissmann N, Rose F, Guenther A, Walmrath D, Seeger W and Grimminger F**. Chronic sildenafil

trearment inhibits monocrotaline-induced pulmonary hypertension in rats. *Am J Respir Crit Care Med* 169: 39-45, 2004.

243. **Segarra M, Vildardell C, Matsumoto K, Esperarza J, Lozano E, Serra-Pages C, Urbano-Marquez A, Yamada K and Cid M**. Dual function of focal adhedsion kinase in gegulating integrin-induced MMP-2 and MMP-9 release by human T lymphoid cells. *FASAEB Journal* 19: 1875-1877, 2005.

244. **Semenza G**. Regulation of oxygen homeostasis by hypoxia-inducible factor 1. *Physiology* 24: 97-106, 2009.

245. **Semenza G and Wang G**. A nuclear factor induced by hypoxia via de novo protein synthesis binds to the human erythropoetin gene enhancer at a site required for transcription activation. *Mol Cell Biol* 12: 5447-5454, 1992.

246. **Seshiah P, Weber D, Rocic P, Valppu L, Taniyama Y and Griendling KK**. Angiotensin II stimulation of NAD(P)H oxidase activity: upstream mediators. *Circ Res* 91: 406-413, 2002.

247. **Sheng L, Zhou W, islop A, Ibe V, Longo L and Rai J**. Role of epidermal growth factor receptor in ovine fetal pulmonary vascular remodeling following exposure to high altitude long-term hypoxia. *High Alt Med Biol* 10: 365-372, 2009.

248. **Shimoda LA, Sylvester JT and Sham JS**. Inhibition of voltage-gated K+ current in rat intrapulmonary arterial mycocytes by ET-1. *Am J Physiol* 274: L842-L853, 1998.

249. **Short M, Nemenoff R, Zawada W, Stenmark KR and Das M**. hypoxia induces differentiation of pulmonary artery adventitial fibroblasts into myofibroblasts. *Am J Physiol Cell Physiol* 286: C416-C425, 2004.

250. **Simonson M and Herman W**. Protein kinase C and protein tyrosine kinase activity contribut to mitogenic signaling by endothelin-1. Cross-talk between G protein-coupled receptors and pp60c-src. *J Biol Chem* 268: 9347-9357, 1993.

251. **Snow JB, Kanagy NL, Walker B and Resta TC**. Rat strain differences in pulmonary artery smooth muscle Ca(2+) entry following chronic hypoxia. *Microcirculation* 16: 603-614, 2009.

252. **Snow JB, Kitzis V, Norton CE, Torres SN, Johnson KD, Kanagy NL, Walker BR and Resta TC**. Differential effects of chronic hypoxia and intermittent hypocapnic and eucapnic hypoxia on pulmonary vasoreactivity. *J Appl Physiol* 104: 110-118, 2008.

253. **Snow J, Sands M, Gonzalez Bosc LV, Walker BR and Resta TC**. Role of mitochondrial reactive oxygen species and actin polymerization in PKC-dependent constriction of small pulmonary but not mesenteric arteries. *FASEB Journal* 26: 873.15, 2012.

254. **Sohn HY, Keller M, Gloe T, Morawietz H, Rueckschloss U and ohl U**. The small G-protein Rac mediates depolarization-induced superoxide formation in human endothelial cells. *J Biol Chem* 275: 18745-18750, 2000.

255. **Somlyo A and Somlyo A**. Ca2+ sensitivity of smooth muscle and nonmuscle myosin II: modulation by G proteins, kinases and myosin phosphatase. *Physiol Rev* 83: 1325-1358, 2003.

256. **Stacher E, Graham B, Hunt J, Gandjeva A, Groshong S, McLaughlin V, Jessup M, Grizzle W, Aldred M, Cook C and Tuder RM**. Modern age pathology of pulmonary arterial hypertension. *Am J Respir Crit Care Med* 186: 261-272, 2012.

257. **Stanbrook H, Morris KG and McMurtry I**. Prevention and reversal of hypoxic pulmonary hypertension by calcium antagonists. *Am Rev Respir Dis* 130: 81-85, 1984.

258. **Stanic B, Pandey D, Fulton D and Miller F**. Increased epidermal growth factor-like ligands are associated with elevated vascular nicotinamide adenine dinucleotide phosphate oxidase in a primate model of atherosclerosis. *Arterioscler Throm Vasc Biol* 32: 2452-2460, 2012.

259. **Stemlicht M and Werb Z**. How matrix metalloproteinases regulate cell behavior. *Ann Rev Cell Dev Biol* 17: 463-516, 2001.

260. **Stenmark KR, Fagan KA and Frid M**. Hypoxia-induced pulmonary vascular remodeling: cellular and molecular mechanisms. *Circ Res* 99: 675-691, 2006.

261. **Stolk J, Hiltermann TJ, Dijkman JH and Verhoeven AJ**. Characteristics of inhition of NADPH oxidase activation in neutrophils by apocynin, a methoxy-substituted catechol. *Am J Respir Cell Mol Biol* 11: 95-102, 1994.

262. **Storme L, Rairigh R, Parker T, Kinsella J and Abman S**. In Vivo evidence for a myogenic response in the fetal pulmonary circulation. *Pediatr Res* 45: 425-431, 1999.

263. **Stover D, Becker M, Liebetanz J and Lydon N**. Src phosphorylation of the epidermal growth factor receptor at novel sites mediated receptor interaction with Src and P85 alpha. *J Biol Chem* 270: 15591-15597, 1995.

264. **Streeter J, Schickling B, Jian S, Stanic B, Thiel W, Gakhar L, Houtman J and Miller F**. Phosphorylation of Nox1 regulates association with NoxA1 activation domain. *Circ Res* 115: 911-918, 2014.

265. **Strongin A, Collier I, Bannikov G, Marmer B, Grant G and Goldberg G**. Mechanism of cell surface activation of 72-kDa type IV collagenase. Isolation of the activated form of the membrane metalloprotease. *J Biol Chem* 270: 5331-5338, 1995.

266. **Suzuki M, Raab G and Fernandez C**. Matrix metalloproteinase-3 releases active heparin-binding EGF-like growth factor by cleavage at a specific juxtamembrane site. *J Biol Chem* 272: 31730-31737, 1997.

267. **Suzuki Y and Ford G**. Redox regulation of signal transcuction in cardiac and smooth muscle. *J Mol Cell Cardiol* 31: 345-353, 199.

268. **Sweeney M, Yu Y, Platoshyn O, Zhang S, McDaniel S and Yuan J**. Inhibition of endogenous TRP1 decreases capacitative Ca2+ entry and attenuates pulmonary artery

smooth muscle cell proliferation. *Am J Physiol Lung Cell Mol Physiol* 283: L144-L155, 2002.

269. **Tabima DM, Frizzell S and Gladwin MT**. Reacitive oxygen and nitrogen species in pulmonary hypertension. *Free Radical Biology and Medicine* 52: 1970-1986, 2012.

270. **Tahara S, Fukuda K, Kodama H, Kato T, Miyoshi S and Ogawa S**. Potassium channel blocker activates extracellular signal-regulated kinases through Pyk2 andepidermal growth factor receptor in rats. *J Am Coll Cardiol* 38: 1554-1563, 2001.

271. **Takaguria A, Shiraia H, Kimuraa K, Hinokia A, Kunie E, Carlile-Klusaceka M, Yang B and Rizzoa V**. Caveolin-1 negatively regulates a metalloprotease-dependent epidermal growth factor receptor transactivation by angiotensin II. *J Mol Cell Cardiol* 50: 545-551, 2011.

272. **Takashima S**. Phosphorylation of myosin regulatory light chain by myosin light chain kinase, and muscle contraction. *Circ J* 73: 208-213, 2009.

273. **Taniguchi K, Xia L, Goldberg H, Lee K, Shah A, Stavar L, Masson E, Momen A, Shikitani E, John R, Husain M and Fantus I**. Inhibition of Src kinase blocks high glucose-induced EGFR transactivation and collagen synthesis in mesangial cells and prevents diabetic nephropathy in mice. *Diabetes* 62: 3874-3886, 2013.

274. **Taniyama Y and Griendling KK**. Reactive oxygen sprecies in the vasculature: molecular and cellular mechanisms. *Hypertension* 42: 1075-1081, 2003.

275. **Thomas S and Brugge J**. Cellular functions regulated by Src family kinases. *Ann Rev Cell Dev Biol* 13: 513-609, 1997.

276. **Tong W, Chen W, Ostrowski R, Ma Q, Souvenir R, Zhang L, Zhang J and Tang J**. Maternal hypoxia increases the activity of MMPs and decreases the expression of TIMPs in the brain of neonatal rats. *Dev Neurobiol* 70: 182, 2010.

277. **Truong T and Carroll K**. Redox regulation of epidermal growth factor receptor signaling through cysteine oxidation. *Biochemistry* 51: 9954-9965, 2012.

278. **Truong T and Carroll K**. Redox regulation of protein kinases. *Crit Rev Biochem Mol Biol* 48: 332-356, 2013.

279. **Tsuchiya T, Okada M, Ueda M and Yasukochi Y**. Activation of the erythropeietin promoter by a point mutation for GATA to TATA in the -30 region. *J Biol Chem (Tokyo)* 121: 193-196, 1997.

280. **Tuder R, Grove B, Badesh D and Voelkel NF**. Exuberant endothelial cell growth and elements of inflammation are present in plexiform lesions of pulmonary hypertension. *Am J Pathol* 144: 275-285, 1994.

281. **Ulu N, Gurdal H, Landheer S, Duin M, Guc M, Buikema H and Henning R**. alpha1-adrenoceptor-mediated contraction of rat aorta is partly mediated via transactivation of the epidermal growth factor receptor. *Br J Pharmacol* 161: 1301-1310, 2010.

282. **Umesh A, Paudel O, Cao Y, Myers J and Sham J**. Alteration of pulmonary artery integrin levels in chronic hypoxia and monocrotaline-induced pulmonary hypertension. *J Vasc Res* 48: 525-537, 2001.

283. **van Hinsbergh V and Koolwjk P**. Endothelial sprouting and angiogenesis: matrix metalloproteinases in the lead. *Cardiovascular Research* 78: 203-212, 2008.

284. **Veit F, Pak O, Egemnazarov B, Roth M, Kosanovic D, Seimetz M, Sommer N, Ghofrani H, Seeger W, Grimminger F, Brandes RP, Schermuly RT and Weissmann N**. Function of NADPH oxidase 1 in pulmonary arterial smooth muscle cells after monocrotaline-induced pulmonary vascular remodeling. *Antioxid Redox Signal* 19: 2213-2231, 2013.

285. **Wang J, Weigand L, Lu W, Sylvester JT, Semenza G and Shimoda LA**. hypoxia inducible factor 1 mediates hypoxia-mediated TRPC expression and elevated basal Ca2+ in pulmonary arterial smooth muscle. *Circ Res* 98: 1528-1537, 2006.

286. **Wang L, Yin J, Nickles H, Ranke H, Tabuchi A, Hoffmann J, Tabeling C, Barbosa-Sicard E, Chanson M, Kwak B, Shin H, Wu S, Isakson B, Wizenrath M, de Wit C, Fleming I, Kupe H and Keubler W**. Hypoxic pulmonary vasoconstriction requires connexin 40-mediated endothelial signal conduction. *J Clin Invest* 122: 4218-4230, 2012.

287. **Wang X, Tong M, Chinta S, Raj J and Gao Y**. Hypoxia-induced reactive oxygen species downregulate ETB receptor mediated contraction of rat pulmonary arteries. *Am J Physiol Lung Cell Mol Physiol* 290: L570-L578, 2006.

288. **Wang X and van Breeman C**. Depolarization-mediated inhibition of Ca(2+) entry in endothelial cells. *Am J Physiol Heart Circ Physiol* 277: H1498-H1504, 1999.

289. **Wanstall JC, Kaye J and Gambino A**. The in vitro pulmonary vascular effects of FK409 (nitric oxide donor):a study in normotensive and pulmonary hypertensive rats. *Br J Pharmacol* 121: 280-286, 1997.

290. **Wanstall JC and O'Donnell S**. Endothelin and 5-hydroxytryptamine on rat pulmonary artery in pulmonary hypertension. *Eur J Pharmacol* 176: 159-168, 1990.

291. **Warnecke C, Zaborowska Z, Kurreck J, Erdmann V, Frei U, Wiesener M and Eckardt K**. Differentiating the functional role of hypoxia-inducible factor (HIF)-1 alpha and HIF-2 alpha (EPAS-1) by the use of RNA interference:erythropoetin is a HIF-2 alpha target gene in Hep3B an Kelly cells. *FASEB Journal* 18: 1462-1464, 2004.

292. **Waterhouse B, Gijsen M, Barber P, Tullis I, Vojnovic B and Kong A**. Assessment of EGFR/HER2 dimerization by FRET-FLIM utilizing Alexa-conjugated secondary antibodies in relation to targeted therapies in cancers. *Oncotarget* 736, 2011.

293. **Waypa GB and Schumacker PT**. Hypoxic pulmonary vasoconstriction: redox events in oxygen sensing. *J Appl Physiol* 98: 404-414, 2005.

294. **Webster N and Crow S**. Matrix metalloproteinases, their production by monocytes and macrophages and their potential role in HIV-related diseases. *J Leukoc Biol* 80: 1066, 2006.

295. **Weigand L, Sylvester JT and Shimoda LA**. Mechanisms of endothelin-1-induced contraction in pulmonary arteries from chronically hypoxic rats. *Am J Physiol Lung Cell Mol Physiol* 290: L284-L290, 2006.

296. **Weir E and Archer S**. The mechanism of acute hypoxic pulmonary vasoconstriction: the tale of two channels. *FASEB Journal* 9: 183-189, 1995.

297. **Wells A**. EGF receptor. *Int J Biochem Cell Biol* 31: 637-343, 1999.

298. **Welsh D, Morielli A, Nelson M and Brayden J**. Transient receptor potential channels regulate myogenic tone of resistance arteries. *Circ Res* 90: 248-250, 2002.

299. **Welsh D, Harnett M, MacLean M and Peacock A**. Proliferation and signaling in fibroblasts: role of 5 hydroxtryptamine2A receptor and transporter. *Am J Respir Crit Care Med* 170: 252-259, 2004.

300. **Will H, Atkinson S, Butler G, Smith B and Murphy G**. The soluble catalytic domain of membrane type 1 matrix metalloproteinase cleaves the propeptide of progelatinase A and initiates autoproteolytic activation: regulation by TIMP-2 and TIMP-3. *J Biol Chem* 271: 17119-17123, 1996.

301. **Wind S, Beuerlein K, Armitage ME, Taye A, Kumar A, Janowitz D, Neff C, Shaw AM, Wingler K and Schmidt H**. Oxidative stress and endothelial dysfunction in aorta of aged spontaneously hypertensive rats by NOX1/2 is reversed by NADPH oxidase inhibition. *Hypertension* 56: 490-497, 2010.

302. **Wolin MS**. Reactive oxygen specie and the control of vascular function. *Am J Physiol Heart Circ Physiol* 296: H539-H549, 2009.

303. **Wort S, Woods M, Warner T, Evans T and Mitchell J**. Endogenously released endothelin-1 from human pulmonary artery smooth muxcle promotes cellular proliferation:relevance to patogenesis of pulmonary hypertension and vascular remodeling. *Am J Respir Cell Mol Biol* 25: 104-110, 2001.

304. **Yang XR, Lin A, Hughs J, Flavahan N, Cao Y, Liedtke W and Sham J**. Upregulation of osmo-mechanosensitive TRPV4 channel facilitates chronic hypoxia-induced myogenic tone and pulmary hypertension. *Am J Physiol Lung Cell Mol Physiol* 302: L555-L568, 2012.

305. **Yang Y, Candelario-Jalil E, Thompson J, Cuadrado E, Estrada E, Rosell A, Montaner J and Rosenberg G**. Increased intranuclear matrix metalloproteinase activity in neurons interferes with osicative DNA repair in gocal cerebral ishemia. *J Neurochem* 112: 134-149, 2010.

306. **Yarden Y and Schlessinger J**. Epidermal growth factor induces rapid, reverible aggregation of the purified epidermal growth factor receptor. *Biochemistry* 26: 1443-1451, 1987.

307. **Yarden Y and Schlessinger J**. Self-phosphorylation of epidermal growth factor receptor: evidence for a model of intermolecular allosteric activation. *Biochemistry* 26: 1434-1442, 1987.

308. **Yu F, White S, Zhao Q and Lee F**. HIF-1á binding to VHL is regulated by stimulus-sensitive proline hydroxylation. *Proc Natl Acad Sci USA* 98: 9630-9635, 2001.

309. **Yu Y, Fantozzi I, Remillard C, Landsberg J, Kunichika M, Platoshyn O, Tigno D, Thistlewaite P, Rubin L and Yuan J**. Enhanced expression of transient receptor potential channels in idiopathic pulmonary arterial hypertension. *Proc Natl Acad Sci USA* 101: 13861-13866, 2004.

310. **Yuan J, Aldinger A, Juhaszova M, Wang J, Conte J, Gaine S, Orens J and Rubin L**. Dysfunctional voltage-gated K+ channels in pulmonary arterial smooth muscle cells of patients with primary pulmonary hypertension. *Circulation* 98: 1400-1406, 1998.

311. **Zempo N, Koyama N, Lea H and Clowes A**. Regulation of vascular smooth muscle cell migration and proliferation in vitro and in injured rat arteries by a synthetic matrix metalloproteinase inhibitor. *Arterioscler Throm Vasc Biol* 16: 28-33, 1996.

312. **Zhang B, Peng F, Wu D, Ingram AJ, Gao B and Krepinsky JC**. Caveolin-1 phosphorylation is required for stretch-induced EGFR and Akt activation in mesangial cells. *Cell Signal* 19: 1690-1700, 2007.

313. **Zhang M, Song P, Xu J and Zou MH**. Activation of NAD(P)H oxidase by thromboxane A2 receptor uncouples endothelial nitric oxide synthase. *Arterioscler Throm Vasc Biol* 31: 125-132, 2011.

314. **Zhang Y, Peng F, Gao B, Ingram AJ and Krepinsky JC**. Mechanical strain-induced RhoA activation requires NADPH oxidase-mediated ROS generation in caveolae. *Antioxid Redox Signal* 13: 959-973, 2010.

315. **Zhao H, Kalivendi S, Zhang H, Joseph J, Nithipatikom K, Vasquez-Vivar J and Kalyanaraman B**. Superoxide reacts with hyroethidine but forms a fluorescent product that distincly different from ethidium: potential implications in detection of superoxide. *Free Radical Biology and Medicine* 34: 1359-1368, 2003.

316. **Zhao Y, Lui Y, Stan R, Fan L, Gu Y, Dalton N, Chu P, Peterson K, Ross J and Chien K**. Defects in caveolin-1 cause dilated cardiomyopathy and pulmonary hypertension in knockout mice. *Proc Natl Acad Sci USA* 99: 11375-11380, 2002.

317. **Zhou X and Agaziea Y**. The signal and transformation potency of the overexpressed HER2 protein is dependent on the normally expressed EGFR. *Cell Signal* 24: 140-150, 2012.

318. **Zwick E, Daub H, Aoki N, Yamaguchi-Aoki Y, Tinofer I and Ullrich A**. Critical role of calcium-dependent epidermal growth factor receptor transactivation in PC12 cell membrane depolarization and bradykinin signaling. *J Biol Chem* 272: 24767-24770, 1997.

319. **Zwick E, Hackel PO, Prenzel N and Ullrich A**. The EGF receptor as central transducer of heterologous signalling systems. *Trends Pharmocol Sci* 20: 408-412, 1999.